THE GUARDIANS OF CELL FATE: PROTECTIVE MECHANISMS THAT ENSURE PROPER CELL FATE AND PATTERNING DURING IMAGINAL DISC REGENERATION IN DROSOPHILA

BY

KEATON JAY SCHUSTER

DISSERTATION

Submitted in partial fulfillment of the requirements
for the degree of Doctor of Philosophy in Cell and Developmental Biology
in the Graduate College of the
University of Illinois at Urbana-Champaign, 2018

Urbana, Illinois

Doctoral Committee:

Professor Lisa Stubbs, Chair
Assistant Professor Rachel Smith-Bolton, Director of Research
Associate Professor Craig Mizzen
Associate Professor Lori Raetzman

Abstract

Regenerating tissue must replace lost structures with cells of the proper identity and pattern in order to restore function. This thesis will describe two major insights into how patterning and cell fate is maintained and restored during the late phases of regeneration in the wing imaginal disc of *Drosophila*. First, the identification of *taranis* as a regeneration-specific patterning gene and its subsequent characterization as a factor that is required to protect the regenerating cells in the wing imaginal disc from inappropriate posterior to anterior cell fate changes that are induced by the powerful JNK signaling cascade at the wound misregulating the expression of *engrailed*. The other chapter will detail the identification of the pioneer transcription factor Zelda as being upstream of *taranis* expression during regeneration. Zelda is found to be expressed at the same place and time as Taranis, and reduction of Zelda levels results in profound anterior and posterior patterning defects. Speculation is provided suggesting that Zelda may also be essential for the large developmental transition from a program devoted to regenerative growth to the repatterning phase that allows for the restoration of cell fate and patterning genes that was lost earlier in regeneration. This work describes identification of a novel gene regulatory network essential for patterning and cell fate during regeneration.

This thesis is dedicated to my mother, Kelly Schuster, who was diagnosed with Amyotrophic Lateral Sclerosis (ALS) less than three weeks before my public thesis defense. Her strength continues to inspire me. I love you, Mom.

Acknowledgements

I would like to thank The Smith-Bolton lab for all the helpful scientific discussions on my work throughout the years. I would like to thank my advisor, Dr. Rachel Smith-Bolton for all the scientific advice throughout the years. I would also like to thank my committee: Dr. Lisa Stubbs, Dr. Craig Mizzen, and Dr. Lori Raetzman for all the helpful advice to make my project the best it can be. I would also like to thank Dr. Jon Chekan for introducing to me Gibson Assembly and helpful advice with cloning and protein purification. I would like to thank members of the Brian Freeman lab (especially Zlata Gvozdenov) with help with the biochemistry equipment they generously let me use. I would also like to thank Laura Martin and Elaine Rodgers for all their help with keeping me organized and keeping with deadlines. They were also very helpful with looking over this thesis for formatting errors. Of course, I would like to thank Chen Wang for the emotional support during the last two years of my graduate career.

I am forever grateful for all of the support from friends and family throughout my PhD. I thoroughly enjoyed my time here in Champaign-Urbana. I would especially like to thank my parents, Kraig and Kelly Schuster, for always supporting me.

Table of Contents

Chapter 1: General Introduction

Regeneration

Regeneration is the fascinating phenomenon where damaged body parts regrow after injury or disease. Indeed, regeneration has captivated biologists since the origins of experimental biology, with Abraham Trembley with *Hydra* (Galliot, 2012) and Lazzaro Spallanzani with salamanders (Dinsmore, 1996) being the first to formally describe regeneration in these species in the mid-1700s. The major reason why the ability to regenerate whole body parts such as limbs, eyes, hearts, etc. has been of great interest to the biomedical community is due to the comparatively poor regenerative abilities of humans. Therefore, understanding how other species can perform regeneration, and why we cannot is of tantamount importance for regenerative medicine.

Regeneration via cell proliferation, classically referred to as “Epimorphosis” by Thomas Hunt Morgan (Sunderland, 2010) is perhaps the most striking example of regeneration, which includes regenerating limbs and hearts, as opposed to “Morphalaxis”, which is simply remodeling of existing tissues. It should be noted that when I refer to regeneration, I am not including homeostatic self-renewal of tissues with adult stem cells within that definition. Epimorphic regeneration typically involves the formation of a blastema, which is a zone of proliferating undifferentiated cells that will eventually form the new structure (Tanaka and

Reddien, 2011). Of course, such classical definitions have been shown to not be absolute, with remodeling and cellular proliferation often accompanying each other in various extents (Tanaka and Reddien, 2011). The cellular origin of the blastema remains contested, depending on the species, but it does seem to primarily be derived from dedifferentiation of the remaining cells (Knopf et al., 2011; Kragl et al., 2009), or resident lineage-restricted progenitors of unknown origin (Rinkevich et al., 2011) with only a few species having pluripotent stem cell contribution to the blastema (Wagner et al., 2011).

Regeneration is accomplished by various means, but proceeds in a sequence of overlapping processes. The first step is almost immediately after injury, the wound needs to close. This step is typically rapid, and in vertebrates, is completely scar-free (Lévesque et al., 2010). The next step is to form the blastema, via either dedifferentiation (Knopf et al., 2011; Kragl et al., 2009) or via expansion of lineage-restricted progenitors (Gargioli and Slack, 2004; Lehoczky et al., 2011; Rinkevich et al., 2011; Sandoval-Guzmán et al., 2014) which may or may not be derived from dedifferentiated cells. The blastema then grows out to replace the missing mass in the precise dimensions of what was lost. The blastema then needs to repattern to restore functionality to the regenerate. All of these steps are essential to successfully regenerate the missing portion. The molecular mechanisms of each step are still poorly understood, so much of the effort over the past decade has been to identify genes and signaling pathways essential for regeneration in a vast menagerie of species. However, progress has

been slow due to the majority of regeneration-competent organisms having poor genetic tractability, and the classical model organisms having limited to no regenerative ability.

Animal Models of Regeneration

Regenerative ability is scattered throughout the animal kingdom, with no clear correlation with level of “complexity”. Invertebrates have a wide range of regenerative capacity, reflecting the extreme diversity within the clade. The very first model of regeneration, and indeed the very first experimental model for biology, is the freshwater polyps in the *Hydra* genus within Cnidarians, particularly *Hydra vulgaris* (Galliot, 2012). *Hydra spp*. are able to regenerate an entire head and/or foot after amputation (Galliot et al., 2006) mostly via morphallaxis. However, some cell divisions at the amputation plane have been observed (Chera et al., 2009), making the distinction between morphalaxis and epimorphosis unclear. *Hydra spp*. are interesting due to the fact that they only have 2 out of the 3 embryonic germ layers present: ectoderm and endoderm, without any mesoderm (Galliot et al., 2006; Technau and Holstein, 1992). Another Cnidarian model of regeneration is the scarlet sea anemone *Nematostella vectensis* (Passamaneck and Martindale, 2012), which has the advantage of having highly tractable embryos allowing for comparisons between development and regeneration that is not possible in the asexually budding *Hydra*. It is interesting that *Nematostella* head regeneration requires cell division, but its foot does not (Passamaneck and Martindale, 2012). *Hydra* have a

rudimentary genetic toolkit, such as transgenesis and RNAi (Galliot et al., 2007; Wittlieb et al., 2006). *Nematostella* has a rapidly expanding toolkit such as morpholinos, mRNA injection, CRISPR-CAS9 for *Nematostella* (Wijesena et al., 2017), a complete and well-annotated genome, and tissue-specific transgenesis which will catapult *Nematostella* into the forefront of cnidarian research. Due to Cnidarians being a sister group to bilaterians, studies in animals within this phyla will uncover highly conserved mechanisms present during regeneration in addition to unique adaptions not found in other phyla.

Among Bilaterians, planarians within the Platyhelminthes clade have the most striking regenerative powers where they are able to regenerate a whole animal after amputation, even when they are cut into extremely small fragments (Karami et al., 2015). They accomplish this via a population of pluripotent somatic stem cells known as neoblasts (Wagner et al., 2011). Therefore the planarian blastema is somewhat unique with its highly plastic progenitor cell population. Other “worms” have variable regenerative capacity, with the nematode *Caenorabdis elegans* (*C. elegans*) having the inability to regenerate anything other than axons in the peripheral nervous system (Wu et al., 2007; Yanik et al., 2004), to more regeneration-competent Annelids. Annelids can indeed regenerate multiple tissues (Bely and Sikes, 2010; Bely et al., 2014). However the mechanisms are not well understood, mostly due to a lack of a genetic toolkit for this species.

Arthropods are well known to be able to regenerate appendages, which is dependent on their ability to undergo successive molts where they shed their old cuticle and generate a new one. Therefore arthropod species such as crustaceans that are able to molt throughout the entirety of their lives are able to regenerate their appendages at all stages of their post-embryonic lifecycle. It is unclear whether crustacean embryos can regenerate limb buds as embryos. Traditionally, the fiddler crab has been a model for regeneration in crustaceans (Das and Durica, 2013; Durica and Hopkins, 1996), but is not genetically tractable. Therefore, a new genetic model crustacean has emerged in the amphipod *Parhyale hawaiensis* (Konstantinides and Averof, 2014). *Parhyale* is able to regenerate its limbs after amputation. It was shown that it regenerates in a mechanism akin to vertebrates where lineage-restricted progenitors contribute to the blastema, including satellite-like cells which contribute to the muscle (Konstantinides and Averof, 2014). *Parhyale* is also amenable to live imaging of the blastema through the cuticle, which allows for in-depth characterization of the cellular dynamics of the blastema (Alwes et al., 2016).

Other arthropods, such as insects, only molt in their juvenile stages. Therefore regenerative capacity in their appendages is limited to the nymphal stages in Hemimetabolous insects, and the imaginal discs of larval holometabolous insects. Among the basally located Holometabolous insects such as the red flour beetle *Tribolium castaneum* their larval stage has both imaginal discs such as the wing imaginal disc, and functional “polymorphic” limbs that are used for

locomotion. Both limbs and imaginal discs can regenerate in this species (Lee et al., 2013a). This species is often used as a comparative model between Holometabolous and Hemimetabolous insects. The genetic toolkit for this species is being developed, with rudimentary transgenics and enhancer traps as well as RNAi technology (Cheng et al., 2014; Shah et al., 2011; Suzuki et al., 2009).

Among Hemimetabolous insects, the two-spotted cricket *Gryllus bimacatulus* has emerged as a promising model system for limb regeneration during the nymphal stages (Mito et al., 2002). The ability to perform grafts has advanced our understanding of positional information during regeneration (Mito and Noji, 2008). Studies in *Gryllus* have the advantage of RNAi (Nakamura et al., 2007), but this has led to a bias in candidate-based approaches where only known developmental signaling pathways have been investigated.

The phylum Chordata where vertebrates and closely related notochord-containing invertebrates reside. Some species of the basal Chordate lineage Cephalochordates, are also known to have regenerative abilities. The model Cephalochordate amphioxus *Branchiostoma lanceolatum* is able to regenerate its tail and buccal cirri after amputation (Somorjai et al., 2012). Genetic techniques such as TALENs and transgenesis were very recently developed for a related species *Branchiostoma floridae*, and improved husbandry techniques will allow for future genetic analysis that was until very recently, considered

impossible. The sister taxon of vertebrates are now know to be the tunicates (Delsuc et al., 2006). The model tunicate *Ciona intestinalis* is able to regenerate multiple tissues as an adult, including heart, neural complex and oral siphon in its immobile adult stage (Evans Anderson and Christiaen, 2016; Jeffery, 2015a, 2015b). Its mobile larval stage, which more closely resembles a classic chordate body plan, is not thought to be able to regenerate (Jeffery, 2015a), which is atypical among metazoans. Most metazoans have higher regenerative capacities as juveniles than adults. Therefore *Ciona* would make an attractive model for acquisition of regenerative capacity after metamorphosis.

Various vertebrate models for regeneration also exist, which are popular due to their relatively close evolutionary relationship to humans, as compared to the distantly related invertebrates. Teleost fish such as zebrafish (*Danio rerio*) are able to regenerate multiple tissues after damage such as: heart (Poss et al., 2002), brain (Kroehne et al., 2011), spinal cord (Mokalled et al., 2016), retina (Lenkowski and Raymond, 2014), liver (Kan et al., 2009), kidney (Diep et al., 2011), pancreas (Hesselson et al., 2009), jaws (Paul et al., 2016; Wang et al., 2012) and fins (Whitehead et al., 2005). Fin and heart regeneration in zebrafish have been the two models most intensely investigated over the past 15 years in this species. Zebrafish also has the advantage of being genetically tractable, and have a complete genetic toolkit at their disposal. The one downside to zebrafish is that it takes over 3 months for a fish to reach sexual maturity, so experiments that require complex genotypes or to generate novel lines take a long time. The

recent introduction of the turquoise killifish *Nothobranchius furzeri*, which is able to reach sexual maturity within a month after fertilization and having a complete lifespan lasting only 3-6 months (Platzer and Englert, 2016). This makes it an attractive alternative genetic model organism for the study of regeneration, aging, and developmental arrest (Platzer and Englert, 2016) on a timescale unheard of for vertebrates. More work is needed to further develop the genetic and molecular toolkit in this promising emerging model organism.

Amphibians, particularly the Urodeles (salamanders) are perhaps the most extreme example of regenerative ability in vertebrates. Salamanders including the eastern newt *Notophthalmus viridescens* and the Mexican axolotl *Ambystoma mexicanum* are the favorite model urodeles to study regeneration. They are famously known to be able to completely regenerate their limbs after amputation in a couple months. The axolotl has been shown to be able to regenerate its tail (Schnapp et al., 2005), lens (Suetsugu-Maki et al., 2012), spinal cord (Diaz Quiroz et al., 2014), brain (Amamoto et al., 2016) and heart (Flink, 2002) after amputation/injury. Newts have also been shown to be able to regenerate their limbs (Kumar et al., 2007) and lens (Tsonis, 2006). The Anurans (frogs) *Xenopus laevis* and *Xenopus tropicalis* also have impressive regenerative powers. *Xenopus spp.* exhibit age-dependent regenerative capacity where they are able to robustly regenerate their limb buds (Slack et al., 2004), spinal cord (Hui et al., 2014a), tail (Love et al., 2011), and lens (Henry and Tsonis, 2010) in the larval tadpole stages, and are unable to effectively regenerate these tissues

as adults (Slack et al., 2004). Interestingly, *Xenopus* tadpoles experience a refractory period during larval development where they transiently lose their ability to regenerate their tail, but regain the ability to regenerate afterwards until the onset of metamorphosis (Slack et al., 2004). This coincides with the development of the immune system, but a convincing functional connection between the refractory period and the immune system has yet to be demonstrated. Despite these amphibian model systems being champions of regenerative capacity, progress in determining the genes and molecular mechanisms of regeneration has been agonizingly slow due to an extremely long generation time in these species. *Xenopus laevis* and the axolotl take almost a year to reach sexual maturity (Harland and Grainger, 2011; Khattak and Tanaka, 2015), and *Notophthalmus viridescens* takes even longer to reach sexual maturity taking 2-3 years (Simon and Odelberg, 2015). Therefore the generation of transgenic and mutant lines is very impractical in these species. *Xenopus tropicalis* has a much shorter generation time making genetic analysis easier, however there has been a stubborn reluctance to adopting *X. tropicalis* over *X. laevis* that has yet to be resolved as evidenced by the dearth of *X. tropicalis* publications. Therefore most functional analysis in amphibian species has been limited to morpholinos, a small number of transgenic lines (Currie et al., 2016; Kragl et al., 2009; Sandoval-Guzmán et al., 2014), and small molecule inhibitors, where off-target effects can- and do- result in spurious, if not absurd conclusions (Adams et al., 2007; Tseng et al., 2010).

Among amniotes, the level of regenerative capacity is limited relative to other vertebrates mentioned previously. Most of the classically defined non-avian reptile groups have not been investigated for regenerative ability with the exception of a few lizard species. The experimental lizard models of the anole (*Anolis carolinensis*) and the leopard gecko (*Eublepharis macularius*) are known to regenerate their tails after the voluntary loss of their tails to evade predation known as autotomy (Fisher et al., 2012; McLean and Vickaryous, 2011). Regeneration of the tails post-autotomy results in a fully functional tail in both species, however these tails are not properly patterned compared to an unamputated tail (Fisher et al., 2012; McLean and Vickaryous, 2011), indicating hypomorphic regenerative ability. While the evolutionary relatedness of anoles and leopard geckos are relatively close to humans compared to other vertebrate models such as fish or amphibians, they are terrible genetic models due to long gestation, long generation time, and seasonal reproductive habits. They can suffice as a comparative model in the greater context of regeneration in vertebrates.

Other amniotes such as birds and mammals have extremely limited regenerative abilities. Birds (Aves) such as the chicken *Gallus gallus* can only regenerate their limbs and spinal cords as embryos (Halasi et al., 2012; Satoh et al., 2010), and they can regenerate their feathers as adults (Chen et al., 2015). It should be mentioned that the data on the embryonic regenerative phenomenon is quite subtle, and is typically considered regulative development, rather than

regeneration. This extreme lack in regenerative ability, in addition to being a poor genetic model system (despite being a powerful embryological model) makes birds an unattractive model system for regeneration.

Mammals, for the most part, while not being as poor regenerators as birds, still have a very limited amount of regenerative ability. This, of course, is why the study of regeneration in other species is of tantamount importance for regenerative medicine. Knowledge gained from flies, worms, fish and amphibians will inform us how to induce regeneration in a medical setting. The common house mouse *Mus musculus* is an incredibly popular model organism in biology. They are also very genetically tractable, but suffer the same problem of having a relatively long generation time compared to *Drosophila* or *C. elegans*. Their regenerative abilities are modest, at best, and can be a corollary to the regenerative capacity of humans. Mice are known to be able to regenerate their heart and digit tips as neonates (Borgens, 1982; Porrello et al., 2011). This regenerative capacity declines rapidly as they mature into adults, and is often only limited to the first couple weeks of life. Clinical investigations in humans infants show that humans are also able to regenerate their digit tips (Muneoka et al., 2008). Much like humans, adult mice can also regenerate their liver after partial hepatectomy or chemical damage, which can be impaired by fibrosis (Michalopoulos, 2017). The reduced regenerative capacity found in mammals is associated with the alternative mode of healing with a scar, which is considered a trade-off for robust regenerative capacity as seen in salamanders (Eming et al.,

2014). This is believed by some to be due to having an advanced adaptive immune system as evidenced by the immunocompromised MRL mouse model exhibiting enhanced regenerative abilities with ear hole punch injury and digit tip regeneration (Heber-Katz and Gourevitch, 2009). However, this conclusion falls short due to MRL mice not having as robust regenerative capacity compared to wild type African Spiny Mice (Gawriluk et al., 2016; Seifert et al., 2012), and that the major effect quantitative trait loci that are associated with the MRL mouse are cell cycle genes, not immunity genes (Bedelbaeva et al., 2010; Heber-Katz et al., 2012).

Recently, there was a notable exception to the general rule of thumb that mammals are poor regenerators. It was discovered that African Spiny Mice (*Acomys spp*.) exhibits remarkable regenerative capacity. They are able to autotomize their back skin and regenerate it completely without formation of a scar (Seifert et al., 2012), and are able to regenerate large ear hole punch injuries via the formation of a blastema (Gawriluk et al., 2016), which requires the innate immune response, primarily through macrophages (Simkin et al., 2017). It will be of great interest to investigate what other tissues *Acomys* can regenerate that other mammals cannot, which could lead to direct comparisons to how to enhance regeneration in other mammals, including humans. Despite the regenerative abilities of *Acomys*, a genetic toolkit has yet to be developed for this species. There could be notable barriers to the development of a genetic toolkit in this species, such as a long generation time where it takes 2-3 months to

sexual maturity, gestation lasting 38-45 days, and small litter sizes (Haughton et al., 2016). Only time and dedicated work on this species will tell if they can be a genetic model for mammalian regeneration.

In conclusion, the majority of these models, while having remarkable regenerative capacity, fall short on a major concern: with the exception of *Drosophila*, mouse and zebrafish, none of the highly regenerative organisms are amenable to genetic analysis or modification. Therefore, I will detail in the next section on the advantages of *Drosophila melanogaster* as a genetic model system for the study of regeneration.

Drosophila melanogaster as a genetic model of regeneration

The common fruit fly, *Drosophila melanogaster* is a popular model organism in the biomedical sciences for the past 100 years. The main advantage *Drosophila* has over other model systems is its high level of genetic tractability that allows an investigator to easily manipulate gene function over a rapid period of time. Indeed, the generation time of Drosophila takes around 10 days from egg to adulthood at 25^{o}C. This is in stark contrast to traditional models of regeneration, where they take months, if not years to reach sexual maturity. Thus making traditional genetic analysis in most regenerative species impractical and time consuming, if not impossible due to other technical concerns. One is also able to culture hundreds of flies of a given strain, which allows investigators to have high

statistical power in their experiments with large sample sizes. Given *Drosophila*'s ideal nature of a genetic model system, there are countless advanced genetic technologies at the disposal of a fly researcher. Robust ways to overexpress genes and RNAi in a tissue specific manner, genome editing, and random mutagenesis with chemical mutagens and mobile genetic elements exist to aid in the in-depth mechanistic investigation of the processes of choice. *Drosophila*, compared to the highly regenerative axolotl or planarian, has modest regenerative capacity, with only a select number of organs being able to regenerate post injury. Perhaps the most extensively studied is the adult midgut, which regenerates after infection or chemical-induced tissue damage via asymmetric and symmetric divisions of intestinal stem cells (Jiang et al., 2016). A more recent discovery is that the adult drosophila brain can undergo neurogenesis after stab injury (Fernández-Hernández et al., 2013), however, it is still unclear whether these newborn neurons can successfully reintegrate into the existing brain circuitry and recover functionality. The reactive gliosis that also accompanies brain injury (Kato et al., 2009) might inhibit such functional recovery, but this remains to be tested. The larval CNS is also able to repair itself after injury, however, this repair is performed by glia and there is no evidence for neurogenesis in this context (Kato et al., 2011). The peripheral nervous system in both larvae and adults is also able to regenerate damaged axons (Soares et al., 2015) and dendrites (Thompson-Peer et al., 2016), much like most species, including mammals (Saijilafu et al., 2013). The contribution of neural stem cells in CNS and PNS repair is still yet to be determined. In the larvae, it is well known

that the imaginal discs are able to regenerate after various forms of tissue damage (Khan et al., 2016a; Smith-Bolton, 2016; Worley et al., 2012).

Imaginal Disc Regeneration

Imaginal discs are internal epithelial precursor organs in the larvae of holometabolous insects that, upon metamorphosis, differentiate into the external cuticular structures such as legs, wings, antennae, eyes, external genitalia, and proboscis. They are composed of two epithelial layers: a columnar epithelium which is considered the “disc proper” and a simple squamous epithelium above the disc proper known as the peripodium. During larval development in *Drosophila*, the imaginal discs grow rapidly from a small population of 22-34 cells set aside during late embryogenesis (Worley et al., 2013) to the final population of approximately 30,000 cells at the end of the 3rd instar (Martin et al., 2009a). During this rapid growth, the imaginal discs are patterned by signals from morphogen gradients and growth factors and undergo specification depending on position within the disc. This, along with tightly controlled size control mechanisms ensures the correct final size and shape of the resulting appendage is reached by the end of larval development.

During the 1960s, Ernst Hadorn, Peter Bryant, and Gerold Schubiger discovered a remarkable property of imaginal discs: they are able to regenerate missing tissue after fragmentation and subsequent *ex vivo* culture within the abdomens of

adult female *Drosophila* (Bryant, 1971; Hadorn, 1968; Schubiger, 1971). An alternative way to physically damage discs is to damage them in situ by closing a forceps on a disc through the cuticle (Bryant, 1971; Díaz-García and Baonza, 2013; Smith-Bolton et al., 2009). This is perhaps a more physiological way to damage an imaginal disc, since it mimics damage done via predation attempt on various larval holometabolous insect species in the wild. However, it is a difficult technique to master and suffers from low reproducibility of the damage type. The fragmented discs regenerate via a localized zone of proliferating cells which is considered a blastema (Bryant and Fraser, 1988; Hadorn, 1968; O'Brochta and Bryant, 1987). The blastema forms prior to wound closure, and robustly regenerates the missing portion of tissue (Bryant and Fraser, 1988; O'Brochta and Bryant, 1987). Following regenerative outgrowth, the regenerating disc repatterns to restore the lost pattern after damage.

A decade after the discovery that imaginal discs can regenerate after physical fragmentation, it was discovered that imaginal discs can lose over 50% of their cells after X-irradiation, and can restore the lost number of cells to the original pre-damage levels by simply undergoing additional divisions (Adler and Bryant, 1977). This response to sporadic cell death within the imaginal disc is referred to as "compensatory proliferation". This form of damage reveals a remarkable plasticity in how an imaginal disc responds to different forms of tissue damage, with the major difference is with cutting and pinching, a loss of positional information results in the formation of a blastema and the restoration of the

missing positional information. During compensatory proliferation, there is no loss in positional information due to individual cells scattered throughout the disc undergo cell death at random locations. Therefore it has been observed that different signaling pathways are required after physical fragmentation and after irradiation (Hariharan and Serras, 2017; Khan et al., 2016a; Martin et al., 2009b; Smith-Bolton, 2016; Worley et al., 2012).

It was later shown that compensatory proliferation after irradiation requires apoptosis (Huh et al., 2004; Pérez-Garijo et al., 2004; Ryoo et al., 2004). They employed an experimental trick to force apoptotic cells to remain in the tissue by inhibiting effector caspase activity by overexpressing the baculovirus protein p35 in the irradiated imaginal disc. This allows for the initiation of apoptosis, but blocks the execution of cell death (Hay et al., 1994). This leads to the formation of “undead cells”, which are cells that are in an abnormal non-physiological cellular state where the cells are not-quite dead and are releasing various signaling proteins that are able to autonomously and non-autonomously induce overgrowth within the tissue (Huh et al., 2004; Pérez-Garijo et al., 2004; Ryoo et al., 2004). This led to the conclusion that apoptotic cells can signal to their neighbors to divide, hence this process was christened “apoptosis-induced compensatory proliferation” or AiP. It was later shown that undead cells and regular apoptotic cells can stimulate non-autonomous apoptosis (Pérez-Garijo et al., 2013), and apoptotic cells could stimulate non-autonomous resistance to irradiation (Bilak et al., 2014). Undead cells induce AiP via different mechanisms

depending on whether the tissue is terminally differentiated, or undifferentiated and therefore still actively dividing (Fan and Bergmann, 2008). While the concept of AiP without undead cells has been validated in other systems such as Hydra (Chera et al., 2009), the use of undead cells in the field has erroneously equated regeneration with AiP. In actuality, AiP with undead cells is more akin to tumorigenesis than a true regenerative response. This also does not seem to be a true regenerative response, since blocking apoptosis after pinch injury has little effect on the regenerative response of the wing disc (Díaz-García and Baonza, 2013). Therefore, AiP, compensatory proliferation, and regeneration should be considered separate processes.

In order to identify novel genes essential for regeneration, the design and implementation of forward genetic screens was essential. However, the method of physical fragmentation and culture in adult female hosts is time consuming, difficult to master, and the necessity of having large numbers of animals made genetic screens for genes involved in imaginal disc regeneration impractical and technically challenging. Therefore, a genetic method to induce tissue damage *in situ* via the transient conditional induction of pro apoptotic genes using the GAL4/UAS/GAL80^{ts} system in large numbers of larvae was developed independently by the Hariharan and Serras labs (Bergantiños et al., 2010; Smith-Bolton et al., 2009). These induced expression of either *eiger* or *reaper* within a spatially defined region within the wing primordia of the wing imaginal disc. Both *eiger* and *reaper* expression results in massive tissue damage via apoptosis, and

the expression of known regeneration genes JNK and Wingless (Bergantiños et al., 2010; Smith-Bolton et al., 2009). A transient loss of patterning information was also observed in the regenerating tissue. Eiger induces a more robust regenerative response that Reaper, which is likely due to Eiger being upstream of JNK, therefore amplifying the regenerative response beyond the normal range (Igaki and Miura, 2014; Smith-Bolton et al., 2009). A few years later, another genetic ablation system using the pro-apoptotic factor Hid to ablate the wing primordium (Herrera et al., 2013). It became obvious that ablation with Hid has different kinetics in inducing cell death than other pro-apoptotic gene. Discs overexpressing Hid have more cleaved Caspase-3 immunoreactivity, yet the pouch size and DAPI staining did not change. It is clear, in this experimental paradigm that cells rapidly replace the dead cells before a change in size or cell number can occur. Wingless is not upregulated and patterning is not lost. Therefore Hid-mediated ablation in wing imaginal discs more closely mimics the scattered cell death that results in compensatory proliferation. The difference between these genetic ablation strategies will allow for easy assessment of genes involved in regeneration and compensatory proliferation with a simple thermal shift during larval development.

Anterior/Posterior Patterning during Normal Wing Imaginal Disc Development

This thesis will extensively describe wing disc regeneration in the context of anterior/posterior patterning of the wing, therefore a brief introduction to AP

patterning is warranted. The AP axis is initially established during late embryogenesis via the segment polarity genes such as Engrailed via the activity of the pair-rule genes (DiNardo and O'Farrell, 1987). Engrailed is the posterior selector gene and is expressed in the posterior compartment of all imaginal discs starting in late embryogenesis (Kornberg et al., 1985; Patel et al., 1989), and is maintained by the action of the PcG family of chromatin modification enzymes throughout the rest of larval development (Chanas et al., 2004; Maschat et al., 1998; Randsholt et al., 2000). Engrailed establishes posterior identity, and represses the transcription of anterior genes such as the Hedgehog pathway transcription factor Cubitus interruptus (Ci) which are the default expression state in the discs when the activity of En is not present (Eaton and Kornberg, 1990). It should be noted that under normal circumstances, the posterior compartment and the anterior compartment are segregated from each other via the anterior-posterior compartment boundary, which suppresses compartment intermixing, yet the mechanisms of how this happens is controversial but likely involves interactions between signaling, tension, and perhaps cell adhesion (Umetsu and Dahmann, 2015). En in the posterior compartment activates the expression of the morphogen Hedgehog (Hh), which then transverses to the anterior compartment as a morphogen gradient and activates the expression of target genes in a concentration-dependent manner via binding to its receptors Patched (Ptc) and Smoothened (Smo) (Briscoe and Thérond, 2013; Taipale et al., 2002). Upon binding of Hh to Ptc, Ptc inhibits Smo from promoting the cleavage of Ci into its repressor form and the full-length Ci is able to translocate into the nucleus

and activate transcription of its targets (Aza-Blanc et al., 1997; Chen et al., 1999; Taipale et al., 2002). At high concentrations of Hh, Ci activates the expression of Ptc in a feed-forward loop that results in the activation of the BMP2/4 homolog *decapetapelegic* (*dpp*) (Capdevila et al., 1994; Tanimoto et al., 2000). Dpp is also a morphogen that acts as the AP organizer where it is transported/diffuses across the entire AP axis in both directions laterally and activates different targets in a concentration dependent manner in a gradient via binding the Type I BMP Receptors Thickveins and Saxophone (Singer et al., 1997), which results in the phosphorylation of the Smad-family transcription factor *Mothers against dpp* (Mad) (Campbell and Tomlinson, 1999a; Matsuda et al., 2016). Phospho-Mad (pMad) can be used as a readout of the Dpp morphogen gradient (Tanimoto et al., 2000). At high concentrations, pMad activates Spalt (de Celis and Barrio, 2000; de Celis et al., 1996), and intermediate concentrations pMad activates *optomotor blind* (*omb*) (del Álamo Rodríguez et al., 2004) and *daughters againsts dpp* (*dad*) (Tabata et al., 1997). At low concentrations of Dpp, pMad activates the expression of *brinker* (*brk*) which is a transcriptional repressor of the Dpp pathway (Campbell and Tomlinson, 1999b; Jaźwińska et al., 1999). Through the concerted action of these different target genes in overlapping or “nested” domains, they establish a groundplan for where the proveins will be positioned along the AP axis to determine the stereotypic five-veined pattern of the adult wing blade (Blair, 2007). Proveins are marked by the notch ligand Delta (Doherty et al., 1996a) and the EGFR signaling targets known as the Iroquois Complex (IroC) (Gómez-Skarmeta et al., 1996; Sugimori et al., 2016) and Rhomboid

(Sturtevant et al., 1993), among others (not shown). Delta in the proveins then activates Notch signaling in the adjacent tissue which will then be specified into intervein territories which are marked by E(spl)Mβ and dSRF/Blistered (Ligoxygakis et al., 1999; Nussbaumer et al., 2000). Therefore, alterations in wing vein patterning can result from defects in anterior/posterior identity, morphogen signaling, and cell fate specification.

Molecular Mechanisms of Imaginal Disc Regeneration

Over the past decade, rapid progress with the understanding of the molecular signals and effectors involved in imaginal disc regeneration has taken place. These factors include Ca^{2+} (Narciso et al., 2015; Restrepo and Basler, 2016), reactive oxygen species (ROS) (Brock et al., 2017; Khan et al., 2017; Santabárbara-Ruiz et al., 2015), JNK signaling (Bergantiños et al., 2010; Bosch et al., 2005, 2008), p38 MAPK signaling (Santabárbara-Ruiz et al., 2015), JAK/STAT signaling (La Fortezza et al., 2016; Katsuyama et al., 2015; Santabárbara-Ruiz et al., 2015), Hippo/ Yorkie/Ajuba signaling (Grusche et al., 2011; Meserve and Duronio, 2015; Repiso et al., 2013; Sun and Irvine, 2011, 2013), dilp8/Lgr3 (Colombani et al., 2012, 2015, Garelli et al., 2012, 2015; Jaszczak et al., 2016; Vallejo et al., 2015), Nitric Oxide Synthase (NOS) (Jaszczak et al., 2015), Wingless/Wnt (Wg) signaling (Smith-Bolton et al., 2009), dMyc (Smith-Bolton et al., 2009), Plexin (Yoo et al., 2016), trithorax (Skinner et al., 2015), the actin chaperonin TCP1 (Álvarez-Fernández et al., 2015), and methionine metabolism (Kashio et al., 2016). Intriguingly, both Dpp (BMP)

signaling (Mattila et al., 2004), inflammation mediated by hemocytes (Katsuyama and Paro, 2013), and apoptosis (Diaz-Garcia et al., 2016) do not appear to have an obvious role during imaginal disc regeneration after physical damage, despite evidence for the involvement of these pathways in compensatory proliferation and AiP (Fogarty and Bergmann, 2015; Fogarty et al., 2016; Perez-Garijo et al., 2005, 2009; Pérez-Garijo et al., 2004; Ryoo et al., 2004). It should be noted that these three studies were not comprehensive in ruling out the role of these factors during imaginal disc regeneration, so more investigation is required to tease out the putative role of these pathways.

A general theme has emerged with these studies, where the Jun N-terminal signaling pathway appears to be the central node within the molecular architecture of regenerative signaling in Drosophila imaginal discs. JNK signaling is a classical MAP Kinase signaling pathway that can respond to multiple upstream developmental and stress-response cues (Igaki and Miura, 2014; Stronach, 2005). In regards to imaginal disc regeneration, ROS signaling is upstream of JNK after physical damage and genetic ablation (Santabárbara-Ruiz et al., 2015). Just about all of the signals mentioned above, other than ROS and Ca^{2+}, are either directly or indirectly regulated by JNK, with the exception of p38 signaling that is activated in parallel to JNK (Santabárbara-Ruiz et al., 2015). Therefore, JNK signaling is absolutely required for both wound healing and regenerative growth during imaginal disc regeneration. JNK signaling has also been associated with the phenomenon of transdetermination (Lee et al., 2005)

which is a form of plasticity in regenerating discs where the fate of one disc transforms into another disc type when damaged at a certain point in the disc known as the weak spot, where it appeared to be required for the fate change. However, transdetermination seems to require regenerative growth (McClure and Schubiger, 2007; Schubiger, 1973), and JNK signaling is essential for regenerative growth (Bergantiños et al., 2010; Bosch et al., 2005, 2008), the true role of JNK signaling and cell fate changes remained obscure since there was no evidence for JNK being sufficient for cell fate changes during regeneration.

My project has largely been focused on the mechanisms of cell fate and patterning during regeneration of the wing disc. Historically, the re-establishment of cell fate and patterning has been considered to be largely due to developmental signals being redeployed in the blastema (Nacu and Tanaka, 2011). Indeed, there has been considerable attention given to understanding how known patterning mechanisms integrate during regeneration in both vertebrates (Nacu et al., 2016; Roensch et al., 2013) and invertebrates (Ishimaru et al., 2015; Lee et al., 2013a; Mito and Noji, 2008). This has largely been due to the inherent biases of candidate-based approaches in studies of non-traditional model organisms, where unbiased forward genetic approaches are not feasible, if not impossible. In the rare instances where a novel factor that is essential for regenerative growth and patterning is discovered via brute-force biochemistry (da Silva et al., 2002; Sugiura et al., 2016), the developmental role was not investigated. Prod1 is a classic example of a factor that is essential for positional

information along the proximal-distal axis during limb regeneration in newts (da Silva et al., 2002). This might have been a candidate for a regeneration-specific molecule involved in patterning, but its developmental role was not investigated for another ~13 years (Kumar et al., 2015). Of course, Prod1 is indeed essential for patterning of the developing limb bud in newts (Kumar et al., 2015), which disqualifies it as a “regeneration-specific patterning factor”. Planarians have this same issue, where numerous signaling pathways are essential for patterning during regeneration. However, since planarian embryogenesis is only now being investigated (Davies et al., 2017), a number of these patterning factors are guaranteed to be shown to be essential for embryonic patterning as well. Therefore, at the time of the start of my PhD, the notion of the existence of factors essential for patterning during regeneration, but not development of the same organ was considered possible, but no evidence for such factors existed.

Despite this assumption that regeneration recapitulates development, there are a number of lines of evidence that point to the possibility of such mechanisms. Gene expression and lineage tracing studies revealed that regenerating leg discs regenerate in proximal tissue first, with cells of distal identity forming later. This is opposite to what is found in developing leg discs, where distal identity is specified first, with proximal identities being specified later (Bosch et al., 2010). The functional plasticity found in regenerating imaginal discs is another point indicating the possibility of factors that are unique to regeneration could exist, and that plasticity is important for regeneration. For example, when a provein

region is ablated within the wing pouch, the adjacent intervein cells transform into provein cells (and vice versa) to regenerate the missing tissue (Repiso et al., 2013). A major challenge in the field is to identify such factors that regulate patterning and cell fate specification during regeneration.

As I will detail in the next chapter, we sought out to identify novel mechanisms that control regeneration in the wing imaginal disc by performing a dominant modifier screen for genes that affect regeneration as heterozygotes (Smith-Bolton et al., 2009). I discovered that *taranis* is factor that is required for cell fate and patterning after tissue damage, but is dispensable for normal development (Schuster and Smith-Bolton, 2015). It is part of an unanticipated regulatory circuit where it acts as a protective factor to prevent aberrant cell fate changes caused by the JNK signaling cascade during regeneration (Schuster and Smith-Bolton, 2015). This ensures the regenerating wing has the proper pattern after tissue damage and regeneration, therefore making a fully functional wing. Finally, the third chapter will detail my investigations in the mechanisms of how cell fate is re-established and how this led me to the discovery that the pioneer transcription factor Zelda (Liang et al., 2008) is upstream of Taranis expression during regeneration. Zelda may also be essential for re-establishing the expression of other patterning factors late in regeneration.

Chapter 2: Taranis Protects Regenerating Tissue from Fate Changes Induced by the Wound Response in *Drosophila* *

Introduction

The replacement of lost or damaged tissues and appendages through regeneration is a fascinating phenomenon that occurs to varying extents among metazoans. The rebuilding of a structure after loss or damage depends on proliferation accompanied by proper cell fate specification and patterning. Recent work in several model organisms has begun to elucidate the genes and signaling pathways that initiate regeneration and promote regenerative growth (Sun and Irvine, 2014). Some of these signals occur in response to wounding, such as the release of reactive oxygen species, activation of JNK signaling, and the production of mitogens such as Fgf20 and other growth-promoting signals such as nAG (Bergantiños et al., 2010; Gauron et al., 2013; Kumar et al., 2007; Love et al., 2013; Whitehead et al., 2005).

While progress has been made identifying early regeneration genes, little is known about the genes that regulate repatterning and adoption or maintenance of appropriate cell fates late in regeneration. While the mechanisms that

---

*This chapter was originally published as: Schuster, K.J., and Smith-Bolton, R.K. (2015). Taranis Protects Regenerating Tissue from Fate Changes Induced by the Wound Response in Drosophila. *Dev. Cell 34*, 119–128. The work and writing in this chapter were performed and written by Keaton J. Schuster and have been adapted with minor modifications for incorporation into this work.

establish these cell fates during regeneration are often thought to recapitulate development (Gupta et al., 2013; Roensch et al., 2013) and regenerative medicine seeks to replicate development (Tonnarelli et al., 2014), deviation from developmental patterning and reprogramming of positional identity can occur in regenerating tissue (Bosch et al., 2010; McCusker et al., 2013). Furthermore, changes in cell lineage can occur when necessitated by depletion of the preferred progenitor pool (Herrera and Morata, 2014; Singh et al., 2012). Moreover, while regeneration can be induced in adult *Xenopus* limbs by grafting progenitor cells onto amputation stumps, application of developmental signaling molecules to provide pattern instruction and positional information did not generate limbs with complete patterning and structure (Lin et al., 2013), indicating that additional factors are needed to ensure the proper regenerated form. Thus, very important open questions remain regarding patterning and cell fate during regeneration. What are the genes and signals that control patterning and cell fate during the later steps of regeneration? Are these genes different from those that control patterning and cell fate in the same tissue during normal development? If so, why is the normal developmental program insufficient during regeneration? Identification of these unknown factors that enable regenerating structures to attain proper cell fates and form will be key to employing regenerative mechanisms in wounded tissue.

Here we describe the identification of *taranis (tara),* a homolog of the vertebrate TRIP-Br (Transcriptional Regulators Interacting with PHD zinc fingers and/or

Bromodomains) family of proteins, as a regeneration-specific patterning gene in *Drosophila*. Vertebrate TRIP-Br proteins can regulate transcription through Dp/E2F (Hayashi et al., 2006; Hsu, 2001), and p53 (Watanabe-Fukunaga et al., 2005), and can regulate the cell cycle through direct binding of CyclinD/Cdk4 (Sugimoto et al., 1999) and by regulating expression of CyclinE (Sim et al., 2006a). *Drosophila* Tara genetically interacts with E2F/Dp (Manansala et al., 2013), and with Polycomb Group and Trithorax Group genes (Calgaro et al., 2002; Fauvarque et al., 2001) but otherwise remains uncharacterized at the molecular and functional level.

We show that regenerating tissue with reduced levels of Tara undergoes posterior-to-anterior fate transformations late in regeneration. These fate changes occur because expression of the posterior selector gene *engrailed* (*en*) becomes deregulated, leading to autoregulatory silencing of the *engrailed* locus, which requires the Polycomb Repressor Complex 1 (PRC1) subunit *polyhomeotic (ph)*. This misregulation and subsequent silencing of *en* is induced by Jun N-terminal Kinase (JNK) signaling, which is essential for wound closure and regenerative growth. Tara is able to suppress these JNK-dependent fate changes without reducing JNK signaling activity. Thus, Tara stabilizes *engrailed* expression downstream of JNK signaling to maintain proper cell fate during regeneration.

Results

To identify regeneration-specific factors that are critical for patterning and cell fate, we used a forward genetic screen to isolate mutants that have altered tissue morphology after regeneration. This screen was carried out using damaged *Drosophila* wing imaginal discs, which are an excellent model system for the study of regeneration (Worley et al., 2012) because of their simple epithelial structure, complex patterning and fate specification, well-characterized development, remarkable regenerative capacity, and unparalleled genetic tractability. To study regeneration *in vivo*, we used a genetic tissue ablation system (Smith-Bolton et al., 2009) to ablate cells in a spatially and temporally defined manner in *Drosophila* larval wing imaginal discs. We ablated over 90% of the primordial wing in early 3rd instar larvae rapidly and efficiently by driving expression of the pro-apoptotic gene *reaper* (*rpr*) within the *rotund* (*rn*) expression domain of the wing pouch for 24 hours. After ablation, the discs regenerated *in situ*. The extent and quality of the regeneration were scored based on the size, shape and patterning of the resulting adult wings. Using this system, we performed a pilot dominant-modifier screen for genes required for regeneration using isogenic deficiencies (Ryder et al., 2007; Smith-Bolton et al., 2009).

taranis is required for posterior cell fate during imaginal disc regeneration

We identified a deficiency, *Df(3R)ED10639*, that, when heterozygous, had phenotypically normal wings when undamaged (data not shown), yet caused dramatic and consistent patterning defects after regeneration that resembled a posterior-to-anterior (P-to-A) transformation, including socketed bristles and ectopic veins on the posterior margin, an ectopic anterior crossvein (ACV), costal bristles on the alula, and an altered shape that has a narrower proximal and wider distal P compartment (Fig. 1A-B). To identify the gene responsible for this phenotype we screened smaller deficiencies and mutant alleles of genes within this region. Four alleles of the gene *taranis* (*tara*) (Calgaro et al., 2002), $tara^{1}$ (Fauvarque et al., 2001), $tara^{03881}$ (Gutiérrez et al., 2003), $tara^{YD0165}$ and $tara^{YB0035}$ (Buszczak et al., 2007), recapitulated the P-to-A transformation phenotype after tissue damage, yet had normal wing patterning when undamaged (Fig. 1C-G, data not shown). By contrast, wild-type regenerated adult wings had few defects in the posterior wing (Fig. 1F-G). Furthermore, the wild-type regenerated wings with patterning errors did not have as severe a phenotype as the $tara^{1}$/+ regenerated wings (Fig. 2A-D). Such aberrations never appeared in undamaged wings of either genotype (Fig. 1A, C).

To confirm that the posterior compartments of $tara^{1}$/+ regenerating wing discs were transforming to an anterior fate, we examined the regenerating wing imaginal discs for ectopic anterior gene expression 72 hours after tissue damage

(recovery time 72 or R72), which is when regeneration and repatterning are largely complete (Smith-Bolton et al., 2009). Achaete (Ac) is a proneural protein that marks sensory organ precursor (SOP) cells that develop into the socketed bristles found on the anterior wing margin (Fig. 1H) (Skeath and Carroll, 1991). Wild-type R72 discs had normal Ac expression along the anterior margin (Fig. 1I), with occasional ectopic Ac^+ cells in the posterior compartment (Fig. 2E). *tara*^{1}/+ R72 discs had a high frequency of many Ac^+ cells in the posterior compartment (Fig. 1J). Additional anterior genes include the co-receptor of the Hedghog (Hh) pathway, *patched* (*ptc*), which is highly expressed adjacent to the anterior-posterior (AP) boundary (Fig. 1K) (Phillips et al., 1990), and *cubitus interruptus* (*ci*), which is expressed in the entire anterior compartment (Fig. 1I) (Eaton and Kornberg, 1990). Most wild-type regenerated wing discs had normal expression patterns of Ptc and Ci (Fig. 1L), with only a subset (27.3%; n=33) having small spots of weak ectopic Ptc expression in the posterior compartment (Fig. 2F). No detectable ectopic Ci was observed. Strikingly, 87.2% (n=39) of the regenerated *tara*^{1}/+ wing discs examined had large areas of strong ectopic Ptc expression in the posterior compartment of the regenerated wing pouch (Fig. 1M). Ci was expressed at low levels anterior to and co-localizing with the ectopic Ptc. This ectopic Ptc was not detected before R60 (Fig. 2G-J), indicating that these fate transformations occurred late in the process of regeneration.

taranis is upregulated during regeneration

Next we examined *tara* expression using the *lacZ* enhancer trap $tara^{03881}$ (Manansala et al., 2013). β-Gal expression was ubiquitous at low levels in undamaged wing discs, was slightly elevated within the regenerating tissue at R24, and elevated at R48 (Fig. 3A-C). This result was confirmed using the *P[lacW]* enhancer trap $tara^{1}$/+ in ablated discs (data not shown), as well as the $tara^{03881}$ enhancer trap in manually wounded discs (Fig. 4).

taranis is required for posterior cell fate only during regeneration

To determine whether Tara is required for posterior wing fate during normal development, we generated homozygous clones of the null allele $tara^{1}$ within the developing wing disc. We did not find any ectopic expression of Ptc in the $tara^{1}$ clones located in the posterior compartment (Fig. 3D, n=30 clones). Expression of the posterior selector gene *engrailed* (*en*) was also not altered within or around these clones (Fig. 3E, n=25 clones). Furthermore, we did not observe any $tara^{1}$ clones crossing the AP boundary, and no P-to-A transformations were observed in adult wings that contained $tara^{1}$ mutant clones (data not shown). Therefore, Tara is not required for posterior wing fate during unperturbed development.

taranis maintains proper *engrailed* expression during regeneration

The transcription factor Engrailed is the posterior selector gene in the wing imaginal disc (Fig. 5A) (Kornberg et al., 1985). During regeneration, En expression was maintained in the posterior compartment (Figs. 5B, 6A-E) (Smith-Bolton et al., 2009). By contrast, in *tara*^{1}/+ R72 discs, domains with elevated En expression and domains lacking En expression were found in the posterior compartment (Fig. 5C). These domains appeared at R60 (Fig. 6F-J), which is when the ectopic Ptc and Ci expression appeared (Fig. 2O). Interestingly, overexpression of En in the posterior compartment of the developing wing causes robust and irreversible silencing of the *en* locus in patches of cells, as well as P-to-A fate transformations visible in the adult wing (Garaulet et al., 2008; Guillen et al., 1995). To determine whether the *tara/*+ regeneration phenotype was similarly caused by transiently elevated En levels, we reduced the levels of En by generating animals heterozygous for both *tara*^{1} and the *en*^{54} loss-of-function allele (Gustavson et al., 1996). Indeed, *en*^{54}/+ robustly suppressed the *tara*^{1}/+ cell fate transformation and *en* silencing phenotypes (Fig. 5D-G), likely by preventing elevation of En expression high enough to induce silencing. These data suggest that Tara may function to stabilize En levels during regeneration. To determine whether the loss of En expression and presence of Ptc and Ci expression in the P compartment truly represented changes in cell fate, we immunostained for phospho-Mad, which is normally found in a bidirectional gradient that has two peaks along the AP boundary (Tanimoto et al., 2000) (Fig. 6K-M). Indeed, we observed ectopic AP boundaries as marked by ectopic

phospho-Mad gradients where Ptc expression was observed (Fig. 6K-L) and where En^+ and En^- patches of cells were juxtaposed (Fig. 6M-N).

These zones of En^- and Ptc^+ and Ci^+ cells in the posterior compartment were not likely due to movement of anterior cells into the posterior compartment for several reasons. First, they were not observed at earlier time points when the regenerating tissue was rapidly growing (Fig. 2M-N). Second, they were not preferentially located at the AP boundary or contiguous with the anterior compartment (Fig. 1M, 2O-P). While clonally related cells that are not along the AP boundary can become separated by intercalating proliferating cells (Umetsu et al., 2014), such an explanation would require seeing the Ptc^+ and Ci^+ cells in the posterior compartment earlier in regeneration and closer to the boundary. Third, when cells from the anterior compartment do cross into the posterior compartment after tissue damage, they are converted to posterior fate (Herrera and Morata, 2014). However, the cells expressing anterior markers in the posterior compartments of the *tara*^{1}/+ regenerated wing discs are not converted to posterior fate, and thus produce the anterior structures observed in the posterior of the adult wings (Fig. 1E). Finally, lineage-tracing experiments using a reporter for *en*, *en-lacZ*, in which the β-gal perdures for some time, demonstrated that the Ptc expression occurred in cells that had once expressed En (Fig. 6O-P). Thus, Tara must be required for maintenance of posterior cell fate after tissue damage.

polyhomeotic is required for the silencing of *engrailed*

The Polycomb Group (PcG) gene *polyhomeotic* (*ph*), a component of the Polycomb repressor complex 1 (PRC1), is activated by En and can repress *en* expression during normal wing development (Maschat et al., 1998; Randsholt et al., 2000). Because the *en* silencing likely involves chromatin modifications via Polycomb Group genes, and *ph* regulates *en* in other contexts, we speculated that *ph* might be required for the *en* silencing in the regenerating discs. Indeed, reducing *ph* levels via one copy of the ph^{504} loss-of-function allele (Dura et al., 1987) suppressed the $tara^{1}$/+ cell fate transformation and *en* silencing phenotypes (Fig. 5H-I). Quantification of En levels within the ph^{504}/+; $tara^{1}$/+ discs at R72 revealed that En expression remained high relative to $tara^{1}$/+ R72 discs, with little to no silencing (Fig. 5K). Therefore *ph* is required for *en* silencing in regenerating $tara^{1}$/+ wing discs.

JNK signaling induces cell fate changes in regenerating tissue

These results indicate that a regeneration-specific mechanism exists for regulating posterior cell fate in which *tara* maintains proper expression of *en*. However, it was unclear why imaginal discs required Tara to prevent cell fate changes during regeneration. Intriguingly, in wild-type regenerating wing discs, a basal level of isolated P-to-A transformations did occur (Figs. 1F-G, 2A-B, 5E, I). Reducing En levels suppressed these transformations (Fig. 5D-G). Interestingly, similar mislocalized socketed bristles have been reported in wing discs that were

physically damaged *in situ* (Szabad et al., 1979) and may account for the "adventitious bristles" observed after fragmentation and *in vivo* culture of wing discs (Bryant, 1975). Because this phenomenon was observed after three methods of inducing tissue damage, we hypothesized that the endogenous wound response can influence posterior cell fate.

The conserved JNK signaling pathway, which is required for wound closure and blastema formation in wing discs (Bergantiños et al., 2010; Bosch et al., 2005, 2008), is important for regeneration in other species such as planaria, zebrafish and mouse (Almuedo-Castillo et al., 2014; Gauron et al., 2013; Wuestefeld et al., 2013). Interestingly, JNK signaling can activate *en* expression during dorsal closure (Gettings et al., 2010), and in anterior cells that cross the AP boundary (Herrera and Morata, 2014). Therefore, JNK signaling might misregulate *en* expression during regenerative growth. We tested this hypothesis by increasing JNK signaling during regeneration via reduction of *puckered* (*puc*), the phosphatase that negatively regulates JNK (Martín-Blanco et al., 1998). Indeed, puc^{E69}/+ regenerated wings had a significant increase in *en* silencing and P-to-A transformations (Fig.7A-C, Fig. 8A-B, G). Reducing the levels of En in the puc^{E69}/+ background resulted in suppression of the transformation phenotype (Fig. 7D-E, Fig. 8C, G), suggesting En was required for the JNK–induced cell fate changes. We also increased JNK signaling by transiently expressing constitutively activated *hemipterous* (JNKK) (*UAS-*hep^{Act}) (Weber et al., 2000) in the *rn*-expressing cells that survived ablation. This second method of increasing

JNK signaling also caused expression of A markers in the P compartment, loss of En, and P to A transformations in the adult wings (Fig. 8E-H). These results are consistent with our hypothesis that the P-to-A transformations are caused by JNK-induced En misregulation and autoregulatory silencing. To support our hypothesis that JNK signaling induces *en* expression, we expressed the activated *hemipterous* in the entire wing pouch of undamaged discs, together with a miRNA targeting *rpr, hid,* and *grim* (Siegrist et al., 2010) to minimize the apoptosis normally induced by prolonged JNK activation. Strikingly, *en* was mis-expressed throughout the A compartment in the pouch, confirming that JNK signaling can induce *en* expression (Fig. 8I).

Taranis does not regulate JNK signaling

Next we sought to clarify the regulatory hierarchy among JNK signaling, *taranis,* and *engrailed*. To determine whether Tara can suppress the fate transformations induced by JNK signaling, we transiently overexpressed Tara in the puc^{E69}/+ background in the *rn*-expressing cells that remained after ablation. This limited Tara overexpression suppressed the puc^{E69}/+ transformation phenotype (Fig. 7F-G, Fig. 8D, G). Tara may suppress this transformation phenotype by negatively regulating JNK signaling, or by acting downstream of the JNK pathway by preventing the JNK-induced *en* misregulation that leads to cell fate changes. To determine whether Tara controls En expression indirectly by negatively regulating JNK signaling, we examined the puc^{E69} enhancer trap, a commonly

used transcriptional reporter of JNK signaling activity. This reporter was not significantly affected by the Tara overexpression that rescued the transformation phenotype (Fig. 7H-J). Furthermore, *puc* transcript levels in regenerating wild-type and $tara^{1}$/+ wing discs were not significantly different (Fig. 7K). We also examined expression of a second JNK target gene, *mmp1* (Uhlirova and Bohmann, 2006). Mmp1 levels were elevated in the puc^{E69}/+ regenerating tissue and were not reduced in the *UAS-tara/+;* puc^{E69}/+ regenerating tissue (Fig. 8J-M), confirming that Tara did not act by reducing JNK activity. To determine whether JNK signaling induced *tara* expression, we examined *tara* transcript levels in wild-type and puc^{E69}/+ wing discs during regeneration. We did not observe a significant difference in the levels of *tara* mRNA (Fig. 7L). Together these data indicate that Tara and JNK signaling do not regulate each other during regeneration, which suggests that Tara prevents cell fate changes downstream of JNK signaling, possibly by stabilizing *en* expression directly, thereby preventing the *ph*-mediated autoregulatory silencing (Fig. 7M).

Discussion

Here we have shown that the endogenous wound response, orchestrated in part by JNK signaling, can induce inappropriate cell-fate changes in regenerating tissue through misregulation of *en*. While this finding was unexpected, it is not surprising that such strong signaling at the wound and in regenerating tissue, which can include ROS and Ca^{2+} release, as well as JNK, FGF, EGF, and WNT

signals (Sun and Irvine, 2014; Vriz et al., 2014) could affect the regenerating tissue in many deleterious ways. Indeed, the presence of this signaling is a primary difference between regenerating tissue and developing tissue, and may account for many of the ways in which regeneration is distinct from development.

We have also identified Taranis as a regeneration factor that protects regenerating tissue from the adverse side effects of JNK signaling. The molecular function of Tara is not known, although genetic interactions with E2F/Dp (Manansala et al., 2013), and with Polycomb Group and Trithorax Group genes (Calgaro et al., 2002; Fauvarque et al., 2001) have been reported. Vertebrate TRIP-Br proteins can bind to and regulate transcription through E2F/Dp and can interact with the CREB-binding protein to activate p53 (Hayashi et al., 2006; Hsu, 2001; Watanabe-Fukunaga et al., 2005). Given these reports, Tara may act by regulating transcription factors directly or by recruiting chromatin modifiers to influence transcription by altering the chromatin landscape. While we have shown that Tara does not regulate *en* expression indirectly through modifying JNK signaling, Tara may regulate *en* directly or indirectly through a different intermediary. In addition, the upstream signals that activate *tara* expression during regeneration are unknown. Clarifying the function of the Tara protein will be important to understanding how cells protect their identity from perturbation by the signaling that orchestrates the wound response and regeneration.

While the regulation of *en* and preservation of P identity could be specific to *Drosophila* wing disc regeneration, it is possible that Tara and vertebrate TRIP-Br proteins regulate expression of relevant genes at other wound sites. Indeed, Tara is also upregulated after pathogen-induced damage in the adult *Drosophila* gut (Chakrabarti et al., 2012). Furthermore, transcriptional profiling of regenerating tissue in *Xenopus tropicalis* tadpole tail reveal the presence, and in , zebrafish spinal cord, and the axolotl limb upregulation, of TRIP-Br family members in regenerating tissue (Hui et al., 2014b; Love et al., 2011; Voss et al., 2015).

It is unlikely that Tara is the only protective factor required for regeneration. Future studies in experimental regeneration systems such as *Drosophila* will likely identify additional genes required for patterning and cell fate after regeneration. Current efforts to engineer regeneration for medical purposes often seek to replicate development (Tonnarelli et al., 2014). However, it is now clear that they must account for the unwanted side effects of regenerative signaling, whether endogenous to the wound or applied as therapy, and seek to deploy such protective factors to aid in regeneration.

Materials and Methods

Ablation and regeneration experiments

Ablation experiments were carried out as previously described (Smith-Bolton et al., 2009) with a few modifications: induction of cell death was caused by

overexpressing *rpr*, and animals were raised at 18^{o}C until 7 days after egg lay (AEL) (early 3rd instar) before the temperature was shifted to 30^{o}C for 24 hours in a circulating water bath. To identify, and select for mutants residing on the X chromosome, the *FM7i, act-GFP* balancer was selected against during the picking of 1st instar larvae on grape juice agar plates. Before fixation of 3rd instar larvae for staining, a second selection against GFP^{+} larvae was conducted to ensure all discs that were stained were the correct genotype. For undamaged controls, animals with the same genotype as the experimental animals were kept at 18^{o}C and dissected at 9-10 days AEL, which is mid-late 3rd instar. Mock ablated animals are the siblings of the flies in the ablation experiments that experienced the same thermal conditions, but they inherited the *TM6B, tubGAL80* containing chromosome instead of the ablation chromosome. For adult wings, control undamaged animals were kept at 18^{o}C until after eclosion.

Mitotic clone induction and overexpression during normal development

For clonal analysis of *tara^{1}* during normal development, animals with the genotype *y^{1}, w^{1118}, hsFLP; FRT82B, ubi-GFP/FRT82B, tara^{1}* were shifted to 37.5^{o}C for 30 min at 2 days after egg lay, then transferred to 25^{o}C. They were dissected 5-6 dAEL which is at the wandering 3rd instar stage. To overexpress activated *hep* during normal development, animals with the genotype *UAS-hep^{Act}/UAS-RHG miRNA; rnGAL4 UAS-EYFP/+* were incubated at 25^{o}C. Wing discs were dissected in the third larval instar for analysis.

Manual wounding of discs

Early to mid-3rd instar larvae of the genotype *rnGAL4, UAS-EYFP/tara*^{03881} were chilled on ice for 20 minutes. One disc was pinched using forceps without disrupting the larval cuticle, leaving the second disc intact as a contralateral control. Larvae were then transferred to fresh food and incubated at 25°C for 30 hours before dissecting, fixing and staining.

Fly Stocks

The following Drosophila stocks were used: *w*^{1118}*; rnGAL4, UAS-rpr, tubGAL80*^{ts}*/TM6B, tubGAL80* (Smith-Bolton et al., 2009), *w*^{1118} (Hazelrigg et al., 1984) (Referred to as “Wild-type” in Chapter 1), *Df(3R)ED10639* (Ryder et al., 2007), *tara*^{1} (Fauvarque et al., 2001), *tara*^{03881} (Gutiérrez et al., 2003), *tara*^{YD0165} and *tara*^{YB0035} (Buszczak et al., 2007) (obtained from the Flytrap Project via Lynn Cooley), *en*^{54}(Nüsslein-Volhard and Wieschaus, 1980), *ph-d*^{504} *ph-p*^{504} (called *ph*^{504} in the text) (Dura et al., 1987), *puc*^{E69} (Martín-Blanco et al., 1998), and *UAS-myc::tara* (called *UAS-tara* in the text) (Manansala et al., 2013) (a gift from Michael Cleary), *UAS-hep*^{Act} (Weber et al., 2000), *UAS-RHG miRNA* (Siegrist et al., 2010) (a gift from Sarah Siegrist), *rnGAL4, UAS-EYFP/TM6B* (Smith-Bolton et al., 2009), *rnGAL4, GAL80*^{ts} (Smith-Bolton et al., 2009) *en-lacZ* (Hama et al., 1990), and *y*^{1} *w*^{1118} *hsFLP; FRT82B, ubi-GFP*. All fly stocks are available from The Bloomington Drosophila Genetic Stock Center unless stated otherwise.

Adult wings

Wings were mounted on glass slides in Gary's Magic Mount (Canada balsam (Sigma) dissolved in methyl salicylate (Sigma)). Images of individual wings were taken with an Olympus SZX10 dissection microscope with an Olympus DP21 camera using the CellSens Dimension software (Olympus). All images were taken at the same magnification (5X).

To quantify the P-to-A transformation phenotype in adult wings, all wings that reached to or past the tip of abdomen were considered fully regenerated and selected for quantification. The wings were scored for five anterior markers within the posterior compartment. These five markers included socketed bristles on the posterior margin, ectopic vein material on the posterior margin, an ectopic anterior crossvein (ACV) in the posterior wing blade, distal costa-like bristles on the alar lobe, and an anterior-like shape characterized by a narrower proximal and wider distal posterior compartment. The frequency of each marker was calculated independently for each genotype. In addition, these wings were scored on a scale of 0-5 markers to assess the strength of the P-to-A transformation in each wing. For all experiments, at least 3 replicates from independent egg lays were performed. Statistics were calculated and graphs were produced in Microsoft Excel. To calculate the Average Transformation Score, the final scores of each wing was averaged in each replicate. These averages were averaged to each replicate to get the scores listed on the graph.

This allowed us to calculate SEM and perform a Student's t-test to assess statistical significance compared to Wild-type.

Immunohistochemistry

Dissections, fixing and staining were done as previously described (Smith-Bolton et al., 2009). Wing imaginal discs were mounted in Vectashield (Vector Labs). Antibodies used were mouse anti-Ptc (1:50) (Capdevila et al., 1994) (DSHB), rat anti-Ci (1:10) (Motzny and Holmgren, 1995) (DSHB), mouse anti-Ac (1:10) (Skeath and Carroll, 1991) (DSHB), mouse anti-En/Inv (1:3) (Patel et al., 1989) (DSHB), mouse anti-Nub (1:100 or 1:200) was a gift from Steve Cohen (Averof and Cohen, 1997), mouse anti-βgal (1:100) (DSHB), and rabbit anti-βgal (1:500 or 1:1000)(MP Biomedicals), mouse anti-Mmp1 (1:10 dilution of 1:1:1 mixture of monoclonal antibodies 3B8D12, 3A6B4, and 5H7B11) (Page-McCaw et al., 2003) (DSHB), rabbit anti-pMad (1:500)(Cell Signaling), rabbit anti-cleaved Dcp-1 (Cell Signaling). The Developmental Studies Hybridoma Bank (DSHB) was created by the NICHD of the NIH and is maintained at the University of Iowa, Department of Biology, Iowa City, IA 52242.

AlexaFluor secondary antibodies (Molecular Probes) were used at 1:1000. TO-PRO-3 iodide (Molecular Probes) was used as a DNA counterstain at 1:500. Specimens were imaged with either an LSM510 or LSM700 Confocal Microscope (Carl Zeiss). Images were compiled using ZEN Black software (Carl Zeiss),

Photoshop (Adobe) or ImageJ (U.S. National Institutes of Health). All confocal images are maximum intensity projections from z-stacks unless otherwise stated.

Average fluorescence intensity was measured in ImageJ using images that were stained in parallel and imaged under identical confocal settings. En fluorescence intensity quantification on projected z-stack images was restricted to the regenerated wing primordium, as defined by the characteristic folding of the pouch. Fluorescence intensity of the rabbit anti-βgal staining of puc^{E69}/+ discs on projected z-stack images was measured within the regenerating wing primordium as defined by Nubbin immunostaining. To quantify Mmp1 fluorescence intensity, a single confocal slice within the disc proper was used. The area of *en* silencing was measured in the P compartment of the wing pouch in projected z-stacks using ImageJ. Regions of the disc lacking En immunostaining but containing cells as determined by TO-PRO-3 staining were selected and area was determined using the “measure” function. For quantifying mouse anti-βgal staining in $tara^{03881}$/+ discs, the morphology of the wing pouch and the upregulated area of *tara-lacZ* was sufficient to draw a circle in ImageJ and quantify fluorescence intensity of the blastema. The Student’s t-test was performed to assess significance.

Quantitative Real-time PCR

qPCR was performed as described previously (Classen et al., 2009). ~20 wing discs were used per sample. Three to six biological replicates were analyzed per genotype and time point. The reference control was *gapdh2*, whose expression levels appear unchanged via qPCR after tissue damage (data not shown). Primers used were as follows: *GAPDH2* (Forward: 5'-GTGAAGCTGATCTCTTGGTACGAC-3'; Reverse: 5'-CCGCGCCCTAATCTTTAACTTTTAC-3'), and *puc* (Forward: 5'-GTCCTAGCAATCCTTCGTCATC-3'; Reverse: 5'-ATCATCGTAATCAAACCCATCC-3'). Primers for *tara-a/β* (Forward: 5'-GCCAGTTGCACCTACCGCAA-3'; Reverse: 5'-GCCGATTGCGAACTGAGGCT-3') were originally reported in (Fukunaga et al., 2012). Significance was assessed by the Student's t-test. Error bars are Standard Error of the Mean (SEM).

Figures

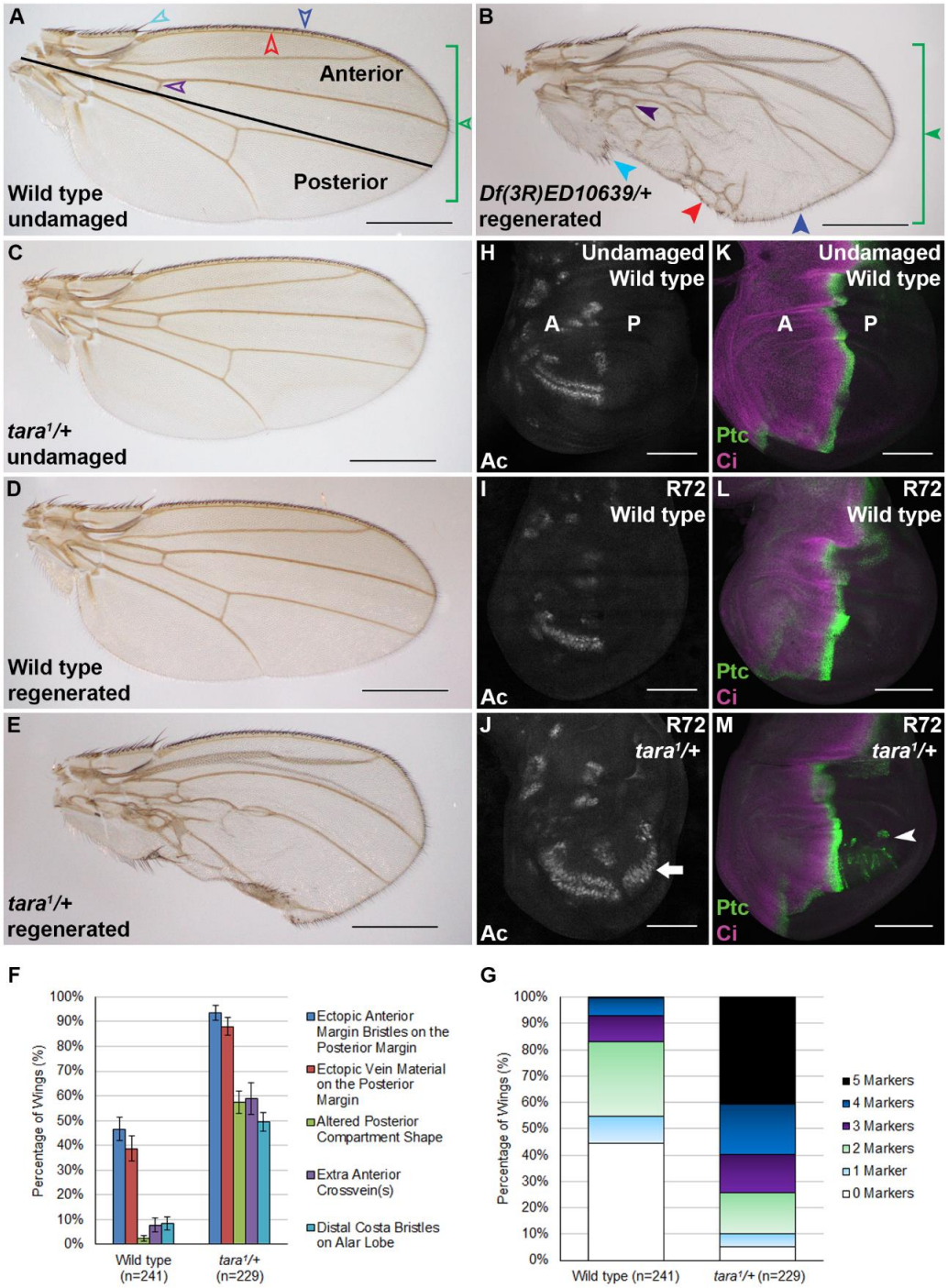

Figure 1. P-to-A transformations after regeneration in *tara*^{1}/+ wings. A) Undamaged wild-type wing. Open arrowheads show distal costa bristles (cyan), anterior crossvein (ACV) (violet), longitudinal vein L1 along the anterior margin (red), socketed sensory bristles along the anterior

Fig. 1 (con't)

margin (blue), and the tapered shape of the wing with the proximal wing blade wider than the distal wing blade (green). B) *Df(3R)ED10639/+* regenerated wing with all 5 ectopic anterior markers in the posterior compartment. Arrowheads colors correspond to the same features as in A and F. C) Undamaged *tara*^{1}/+ wing. D) Wild-type regenerated wing. E) *tara*^{1}/+ regenerated wing with all 5 ectopic anterior features in the posterior compartment . F) Quantifications of the frequency of each ectopic anterior marker in wild-type and *tara*^{1}/+ regenerated wings. Error bars: SEM. $p<0.01$ for all markers between the two genotypes. G) Quantification of the strength of P-to-A transformation, by counting the number of different ectopic anterior markers in each wing. H) Undamaged wild-type wing disc stained for Ac. Anterior (A) is left, and posterior (P) is right in all imaginal disc images. I) Wild-type regenerating wing disc at R72 stained for Ac. J) *tara*^{1}/+ regenerating wing disc at R72 stained for Ac. Arrow: Ac-expressing cells in the posterior compartment. K-L) Wing discs stained for Ptc (green) and Ci (magenta). K) Undamaged wild-type wing disc L) Wild-type regenerating wing disc at R72. M) *tara*^{1}/+ regenerating wing disc at R72 with ectopic Ptc (arrowhead) and Ci-expressing cells within the posterior compartment. Scale bars: 500 µm for adult wings,100 µm for discs.

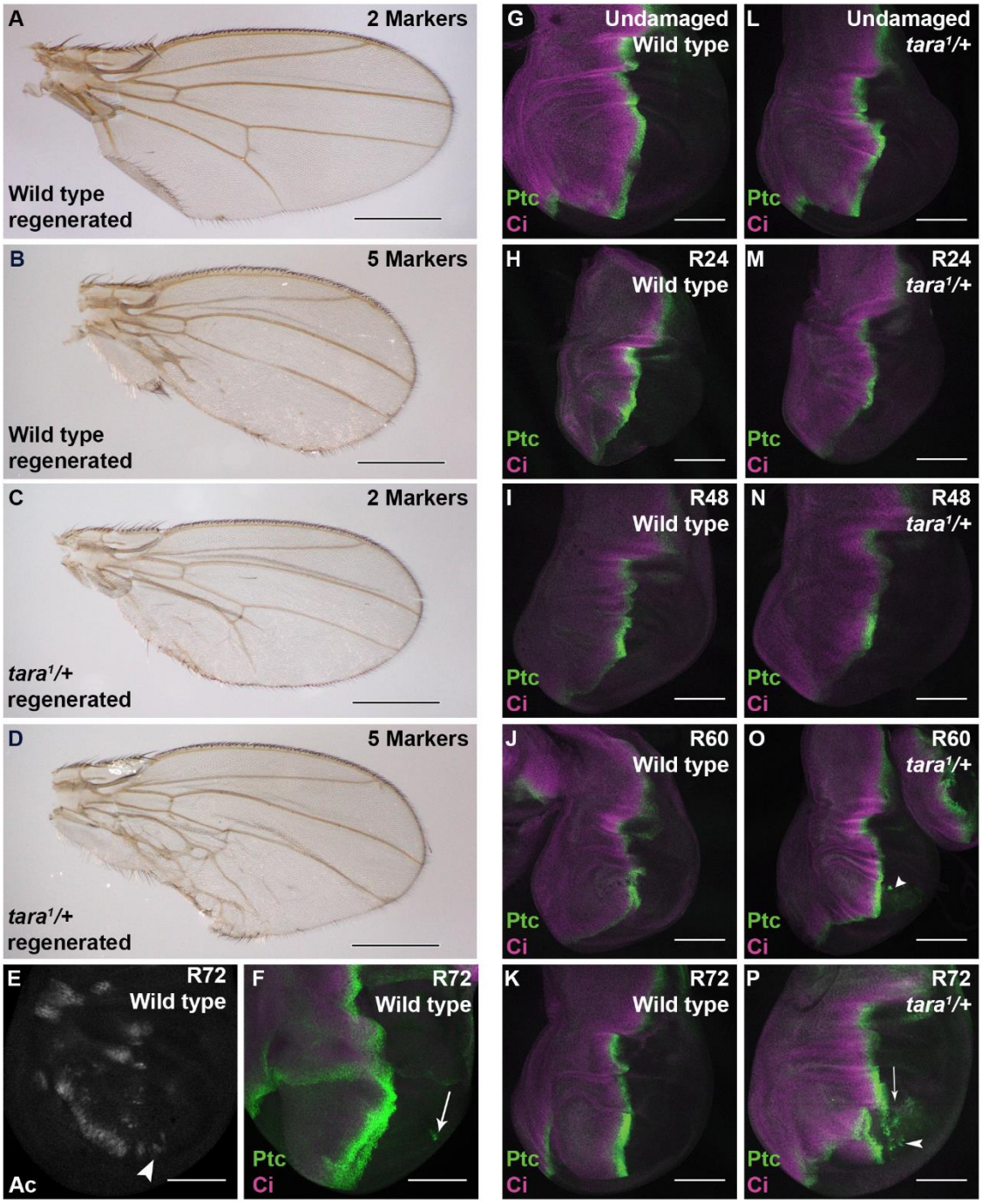

Figure 2. P-to-A transformations in wild-type and *tara*^{1}/+ wings. A) Example of wild-type regenerated adult wing that displayed 2 markers of anterior fate (socketed bristles and veins on the posterior margin). These wings were 28.2%-32.4% of each wild-type population analyzed. B) Example of wild-type regenerated adult wing that displayed all 5 markers of anterior fate in the

Fig. 2 (con't)

posterior compartment. These wings were 0.42%-1.75% of each wild-type population analyzed. C) Example of *tara*^{1}/+ regenerated adult wing that displayed 2 markers of anterior fate (socketed bristles and veins on the posterior margin). These wings were 4.5%-15.7% of each *tara*^{1}/+ population analyzed. D) Example of *tara*^{1}/+ regenerated adult wing that displayed all 5 markers of anterior fate in the posterior compartment. These wings were 40.6%-58.2% of each *tara*^{1}/+ population analyzed. E) Example of wild-type regenerating disc at R72 stained for Ac. Note the small cluster of ectopic Ac^{+} cells in the P compartment (arrowhead). F) Example of wild-type regenerating disc at R72 stained for Ptc (green) and Ci (magenta). Note the single cell of Ptc expression in the P compartment (arrow). G) Undamaged 3rd instar wing disc stained for Ptc (green) and Ci (magenta). H-K) Wild-type regenerating wing discs stained for Ptc and Ci at R24 (H), R48 (I), R60 (J), and R72 (K). L) *tara*^{1}/+ undamaged 3rd instar wing disc stained for Ptc and Ci. M-P) *tara*^{1}/+ regenerating wing discs stained for Ptc and Ci at R24 (M), R48 (N), R60 (O), and R72 (P). Ectopic Ptc expression (arrowhead) becomes detectable by R60 (O). Low levels of Ci (arrow) become apparent either with or near the ectopic Ptc (arrowhead) (P). Scale Bar: 500µm for adult wings, 100µm for discs.

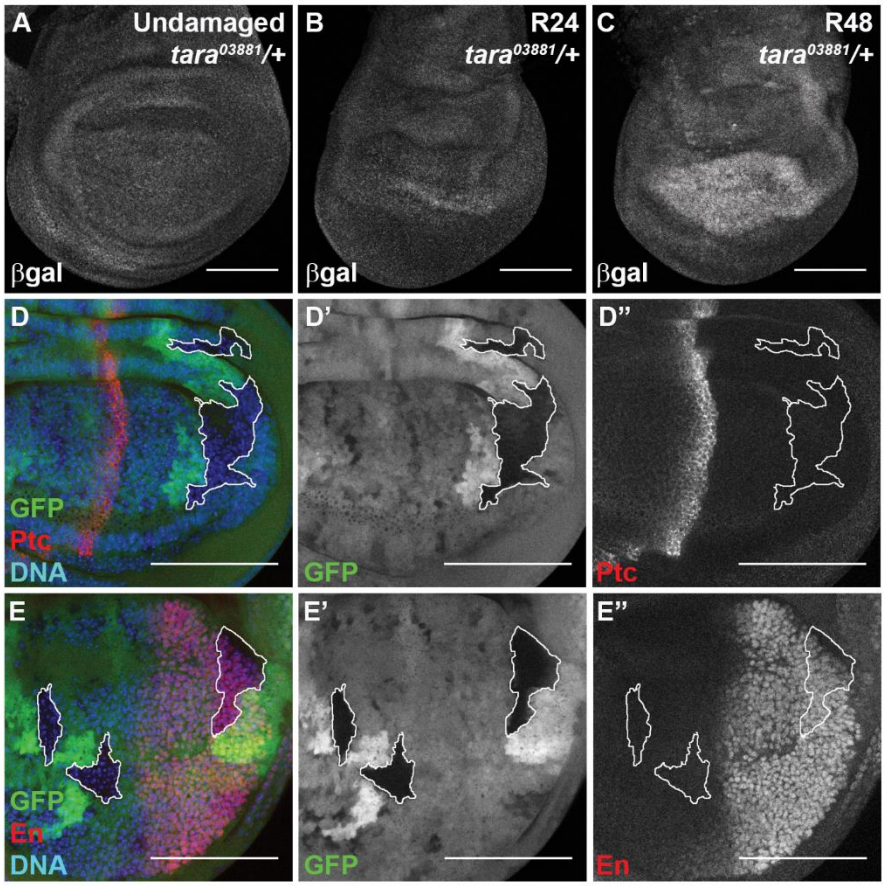

Figure 3. *taranis* regulates posterior cell fate only during regeneration. A-C) *tara*^{03881}/+ wing discs stained for β-Gal. A) Undamaged 3rd instar. B) R24. C) R48. D) Homozygous *tara*^{1} clones (GFP-) in a *tara*^{1}/+ background (GFP+) stained for Ptc (red) and DNA (blue). D') GFP only. D'') Ptc expression with clones outlined. E) *tara*^{1} clones (GFP-) stained for En (red) and DNA (blue). E') GFP only. E'') En expression with clones outlined. Scale bar: 100μm.

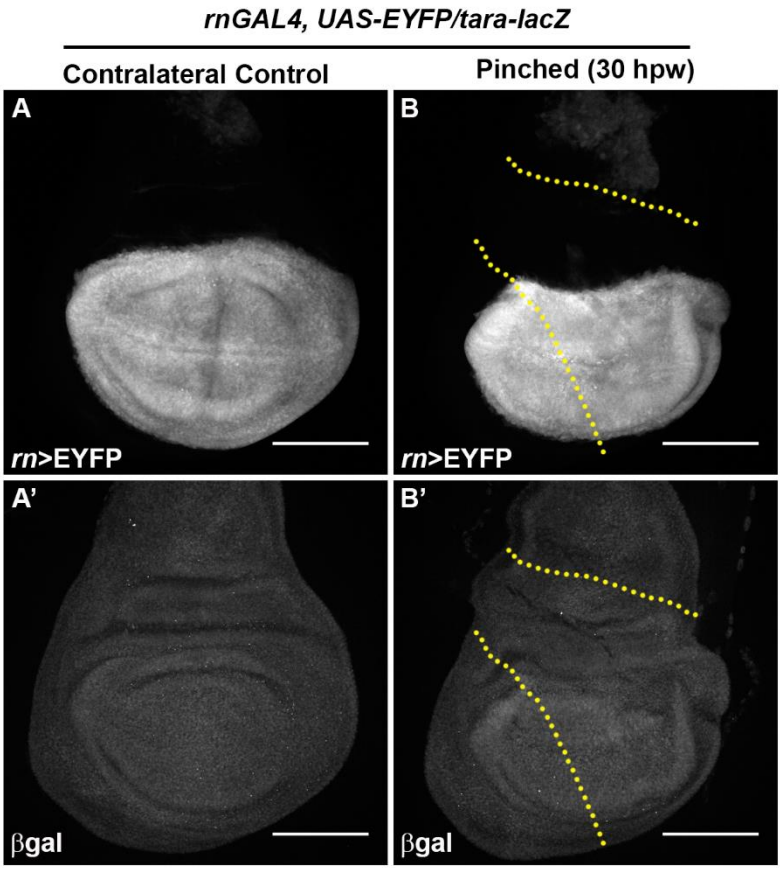

Figure 4. Manual wounding induces increased *tara-lacZ* expression. Disc pinched through the larval cuticle and its contralateral undamaged control allowed to recover for 30 hours. A, B) rn-GAL4, UAS-EYFP used to visualize wing pouch while pinching. A', B') βgal expression from *tara-lacZ* enhancer trap (*tara*^{03881}). A, A') undamaged contralateral control. B, B') Pinched disc 30 hours post wounding (hpw). Approximate path of the pinch is between dotted lines. Note increased expression of *tara-lacZ* throughout the wing pouch. Similar results were observed in 5 discs. Scale Bar: 100μm.

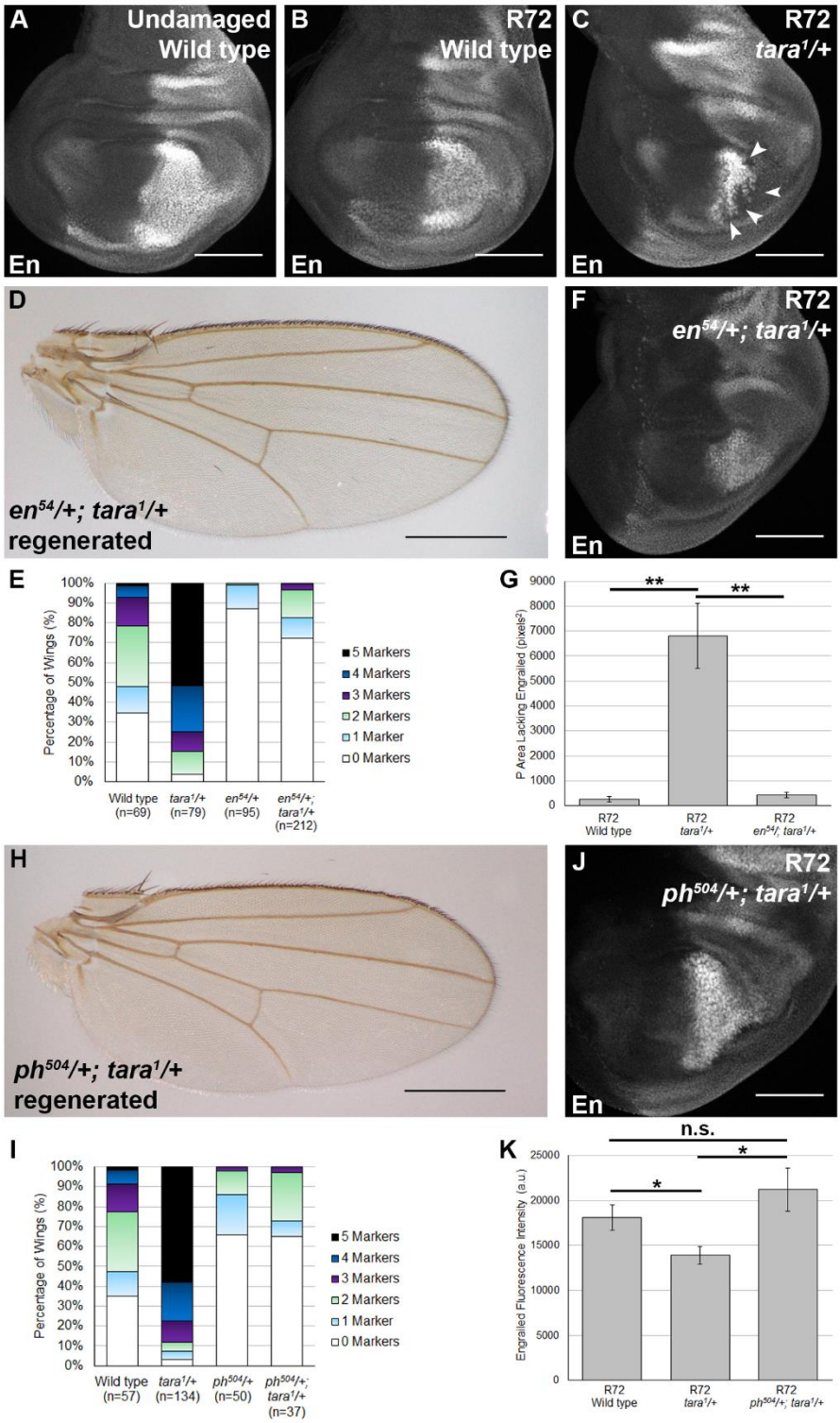

Figure 5. *taranis* regulates *engrailed* expression during regeneration. A-C) En immunostaining. A) Undamaged wild-type wing disc B) R72 wild-type wing disc C) R72 *tara*^{1}/+ wing disc. Arrowheads mark regions that have lost *en* expression. The pattern of *en* silencing

Fig. 5 (con't)

varied with each disc. D) *en^{54}/+; tara^{1}/+* regenerated wing. E) Quantification of extent of P-to-A transformation of regenerated wings that were wild type, *tara^{1}/+*, *en^{54}/+* and *en^{54}/+; tara^{1}/+*. F) En expression in *en^{54}/+; tara^{1}/+* R72 wing disc. F) Quantification of area that lacked En in the posterior wing pouches of wild-type (n= 10), *tara^{1}/+* (n=15), and *en^{54}/+; tara^{1}/+* (n=23) R72 wing discs. **p<0.01. H) *ph^{504}/+; tara^{1}/+* regenerated wing. I) Quantification of extent of P-to-A transformation of regenerated wings that were wild type, *tara^{1}/+*, *ph^{504}/+* and *ph^{504}/+; tara^{1}/+*. J) R72 *ph^{504}/+; tara^{1}/+* wing disc stained for En. K) Average fluorescence intensity of En staining within the posterior compartment of the regenerating pouch in R72 wild-type, *tara^{1}/+* and *ph^{504}/+; tara^{1}/+* wing discs. n=6 for each genotype. *p<0.05, n.s.: not significant. Scale bars: 100μm for discs, 500μm for adult wings.

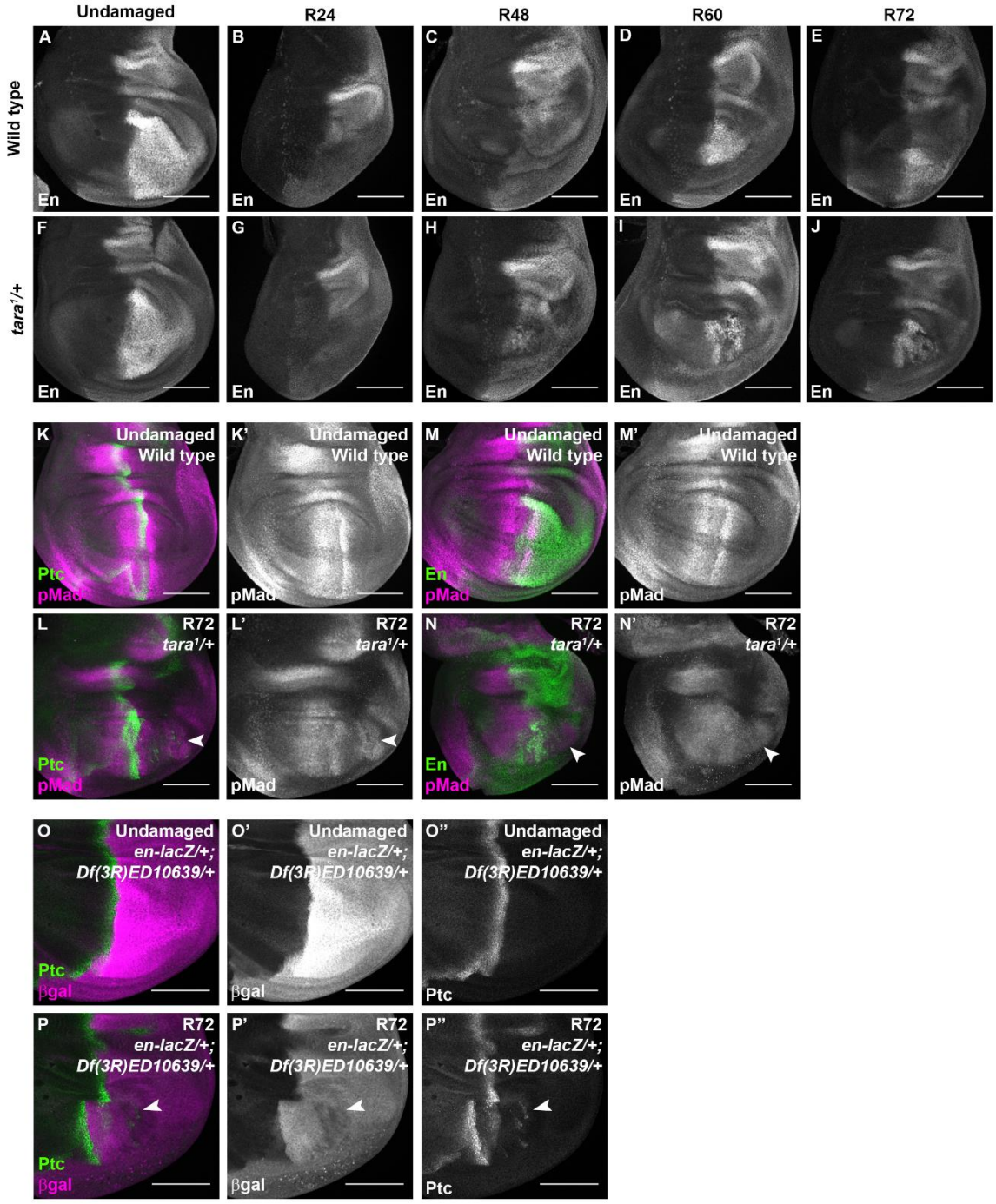

Figure 6. Engrailed expression dynamics during wing imaginal disc regeneration. A-J) En expression timecourse in wild-type and *tara*^{1}/+ wing discs. A) Undamaged 3rd instar wing disc immunostained for En. B-E) Wild-type regenerating wing discs immonustained for En at R24 (B), R48 (C), R60 (D), and R72 (E). F) *tara*^{1}/+ undamaged 3rd instar wing disc immunostained for En. G-J) *tara*^{1}/+ regenerating wing discs immunostained for En at R24 (G), R48 (H), R60 (I), and

Fig. 6 (con't)

R72 (J). Silencing was first observed at R60 (I). K-N) Immunostaining for phospo-Mad revealed new gradients at ectopic AP boundaries within the P compartment. K) Undamaged wild type disc showing Ptc (green) and pMad (magenta). K') pMad alone. L) R72 *tara*^{1}/+ disc showing Ptc (green) and pMad (magenta). Arrowhead marks ectopic AP boundary. L') pMad alone. M) Undamaged wild-type disc showing En (green) and pMad (magenta). M') pMad alone. N) R72 *tara*^{1}/+ disc showing En (green) and pMad (magenta). Arrowhead marks ectopic AP boundary. N') pMad alone. O-P) Lineage tracing using *en-lacZ* to mark P cells. The deficiency was used for these experiments because the *tara* alleles are themselves *lacZ* insertions. O) Undamaged *en-lacZ/+; Df(3R)ED10639/+* disc showing Ptc (green) and βgal (magenta). O') βgal alone. O'') Ptc alone. P) R72 *en-lacZ/+; Df(3R)ED10639/+* disc showing Ptc (green) and βgal (magenta). Arrowhead points to cells containing both Ptc and βgal. P') βgal alone. P'') Ptc alone. Scale Bars: 100μm.

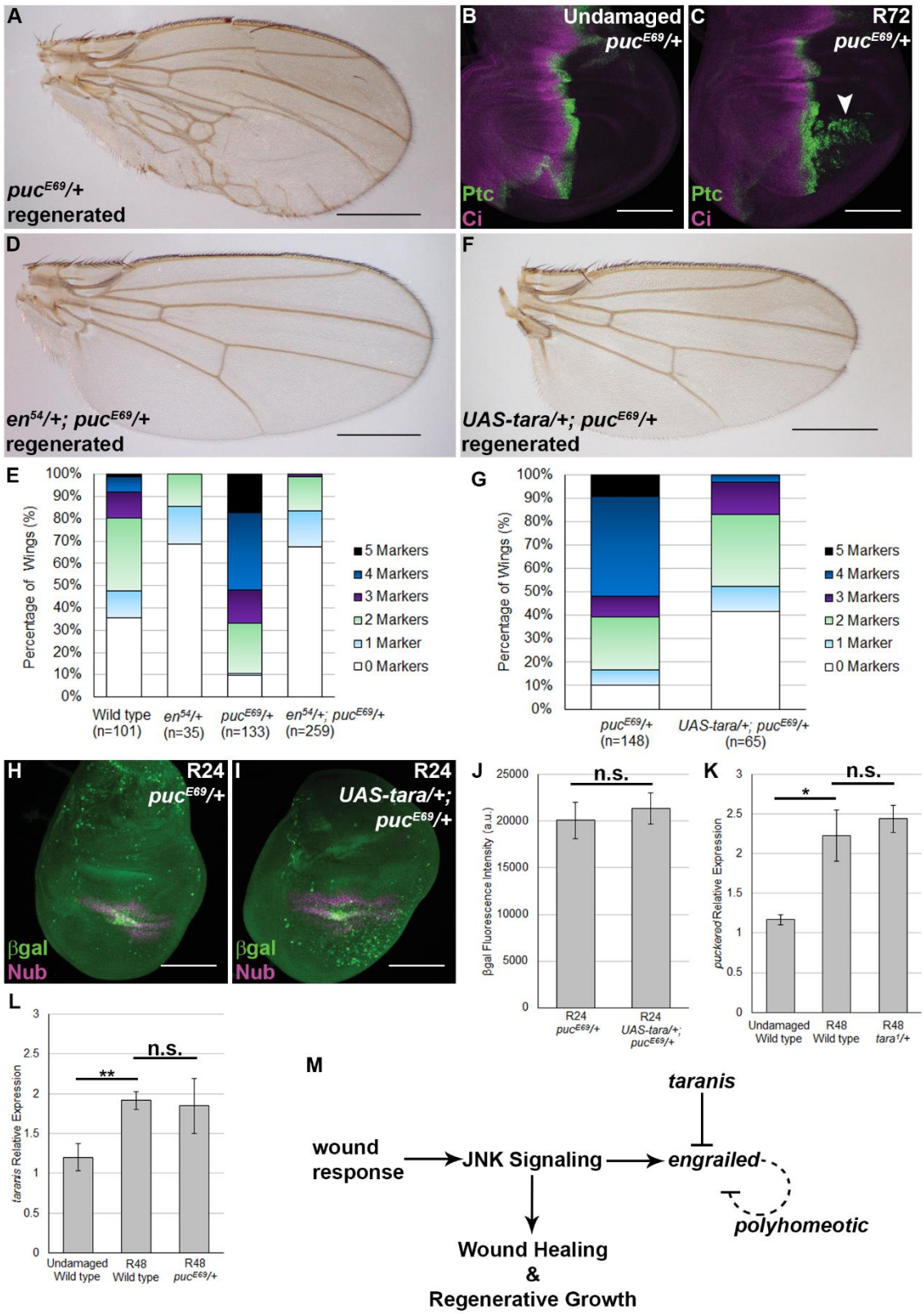

Figure 7. JNK signaling induces P-to-A fate transformations during regeneration.

Fig. 7 (con't)

A) *puc*^{E69}/+ regenerated wing. B) Undamaged *puc*^{E69}/+ wing disc stained for Ptc (green) and Ci (magenta). C) R72 *puc*^{E69}/+ wing disc stained for Ptc and Ci. Arrowhead: ectopic Ptc in the P compartment. D) *en*^{54}/+; *puc*^{E69}/+ regenerated wing. E) Quantification of extent of transformation of regenerated wings that were wild type, *en*^{54}/+, *puc*^{E69}/+, and *en*^{54}/+; *puc*^{E69}/+. F) *UAS-tara*/+; *puc*^{E69}/+ regenerated wing. G) Quantification of extent of transformation of regenerated wings that were *puc*^{E69}/+ and *UAS-tara*/+; *puc*^{E69}/+. H-I) R24 *puc-lacZ* wing discs stained for βgal (green), and the regenerating wing primordium (Nubbin, magenta). H) *puc*^{E69}/+. I) *UAS-tara*/+; *puc*^{E69}/+. J) Quantification of the βgal staining within the wing primordium, defined by Nubbin, in R24 *puc*^{E69}/+ (n=16) and R24 *UAS-tara*/+; *puc*^{E69}/+ (n=12) wing discs. p=0.637. K) qRT-PCR of *puc* transcript in undamaged wild-type, R48 wild-type, and R48 *tara*^{1}/+ wing discs. *p=0.03. L) qRT-PCR of *taranis* transcript in undamaged wild-type, R48 wild-type, and R48 *puc*^{E69}/+ wing discs. **p<0.01 M) Model describing Tara stabilizing *en* expression to protect the regenerating tissue from cell fate changes induced by JNK signaling. Scale bars: 100μm for discs, 500μm for adult wings.

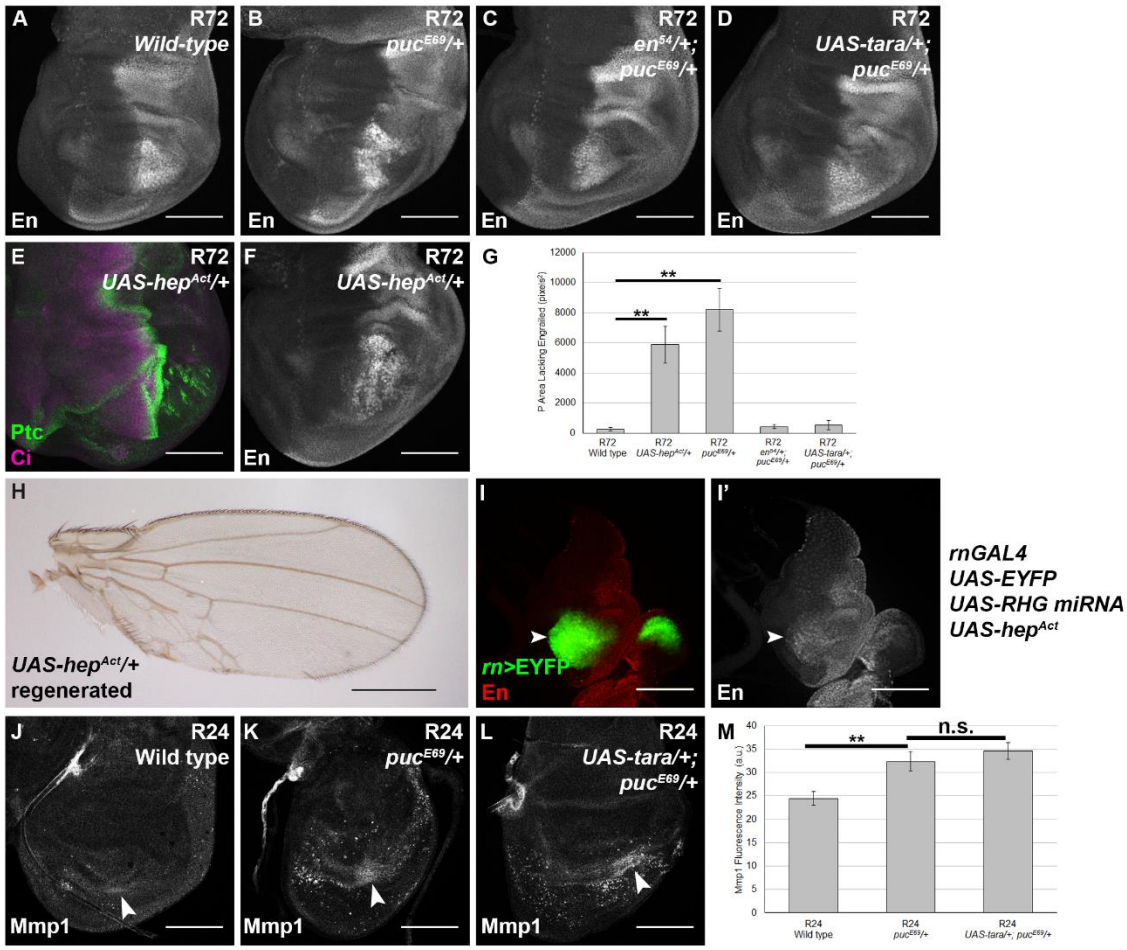

Figure 8. JNK signaling can mis-regulate *en* expression. A, B) Activation of JNK signaling by *puc*^{E69}/+ causes loss of En expression. A) En immunostaining in WT R72 disc. B) En in *puc*^{E69}/+ R72 disc showing loss of En. C) En in *en*^{54}/+; *puc*^{E69}/+ R72 disc showing reduced loss of En. D) En in *UAS-tara/+; puc*^{E69}/+ regenerated disc at R72 showing no loss of En. E-F) Fate transformations in regenerated discs that transiently expressed *UAS-hemipterous*^{CA} *(UAS-hep*^{Act}*)* via *rn-GAL4* in the cells that survived ablation. E) Ptc and Ci immunostaining, with extensive signal in the P compartment. F) En immunostaining, with loss of expression in P compartment. G) Quantification of area lacking En in the P compartment of the wing pouch in the genotypes in A-D and F. Wild type n=10 discs, *UAS-hep*^{Act}/+ n=15 discs, *pucE69*/+ n=11 discs, *en*^{54}/+; *puc*^{E69}/+ n=13 discs, *UAS-tara/+; puc*^{E69}/+ n=13 discs. **p<0.01 H) Adult wing from regenerated disc expressing *UAS-hep*^{Act}. Note the bristles and vein material along the posterior margin. I) Expression of EYFP, *hep*^{Act}, and *RHG miRNA* in an undamaged wing pouch via *rnGAL4*. EYFP

Fig. 8 (con't)

marks the expression domain (green in I). En is expressed throughout the pouch (I and I'). J-L) Anti-Mmp1 immunostaining (arrowheads) in wild-type (J), *puc*^{E69}/+ (K), and *UAS-tara/+; puc*^{E69}/+ (L) R24 discs. M) Quantification of Mmp1 immunostaining in the same genotypes. Wild type n=13 discs, *puc*^{E69}/+ n=17 discs, *UAS-tara/+; puc*^{E69}/+ n=16 discs. **p<0.01. Scale bars are 100μm, except in H where it is 500μm. Error bars are SEM.

Chapter 3: The Pioneer Transcription Factor Zelda is Essential for Patterning during Imaginal Disc Regeneration

Introduction

During epimorphic regeneration, such as is found in the salamander limb or zebrafish fin and heart, a dynamic interplay of cellular behaviors must be coordinated and faithfully executed in order to restore form and functionality to the damaged part. The molecular mechanisms and genes involved in regeneration is only beginning to be revealed. In particular, the regulation of cell fate and patterning is dynamic during regeneration. The first major change in cellular plasticity is the formation of a proliferative zone of progenitor cells that are derived from the surviving cells spared from injury that dedifferentiated and re-entered the cell cycle (Gupta et al., 2013; Knopf et al., 2011; Kragl et al., 2009; Lehoczky et al., 2011; Rinkevich et al., 2011; Sousa et al., 2011; Stewart and Stankunas, 2012). The blastema then grows out and restores the missing tissue mass. Importantly, the regeneration blastema needs to repattern in order to restore the proper number and types of cells in the right anatomical configuration in order to restore functionality to the regenerate. While progress has been made understanding the mechanisms of regrowth during regeneration in a wide variety of phyla (Khan et al., 2016a; Tanaka and Reddien, 2011), the mechanisms of dedifferentiation and repatterning have lagged behind and only a handful of studies have attempted to interrogate functional relationships between genes that could be involved. Part of the reason why progress on how the blastema is able

to pattern effectively has been due to the assumption that, trivially, embryonic patterning mechanisms are just simply re-initiated to repattern the blastema (Nacu and Tanaka, 2011). We recently identified hitherto unpredicted regeneration-specific patterning mechanism in the regenerating wing imaginal disc of *Drosophila* (Schuster and Smith-Bolton, 2015) that directly challenged that view and opened up the field for the search for regeneration-specific patterning factors (see a more in depth discussion in Chapter 2 of this thesis).

Pioneer transcription factors are a unique family of transcription factors that are able to open-up closed chromatin and recruit additional chromatin modifiers, remodelers, and transcription factors to induce large changes in developmental fate (Iwafuchi-Doi and Zaret, 2014, 2016). Indeed, many pioneer transcription factors are associated with cellular reprogramming. For example, three of the Yamanaka factors Oct4, Sox2, and Klf4 have all been shown to have some pioneering activity (Iwafuchi-Doi and Zaret, 2014). This association of pioneer transcription factors and reprogramming has led to hypotheses that they are important for adult stem cell biology and regeneration, particularly in the early phases of regeneration when terminally differentiated cells revert to a progenitor cell state as is the case for Ascl1a during retinal regeneration in zebrafish (Ramachandran et al., 2010) and Sox2 during regeneration of the axolotl spinal cord and murine epithelial stem cells (Arnold et al., 2011; Fei et al., 2014). Paradoxically, the principle pluripotency factor Oct4 has been shown to be

dispensable for homeostatic tissue regeneration in multiple tissues that have well-characterized adult stem cells in mice (Lengner et al., 2007).

In addition to regulating the various aspects of stem cell biology, a select group of pioneer transcription factors have also been shown for one of the most drastic early developmental transitions the embryo experiences: the maternal to zygotic transition (MZT). The MZT is when the maternally contributed mRNAs essential for very early development become depleted, and the embryo activates its zygotic genome so development can proceed under the control of embryo's own genome. Two pioneer factors in various species have been shown to be essential for the activation of the zygotic genome: Oct4/pou5f1 in zebrafish (Lee et al., 2013b; Leichsenring et al., 2013) and Zelda in *Drosophila* (Liang et al., 2008). These pioneer factors have perhaps the most drastic role in development, and seem to be among the few pioneer transcription factors that are not restricted to a single germ layer, such as FoxA or GATA3 during endoderm development (Cirillo et al., 2002). Therefore, these pioneer transcription factors have the potential to be involved in multiple developmental transitions. Despite this potential, neither Zelda nor Oct4/pou5f1 have not been shown to be essential for similar large developmental transitions. Most phenotypes looking at *zelda* or *pou5f1* loss of function in other contexts beyond the early embryo have been subtle at best (see below).

Despite Zelda being an essential factor for the MZT, its role in other tissues later in development or in the adult fly has not been extensively studied. It has been observation that Zelda is expressed in multiple tissues including the imaginal discs (Staudt et al., 2006), thus pointing to a potential role in other tissues. Zelda was first shown to be important for development of the embryonic nervous system with the help of a tissue-specific cofactor, Link (Pearson et al., 2012). There was also a report were a Zelda isoform was overexpressed within the wing disc, and these wings exhibited growth defects (Giannios and Tsitilou, 2013). However, the isoform expressed in this study is not normally found in the wing disc, and does not have its DNA binding domain (Hamm et al., 2015) thus these results are non-physiological. Recently, Zelda was shown to have subtle growth phenotypes when knocked down by systemic RNAi in developing appendages in *Tribolium castaneum* (Ribeiro et al., 2017), but it is not known if these phenotypes are due to cell autonomous effects on the appendages, or systemic effects such as ecdysone signaling. The role of Zelda in adult stem cells or regenerating tissues in *Drosophila* has not been investigated.

We have previously identified and characterized a mechanism where the Sertad protein *taranis* functions to protect regenerating imaginal discs from inappropriate cell fate changes that are induced by the powerful pro-regenerative signaling at the wound, primarily orchestrated by the JNK signaling cascade (Schuster and Smith-Bolton, 2015). An open question coming from this study was that we did not know what the upstream signals/transcription factors that induce the

expression of *taranis* so it can exert its protective function. The obvious first candidate, JNK signaling, acted in parallel to taranis. Acting on the expression of *engrailed* rather than *taranis* itself. Therefore, I set out to identify potential regulators of taranis reporter expression during regeneration. From this candidate screen, I identified the pioneer transcription factor Zelda (Liang et al., 2008) as a regulator of *taranis* expression. It is surprisingly required for both anterior and posterior patterning, and might be important for the re-appearance of developmental patterning during imaginal disc regeneration.

Results

Patterning is dynamic during imaginal disc regeneration

Since taranis is expressed late in regeneration, we set out to understand how patterning is re-established during wing imaginal disc regeneration. We performed a regeneration time course investigating the expression of various known patterning genes/proteins essential for developmental patterning during regeneration of the wing imaginal disc after transient *reaper* (UAS-*rpr*) induced tissue ablation under the temporal and spatial control of *rnGAL4 GAL80^{ts}* during the third larval instar of *Drosophila* (Brock et al., 2017; Schuster and Smith-Bolton, 2015; Smith-Bolton et al., 2009). It has been previously shown that patterning changes drastically during regeneration of the wing imaginal disc after tissue ablation (Smith-Bolton et al., 2009) and after manual wounding in situ (Díaz-García and Baonza, 2013). To get a better understanding of the extent of

patterning changes during regeneration, we performed a small-scale expression screen of known wing patterning genes over a time course throughout regeneration sampling every 24 hours after damage over a three-day period until regeneration was largely complete (R0-R72) (Fig. 9 and data not shown). We first examined the expression of Wingless (Wg) throughout regeneration and found as previously described, that its expression pattern is dynamic during regeneration (Fig. 9A-E). In wandering 3rd instar wing discs that did not experience tissue damage, Wg is expressed in a theta pattern, with two concentric rings along the hinge and a stripe at the dorsal-ventral boundary in the wing blade (Fig. 9A) (Couso et al., 1993). Immediately after damage during wound healing (R0), the expression of Wg in the pouch is largely absent except in cellular debris, and in some discs being faintly expressed in the damaged area (Fig. 9B). By R24, which is when the blastema is fully formed and robustly proliferating, Wg expression is markedly upregulated in the regenerating tissue (Fig. 9C), which is when Wg is required for regenerative growth through dMyc (Smith-Bolton et al., 2009). This persists until approximately R48, where we observe Wg going through a transition-state that is clearly in the process of resolving and/or remodeling into the original theta pattern found in undamaged wings (Fig. 9D). These transition states are different in a population of discs, with a pattern resembling an “infinity” (∞) symbol manifesting before the circle opens-up (data not show). Finally, by R72, the Wg pattern is fully resolved into the theta pattern found in normally developing 3rd instar wing discs (Fig. 9E).

Next, we wanted to determine the temporal dynamics of another previously characterized patterning change during regeneration. We chose to look at the expression of the Notch (N) ligand, Delta (Dl), during regeneration. Dl is expressed within the proveins as well as along two cell rows aligning the DV boundary in the 3rd instar wing imaginal disc (Fig. 9F) (Doherty et al., 1996a), which is set up by the Dpp signaling gradient (Blair, 2007). It was previously shown that other vein markers are transiently lost during regeneration after *eiger*-induced ablation, but is restored to a largely normal pattern by the end of regeneration (Smith-Bolton et al., 2009). Interestingly, this loss of provein pattern does not require cell division, and still occurs in manually wounded discs that are at a stage where they have lost their regenerative capacity (Díaz-García and Baonza, 2013). To characterize the dynamics of Dl expression (provein patterning) during regeneration, we performed the same time course in wild-type regenerating discs and examined Dl expression. As expected, Dl is localized in the proveins and margin in undamaged 3rd instar wing discs (Fig. 9F). During the early stages of regeneration from R0-R24, the pattern of Dl is lost in the provein regions (Fig. 9G-H), and the marginal Dl pattern becomes disconnected by a gap of dead cells at R0 (Fig. 9G), but eventually becomes reconnected to form a continuous margin by R24 (Fig. 9H), if not shortly after this time point (data not shown). By R48, we see Dl expression beginning to come back broadly throughout the blastema, and has not resolved any fine discerning features such as proveins (Fig. 9I). Finally, Dl is restored more or less in its typical provein pattern by R72 (Fig. 9J).

This data (Fig. 9A-I), combined with other patterning changes previously described (Schuster and Smith-Bolton, 2015; Smith-Bolton et al., 2009), suggested that the regenerating wing disc might revert to a second-instar like state due to Wg being expressed throughout the pouch (Ng et al., 1996) and Dl not being present in the provein pattern (Doherty et al., 1996a) during the second instar. Therefore, to test this hypothesis, we examined the expression of reporters for two major enhancers of the wing selector gene *vestigial* (*vg*) during regeneration. Vestigial is both necessary and sufficient for the wing to develop and has been dubbed the “wing selector gene” by some, but not others (Baena-López and García-Bellido, 2003; Halder et al., 1998; Williams et al., 1991). It has two primary enhancers active in the wing disc that become activated at different stages of development. The boundary enhancer (*vgBE*) is expressed along the DV boundary starting in the second larval instar, continuing through the third instar where it gains expression along the anterior-posterior (AP) boundary (Fig. 9K) (Williams et al., 1994) during normal development. Examining the expression of *vgBE-lacZ* during regeneration revealed that *vgBE* remains active at the DV boundary throughout regeneration, albeit at lower levels (Fig. 9L-O). Therefore, the blastema maintains the second instar pattern and does not appear to revert to an earlier point in developmental time, such as embryonic development, which is consistent with a previous report on the cell cycle dynamics of regenerating leg discs (Sustar and Schubiger, 2005).

In contrast, in undamaged wing discs, the quadrant enhancer (*vgQE*) is expressed within the entire wing blade, except in the AP and DV boundaries giving expression in four quadrants, starting in the third instar (Fig. 9P) (Kim et al., 1996). Examination of the *vgQE-lacZ* expression throughout regeneration revealed a striking result: *vgQE-lacZ* is completely lost within the blastema during the early phase of regeneration where regenerative growth is most prominent, from R0-R24 (Fig. 9Q-R). Which is surprising due to the *vgQE* being thought to be critical for wing growth and recruits non-wing cells into the already existing wing field and converting them into wing cells (Zecca and Struhl, 2007b, 2007a, 2010). By R48, *vgQE-lacZ* is starting to return, starting in the distal tip of the blastema (Fig. 9S) and growing out. The expression of *vgQE-lacZ* returns to the normal quadrant expression pattern by R72 (Fig. 9T). Despite this loss of *vgQE* activity, the expression of Nubbin remains throughout regeneration (Khan et al., 2016b; Smith-Bolton et al., 2009), thus suggesting that wing identity is not completely lost, and that the loss of *vgQE-lacZ* is not simply a result of a completely ablated wing. Therefore, the regenerating wing disc appears to lose expression of third instar gene expression, but maintains and/or induces second instar gene expression during the early phases of regenerative growth. The regenerating wing disc eventually repatterns and restores the expression of late patterning genes to allow for the regenerating tissue to restore the original pattern so the wing can be functional after metamorphosis. These results also point to two major phases of regeneration that are major developmental transitions: the early phase of regenerative growth (R0-R24) where many

previously characterized growth promoting factors are induced to provide a pro-regenerative environment (Bergantiños et al., 2010; Brock et al., 2017; La Fortezza et al., 2016; Grusche et al., 2011; Katsuyama et al., 2015; Santabárbara-Ruiz et al., 2015; Smith-Bolton et al., 2009; Sun and Irvine, 2011; Yoo et al., 2016), and the late repatterning phase (R48-R72) where the regenerating tissue restores the lost patterning information thus allowing for proper form and function of the resulting wing. This transient loss and later restoration of pattern is also very reminiscent of regeneration in salamanders and zebrafish that regenerate their limbs and hearts via dedifferentiation of surviving cells in the stump (Gupta et al., 2013; Knopf et al., 2011; Kragl et al., 2009; Sandoval-Guzmán et al., 2014; Stewart and Stankunas, 2012). The results described above demonstrate that the repatterning phase of regeneration is a large developmental transition where likely a large number of patterning genes need to be re-activated following successful regenerative growth.

Zelda is upregulated late during regeneration, and coincides with *taranis* expression.

It has previously been shown that *taranis* has a dynamic expression pattern during regeneration (Schuster and Smith-Bolton, 2015). In undamaged 3rd instar wing discs, *tara-lacZ* is expressed ubiquitously and at relatively low levels (Fig. 10A). The expression *tara-lacZ* expression is low, yet relatively enriched within some cells in the blastema during the early phase of regeneration at R24 (Fig. 10B), and is upregulated within the blastema at R48 (Fig. 10C). This suggests

that *taranis* expression is activated in discs that are undergoing repatterning. We reasoned that whatever could be activating the large cohort of repatterning events could also be regulating the expression of *taranis*. Searching through the literature, one promising candidate was in the pioneer transcription factor Zelda (Zld), which is essential for activation of the zygotic genome during the maternal to zygotic transition during early embryogenesis in *Drosophila* (Liang et al., 2008). Zld is able to open-up closed chromatin, recruit other transcription factors, and bind to a large number of patterning genes before their activation in the early embryo (Foo et al., 2014; Harrison et al., 2011; Liang et al., 2008; Nien et al., 2011; Schulz et al., 2015). Importantly, the *taranis* locus contains two Zld consensus sequences known as TAGteam elements, and Zld is found to be bound there in embryos (Harrison et al., 2011), but the functional significance of this interaction is not known. Therefore, Zelda was an attractive candidate for both the regulation of *taranis* expression, and the activation of other patterning genes during the repatterning phase of regeneration. We first examined the expression of Zld during regeneration and found that Zld and *tara-lacZ* have near identical expression patterns during regeneration and normal development (Fig. 10A-I). Zld was expressed ubiquitously at low levels throughout the undamaged third instar wing disc (Fig. 10D). Zld was found to be expressed at low levels in the blastema at R24 (Fig. 10E), and was markedly upregulated in the blastema at R48 (Fig 10F). Zld and *tara-lacZ* colocalized at all timepoints examined, especially in the blastema (Fig. 10G-I). These near-identical expression

dynamics suggests that Taranis and Zelda might be either in the same pathway, or may be acting in parallel during regeneration.

Zelda is upstream of *taranis* expression

Since Zld and *tara-lacZ* have identical expression patterns, we wanted to see if Zld could be upstream of *taranis* expression. To test this hypothesis, we reduced the dose of *zld* in the *tara-lacZ* background and looked at the expression levels of *tara-lacZ* in $tara^{03881}$/+ and zld^{294}/+; $tara^{03881}$/+ at R48. Indeed, the fluorescence intensity of *tara-lacZ* is significantly reduced in the zld^{294}/+ background compared to control regenerating wing discs (Fig. 11A-C). This suggests that *tara* is downstream of *zld*. Further experiments need to confirm this, including qPCR of taranis transcripts in w^{1118} and zld^{294}/+ R48 discs as well as looking at the expression of *tara-lacZ* in homozygous mutant clones of zld^{294} during regeneration and normal development. The clone induction experiments are currently being optimized for experiments at 18^{o}C, however due to the nature of clones being randomly generated, perhaps the best way to obtain strong, uniform knockdown of zld levels would require use of a second binary system to drive RNAi independently from the *rpr* expression.

Strong Knockdown of Zelda Results in both Anterior and Posterior Defects during Regeneration

If *zld* is indeed upstream of *tara*, then reduction of *zld* levels should phenocopy *tara/+* regeneration phenotype, with massive P to A transformations. Initial experiments with looking at zld^{294}/w^{1118} adult regenerated wings suggested that further reduction of *zld* levels beyond simply being heterozygous was required to get more penetrant phenotypes (data not shown). Ideally, homozygous mutant clones of zld^{294} would be the best way to assess complete loss of *zld* function during regeneration, however, preliminary experiments attempting to induce clones in regenerating tissue have been largely unsuccessful due to differences in developmental timing between larvae grown at 25^{o}C versus larvae grown at 18^{o}C, and having difficulty isolating clones within the blastema itself. Therefore, as an alternative to clones, I combined a *UAS-zldRNAi* line with the zld^{294} mutation to knock down as much *zld* transcripts as possible during regeneration (see appendix for a discussion on RNAi experiments). Control *attP40/+* adult wings that undergone regeneration as wing discs ("adult regenerated wings" for simplicity) had a minimum amount of P to A transformation defects (Fig. 12A, E-F). *UAS-zldRNAi/+* adult regenerated wings had a small increase in P to A transformation defects (Fig. 12B, E-F), however there was a large amount of variability in the phenotype which made the results not statistically significant (Fig. 12F). Adult regenerated wings of zld^{294}*/+; attP40/+* also had a small, yet statistically significant, increase in P to A transformations (Fig. 12C, E-F). Surprisingly, a large frequency of patterning defects found in the anterior

compartment is found in *zld*^{294}*/+; attP40/+* regenerated wings (Fig. 12C, G). Such phenotypes included missing or extra anterior crossveins (ACV), ectopic vein material that was either extensions of longitudinal veins, or perhaps more strikingly: unpatterned, almost amoeboid-shaped vein material was also found in the anterior compartment (Fig. 12C). These striking anterior defects were very rare in *attP40/+* controls, with a slight yet statistically insignificant increase in *UAS-zldRNAi/+* regenerated animals (Fig. 12G), which is likely due to the large amount of phenotypic variation found in this genotype. Importantly, they were never found in undamaged wings (data not shown). The *zld*^{294}*/+; UAS-zldRNAi/+* adult regenerated wings had a large amount of both P to A transformations and anterior defects compared to controls (Fig. 12D-G). The anterior phenotypes appeared more severe in the *zld*^{294}*/+; UAS-zldRNAi/+* adult regenerated wings compared to *zld*^{294}*/+; attP40/+* adult regenerated wings, but the frequency of them appearing in an individual wing was not statistically different between these two genotypes (Fig. 12C-D, G). One major limitation to this experiment was that the sample size of *zld*^{294}*/+; UAS-zldRNAi/+* adult regenerated wings was very small (n=16) compared to other genotypes (n=50-90 depending on the genotype). This was due to most *zld*^{294}*/+; UAS-zldRNAi/+* regenerating poorly compared to the other genotypes, with over 80% of the regenerated wings being between 25-50% regenerated categories (Fig. 12H). Therefore, many patterning phenotypes are likely to be obscured due to the small adult regenerated wing size, which are excluded from the analysis of patterning phenotypes in adult regenerated wings. Analysis of the regenerating wing discs themselves should

shed light on the extent of all patterning phenotypes found in *zld*^{294}*/+; UAS-zldRNAi/+* regenerating wing discs. Given these above results, *zld* is required for both anterior and posterior patterning during regeneration.

Validation of Zelda Reagents

In order to further interrogate Zelda function during regeneration, we needed to validate the available reagents for Zelda. There is a TRiP UAS-RNAi line available that is predicted to target the *zelda* transcripts that is inserted within the *attP40* locus (referred to as *UAS-zldRNAi*). However, it has never been validated in imaginal discs. To test for efficient knockdown, I crossed the *UAS-zldRNAi* with *apGAL4 UAS-EGFP* where the GAL4 is expressed in the dorsal compartment of the wing disc (Fig. 13A-B) and dissected out 3rd instar wing discs and stained for Zld protein expression, which is normally ubiquitously expressed in the wing disc (Fig. 10D, 13E). I found that Zld protein was strongly reduced in the dorsal compartment, but remained in the ventral compartment (Fig. 13A). Therefore the *UAS-zldRNAi* line is effective at knocking down Zelda transcripts during normal development. These *apGAL4 UAS-EGFP/UAS-zldRNAi* flies survived to adulthood without any abnormal patterning defects compared to normal wings (Fig. 13B). This was confirmed using independent *rnGAL4* and *hhGAL4* drivers (data not shown).

Next, we wished to validate the specificity of the Zld antibody by inducing homozygous mutant clones for the null mutant *zld*^{294} in the developing wing disc. Staining for the Zld protein revealed a loss of Zld in the homozygous mutant tissue, as expected (Fig. 13C). Examining adult wings of flies that experienced the same heat shock conditions revealed perfectly patterned wings and eyes (Fig. 13D). It should be noted that it was impossible to see the clones within the wing due to the genetic background not containing a visible marker in adult wings. Therefore, clone induction and maintenance was confirmed by finding mosaic red/white eyes (Fig. 13D-inset). These data demonstrate that the reagents used to detect and abrogate Zld expression are specific and potent. Therefore, they are valid to use for assessing Zld expression and phenotypic analysis of Zld function.

Discussion

This study identified the pioneer transcription factor Zelda as a factor that is both upstream of taranis expression, and is essential for both anterior and posterior patterning during regeneration. These extreme patterning phenotypes found when *zld* is strongly reduced, along with a large portion of regenerated wings being smaller than average suggests that *zld* may be essential for more than just maintaining anterior-posterior patterning. Indeed, Zld expression coincides with the onset of repatterning during regeneration, where a large number of patterning genes are known to be reactivated and/or resolved into their original patterns that are found in undamaged wing discs. Zelda is most well characterized in the

maternal to zygotic transition, where a very large set of zygotic genes are directly activated by Zelda (Harrison et al., 2011). Therefore, Zelda may also be essential for activating a large cohort of patterning genes to reactivate the developmental patterning gene regulatory module in regenerating imaginal discs that have largely completed their regenerative growth. This hypothesis that Zelda is the factor responsible for the “regenerative growth to repatterning transition” is an attractive one, but needs to be directly tested by examining the expression of a number of patterning genes including Wg, Dl, vgBE, and vgQE (Fig. 9). In addition to these, less well characterized patterning genes during regeneration will need to be assessed such as Dpp signaling components pMad, Spalt (Sal), Optomotor blind (Omb), and Brinker (Brk) (Restrepo et al., 2014) as well as other DV patterning genes such as Distalless (Dll), Serrate (Ser), Cut, etc (Couso et al., 1995; Doherty et al., 1996b; Neumann and Cohen, 1996; Zecca et al., 1996). While a candidate gene approach will be a necessary starting point, an unbiased genome-wide approach is also warranted. It would be interesting to see the comprehensive set of Zld targets that are regulated at the regenerative growth to repatterning transition. A ChIP-seq coupled to RNA-seq in undamaged 3rd instar and R48 wild type regenerating wing discs would be a good way to identify potential Zld targets. An ATAC-seq of blastema cells in regenerating (at multiple timepoints) and undamaged 3rd instar wing discs will also be a valuable resource and would further demonstrate the extent of Zelda’s pioneering activity during regeneration.

The identification of Zelda as being an upstream regulator of *taranis* expression still leaves a large number of unanswered questions. Zelda is still a transcription factor, so the upstream signals that regulates Zelda expression still remain to be identified. The number of signaling pathways known to be essential for regeneration are few in number, which include ROS, JNK, hippo/yorkie, Wg, and JAK/STAT signaling. All of these signaling pathways either regulate, or are regulated by JNK signaling, and it was previously shown that *taranis* is not regulated by JNK signaling at the transcriptional level (Schuster and Smith-Bolton, 2015) (Fig. 7L). The only signaling pathway that is thought to act in parallel to JNK signaling during regeneration is p38 MAPK signaling (Santabárbara-Ruiz et al., 2015). Unfortunately, I was unable to replicate their finding that *p38a* is essential for regeneration (data not shown), therefore p38 signaling may not regulate Zelda and/or Taranis expression. One possible candidate is Dpp/pMad signaling, which has not been shown to have a role in imaginal disc regeneration to date, but has a unique expression pattern during regeneration (Smith-Bolton et al., 2009) (data not shown). Dpp signaling is known to be important for dorsal closure, where it is essential for canalizing this robust developmental process (Ducuing et al., 2015), and protects the leading edge cells from apoptosis through Schnurri (Beira et al., 2014). Egfr signaling may also be a candidate regulator of Zld/Tara, especially since it was shown to be essential for both dorsal closure and AiP (Fan et al., 2014). It should be noted that both EGFR and Dpp signaling is activated by JNK during dorsal closure. If this holds true during regeneration, we are back to the same problem as before:

everything but *tara* is regulated by JNK. However, there are notable differences between dorsal closure and regeneration, so Dpp/pMad and EGFR signaling might be independent of JNK signaling in the regenerative context. Future work needs to be done to rule out such possibilities. Finally, the role of the innate immune signaling pathways such as Toll and IMD (Lindsay and Wasserman, 2014; Myllymaki et al., 2014) have yet to be explored in imaginal disc regeneration. These pathways could also regulate Zld/Tara in this context, provided they work in our system. Other possible signaling factors may also be the activating signal for Zld/Tara, but the identification of these pathways will require identification of novel signaling pathways essential for regeneration.

Materials and Methods

Ablation and regeneration experiments

Ablation experiments were carried out as previously described (Smith-Bolton et al., 2009) with a few modifications: induction of cell death was caused by overexpressing *rpr*, and animals were raised at 18^{o}C until 7 days after egg lay (AEL) (early 3rd instar) before the temperature was shifted to 30^{o}C for 24 hours in a circulating water bath. To identify, and select for mutants residing on the X chromosome, the *FM7i, act-GFP* balancer was selected against during the picking of 1st instar larvae on grape juice agar plates. Before fixation of 3rd instar larvae for staining, a second selection against GFP^{+} larvae was conducted to ensure all discs that were stained were the correct genotype. For undamaged

controls, animals with the same genotype as the experimental animals were kept at 18^{o}C and dissected at 9-10 days AEL, which is mid-late 3rd instar. Mock ablated animals are the siblings of the flies in the ablation experiments that experienced the same thermal conditions, but they inherited the *TM6B, tubGAL80* containing chromosome instead of the ablation chromosome. For adult wings, control undamaged animals were kept at 18^{o}C until after eclosion.

Mitotic clone induction and overexpression during normal development

For clonal analysis of *zld*^{294} during normal development, animals with the genotype *w*, zld*^{294}*, FRT19A/ubi-mRFPnls, w*, hsFLP, FRT19A* were shifted to 37.5^{o}C for 30 min at 2 days after egg lay, then transferred back to 25^{o}C. They were dissected 5-6 dAEL which is at the wandering 3rd instar stage. Current efforts are to optimize this protocol for larvae at 18^{o}C for ablation experiments.

Manual wounding of discs

Early to mid-3rd instar larvae of the genotype *rnGAL4, UAS-EYFP/tara*^{03881} were chilled on ice for 20 minutes. One disc was pinched using forceps without disrupting the larval cuticle, leaving the second disc intact as a contralateral control. Larvae were then transferred to fresh food and incubated at 25°C for 30 hours before dissecting, fixing and staining.

Fly Stocks

The following Drosophila stocks were used: *w^{1118}; rnGAL4, UAS-rpr, tubGAL80^{ts}/TM6B, tubGAL80* (Smith-Bolton et al., 2009), *w^{1118}* (Hazelrigg et al., 1984) *y^1v^1; attP40* (Markstein et al., 2008) (genetic background control for RNAi experiments), *vgBE-lacZ* (Williams et al., 1994) and *vgQE-lacZ* (Kim et al., 1996) were kind gifts from Sean Carroll. *y^1sc*v^1; UAS-zldRNAi* (TRiP#HMS02441) (Ni et al., 2011), *apGAL4^{md544}* (Brand and Perrimon, 1993; Calleja et al., 1996) (this line is now recombined with UAS-EGFP), *ubi-mRFPnls w* hsFLP FRT19A*, *w* zld^{294} FRT19A* and *w* zld^{294}* (Liang et al., 2008) were provided by Melissa Harrison. All fly stocks are available from The Bloomington Drosophila Genetic Stock Center unless stated otherwise.

Adult wings

Wings were mounted on glass slides in Gary's Magic Mount (Canada balsam (Sigma) dissolved in methyl salicylate (Sigma)). Images of individual wings were taken with an Olympus SZX10 dissection microscope with an Olympus DP21 camera using the CellSens Dimension software (Olympus). All images were taken at the same magnification (5X).

To quantify the P-to-A transformation phenotype in adult wings, all wings that reached to or past the tip of abdomen were considered fully regenerated and selected for quantification. The wings were scored for five anterior markers within

the posterior compartment. These five markers included socketed bristles on the posterior margin, ectopic vein material on the posterior margin, an ectopic anterior crossvein (ACV) in the posterior wing blade, distal costa-like bristles on the alar lobe, and an anterior-like shape characterized by a narrower proximal and wider distal posterior compartment. The frequency of each marker was calculated independently for each genotype. In addition, these wings were scored on a scale of 0-5 markers to assess the strength of the P-to-A transformation in each wing. For all experiments, at least 3 replicates from independent egg lays were performed. Statistics were calculated and graphs were produced in Microsoft Excel. To calculate the Average Transformation Score, the final scores of each wing was averaged in each replicate. These averages were averaged to each replicate to get the scores listed on the graph. This allowed us to calculate SEM and perform a Student's t-test to assess statistical significance compared to Wild-type. To quantify the percentage of wings having an anterior defect, anterior defects were defined as ectopic or missing vein material in the anterior compartment starting at L1 and ending at the AP boundary which is marked by the L3 vein. Wings were then scored for having an anterior defect and the average percentage of wings having an anterior defect was averaged over at least three replicates. Error bars are SEM and statistical significance was determined by the Student's t-test.

Extent Regeneration and Pupariation Rate experiments were performed as previously described (Brock et al., 2017; Khan et al., 2017; Skinner et al., 2015; Smith-Bolton et al., 2009).

Immunohistochemistry

Dissections, fixing and staining were done as previously described (Smith-Bolton et al., 2009). Wing imaginal discs were mounted in Vectashield (Vector Labs). mouse anti-βgal (1:100) (DSHB), mouse anti-Dl (1:500) (Sun and Artavanis-Tsakonas, 1996) (DSHB), mouse anti-Wg (1:100) (Brook and Cohen, 1996) (DSHB), rat anti-DECAD2 (1:100), and rabbit anti-Zld (1:1000) (Staudt et al., 2006) was a gift from Melissa Harrison. The Developmental Studies Hybridoma Bank (DSHB) was created by the NICHD of the NIH and is maintained at the University of Iowa, Department of Biology, Iowa City, IA 52242.

AlexaFluor secondary antibodies (Molecular Probes) were used at 1:1000. TO-PRO-3 iodide (Molecular Probes) was used as a DNA counterstain at 1:500. Specimens were imaged with either an LSM510 or LSM700 Confocal Microscope (Carl Zeiss). Images were compiled using ZEN Black software (Carl Zeiss), Photoshop (Adobe) or ImageJ (U.S. National Institutes of Health). All confocal images are maximum intensity projections from z-stacks unless otherwise stated.

Average fluorescence intensity was measured in ImageJ using images that were stained in parallel and imaged under identical confocal settings. For quantifying mouse anti-βgal staining in *tara*^{03881}/+ discs, the morphology of the wing pouch and the upregulated area of *tara-lacZ* was sufficient to draw a circle in ImageJ and quantify fluorescence intensity of the blastema. The Student's t-test was performed to assess significance.

Figures

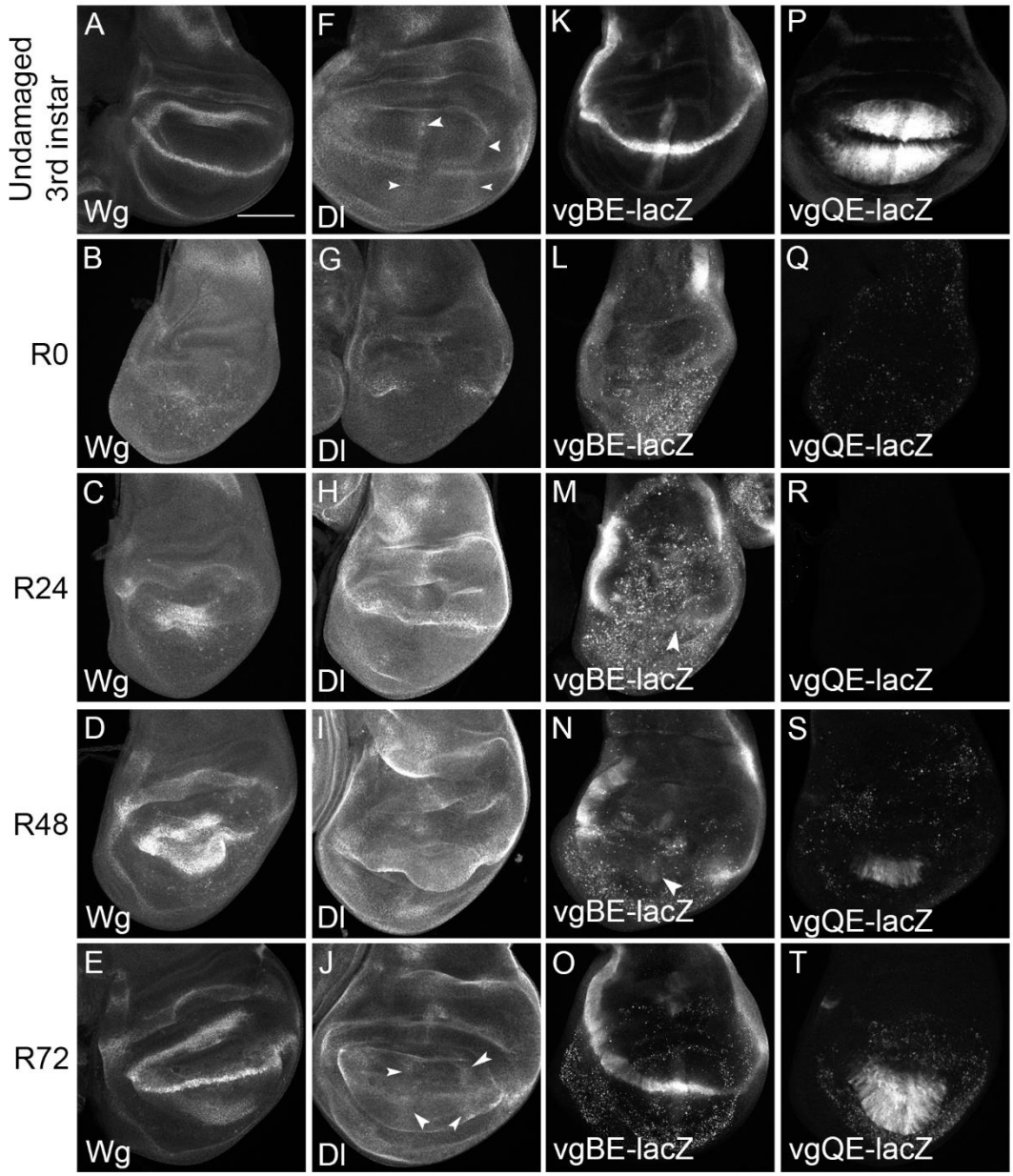

Figure 9. Repatterning is a large developmental transition. A-E) Timecourse of Wg expression in undamaged and regenerating wild type wing discs. A) Undamaged mid-3rd instar wing disc stained for Wg. Note the theta (θ) pattern. B) R0 wing disc with Wg staining. Very little Wg is present. C) R24 wing disc stained for Wg. Wg is upregulated within the blastema (damaged area). D) R48 wing disc stained for Wg. Wg pattern is beginning to resolve and repattern.

Fig.9 (con't)

E) R72 wing disc with pattern restored back to the theta pattern. F-G) Timecourse of Dl expression in undamaged and regenerating wild type wing discs. F) Undamaged mid-3rd instar wing disc stained for Dl. Dl stains margin and proveins (arrowheads). G) R0 wing disc stained for Dl. Dl is lost except at the DV boundary separated by the dead domain. H) R24 wing disc stained for Dl. Dl is restored at the margin in some discs. I) R48 wing disc stained for Dl. Dl is upregulated in the pouch but does not have the provein pattern yet. J) R72 wing disc stained for Dl. Dl expression is restored in the proveins (arrowheads). K-O) *vgBE-lacZ* expression timecourse in undamaged and regenerating *vgBE-lacZ*/+ wing discs. K) Undamaged mid-3rd instar wing disc stained for βgal (vgBE-lacZ). *vgBE-lacZ* is expressed at high levels along the DV boundary L) R0 wing disc with *vgBE-lacZ* expression. *vgBE-lacZ* expression appears lost in the damaged region full of cellular debris. M) R24 wing disc with *vgBE-lacZ* expression. *vgBE-lacZ* is expressed at low levels at the DV boundary (arrowhead), with some gaps. N) R48 wing disc with *vgBE-lacZ* expression. *vgBE-lacZ* is expressed at low levels at the DV boundary (arrowhead), with some gaps. O) R72 wing disc with *vgBE-lacZ* expression. *vgBE-lacZ* levels are restored along the complete margin. P-T) *vgQE-lacZ* expression timecourse in undamaged and regenerating *vgQE-lacZ*/+ wing discs. P) Undamaged mid-3rd instar wing disc stained for βgal (*vgQE-lacZ*). *vgQE-lacZ* is expressed in the wing blade with exception at the AP and DV boundaries, giving it the quadrant pattern. Q) R0 wing disc that has completely lost *vgQE-lacZ* expression. R) R24 wing disc that has completely lost *vgQE-lacZ* expression. S) R48 wing disc with *vgQE-lacZ* expression returning in the distal wing blade region of the blastema. T) R72 wing disc with vgQE-lacZ expression restored to the quadrant pattern. Scale bar: 100μm. All discs imaged at same magnification.

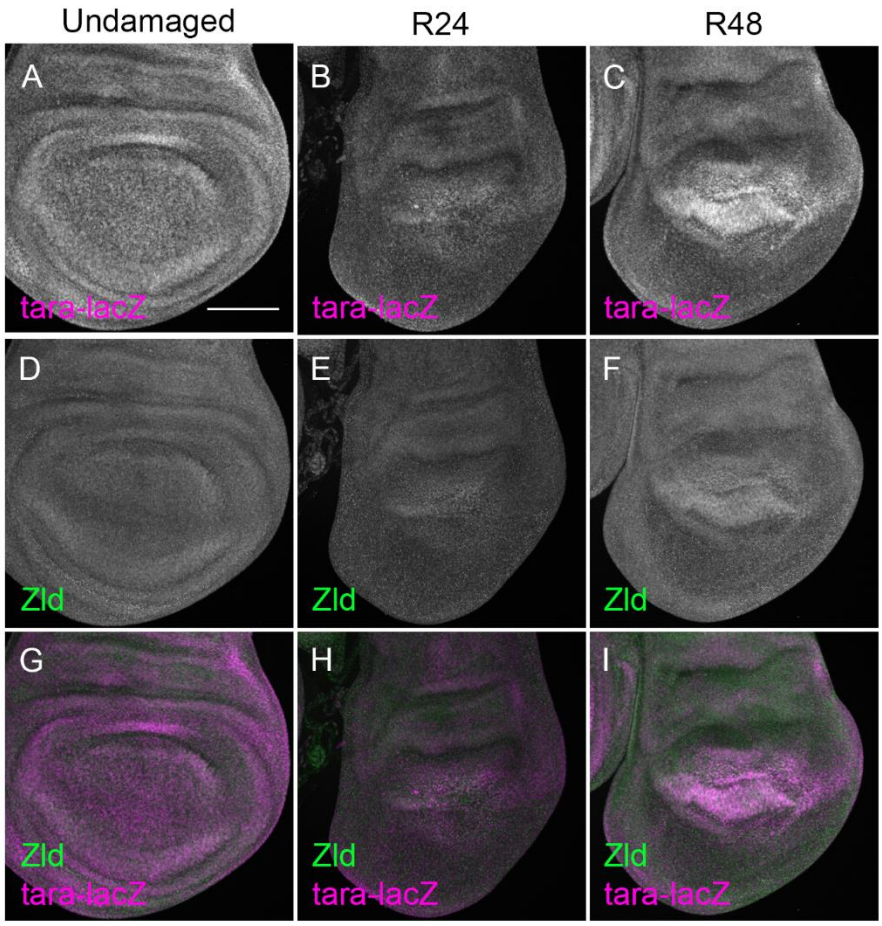

Figure 10. Taranis and Zelda expression dynamically overlap during regeneration. A) Undamaged 3rd instar *tara*^{03881}/+ wing disc stained for βgal (*tara-lacZ*). *tara-lacZ* is ubiquitously expressed at low levels. B) R24 *tara*^{03881}/+ wing disc stained for βgal (*tara-lacZ*). *tara-lacZ* is expressed in the blastema at low levels. C) R48 *tara*^{03881}/+ wing disc stained for βgal (*tara-lacZ*). *tara-lacZ* is expressed in the blastema at high levels. D) Undamaged 3rd instar *tara*^{03881}/+ wing disc stained for Zld. Zld is ubiquitously expressed at low levels. E) R24 *tara*^{03881}/+ wing disc stained for Zld. Zld is expressed in the blastema at low levels. F) R48 *tara*^{03881}/+ wing disc stained for Zld. Zld is expressed in the blastema at relatively high levels. G-H) Merged images of *tara-lacZ* (magenta) and Zld (green). *tara-lacZ* and Zld overlap extensively. G) Undamaged 3rd instar. H) R24. I) R48. Scale bar: 100µm. All discs are imaged at the same magnification.

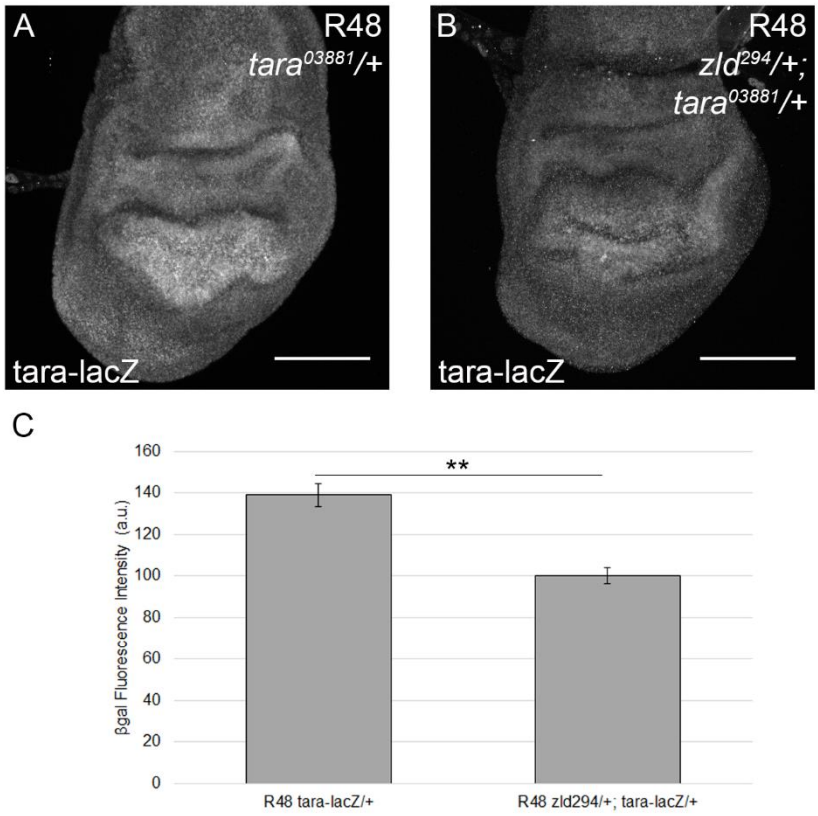

Figure 11. Zelda is upstream of Taranis expression. A) R48 *tara*^{03881}/+ regenerating wing disc stained for βgal to visualize *tara-lacZ* expression. B) R48 *zld*^{294}/+; *tara*^{03881}/+ regenerating wing disc stained for βgal to visualize *tara-lacZ* expression. C) Quantification of average fluorescence intensity of βgal within the blastema of R48 *tara*^{03881}/+ (n=15) and R48 *zld*^{294}/+; *tara*^{03881}/+ (n=13) regenerating wing discs. Scale bar: 100µm. Error bars: SEM. ** p<0.01.

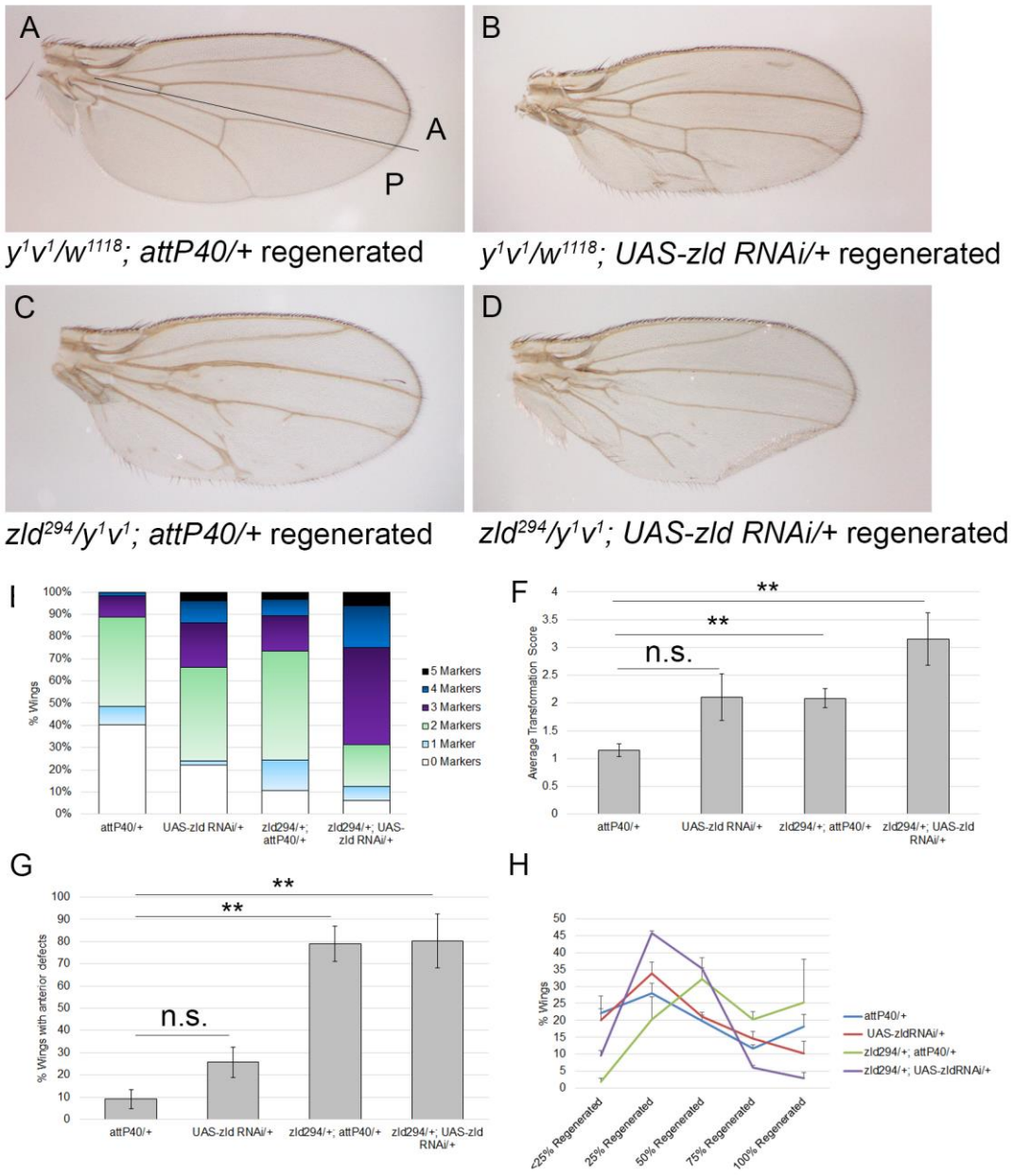

Figure 12. Strong knockdown of Zelda results in both anterior and posterior defects during regeneration. A) Example of an *attP40/+* regenerated wing (wild type control). Anterior (A) and posterior (P) compartments are noted with a line that crosses the AP boundary. B) Example of a *UAS-zldRNAi/+* regenerated wing. Wing has minor posterior defects such as ectopic veins and bristles. The gap in the L2 is due to the wing not being 100% regenerated and is a nonspecific phenotype. C) Example of a *zld^{294}/+; attP40/+* regenerated wing. Note that there is a gap where the anterior crossvein should be and ectopic unpatterned veins near that site as well in the

Fig. 12 (con't)

anterior compartment. Posterior defects such as bristles and ectopic veins are also present. D) Example of a *zld*^{294}*/+; UAS-zldRNAi/+* regenerated wing with both anterior and posterior defects. An ACV that is faint and disorganized, ectopic veins, and a large gap in the proximal L3 longitudinal vein are present in the anterior compartment. The posterior compartment has overgrown (anteriorized shape), with ectopic veins, bristles and crossveins. E) Quantification of extent of P-to-A transformation of regenerated wings that were *attP40/+* (n=62), *UAS-zldRNAi/+* (n=50), *zld*^{294}*/+; attP40/+* (n=94), and *zld*^{294}*/+; UAS-zldRNAi/+* (n=16). F) Average P to A transformation score of adult fully regenerated wings that were *attP40/+* (n=62), *UAS-zldRNAi/+* (n=50), *zld*^{294}*/+; attP40/+* (n=94), and *zld*^{294}*/+; UAS-zldRNAi/+* (n=16). G) Quantification of the frequency of wings (%) that had an anterior defect that were *attP40/+* (n=62), *UAS-zldRNAi/+* (n=50), *zld*^{294}*/+; attP40/+* (n=94), and *zld*^{294}*/+; UAS-zldRNAi/+* (n=16). H) Extent regeneration semi-quantitative measurements of adult regenerated wings in *attP40/+*, *UAS-zldRNAi/+*, *zld*^{294}*/+; attP40/+*, and *zld*^{294}*/+; UAS-zldRNAi/+.* Error bars: SEM. ** $p<0.01$, n.s.: not significant ($p>0.05$). All adult wing images were taken at the same magnification.

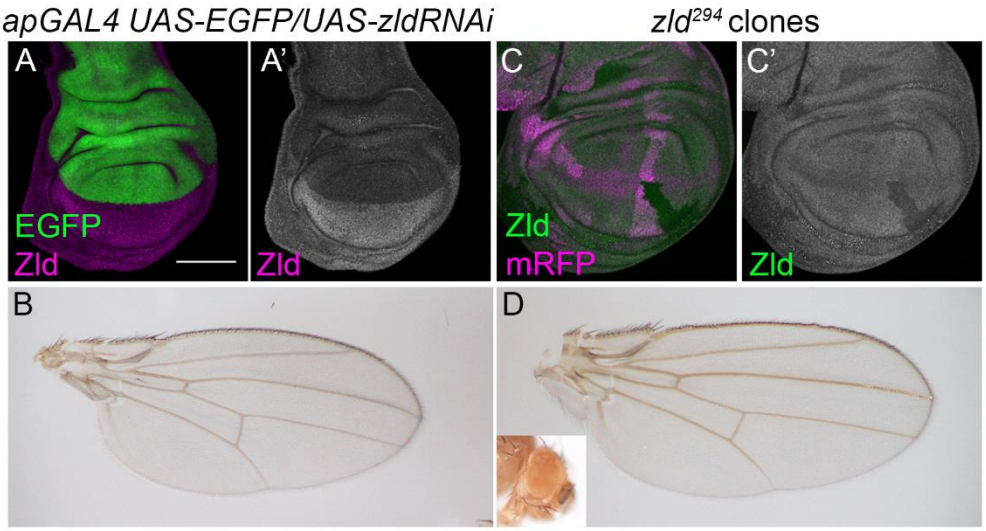

Figure 13. Validation of Zelda Reagents. A) Single confocal slice of *apGAL4 UAS-EGFP/UAS-zldRNAi* 3rd instar wing disc stained for Zld (magenta) and visualized for EGFP expression (green). A') Zld staining alone. Note the strong knockdown of Zld protein in dorsal compartment compared to ventral compartment. B) *apGAL4 UAS-EGFP/UAS-zldRNAi* adult wing. No visible patterning phenotypes are found. C) *zld*^{294} homozgous mutant clones generated in *w* zld*^{294} *FRT19A/ubi-mRFPnls w*^{1118} *hsFLP FRT19A* larvae by heatshock on d2AEL at 25^{o}C (30min) and fixed/stained at wandering 3rd instar (5-6dAEL) stained for Zld (green). Homozygous mutant clones are identified by lack of mRFP (magenta). D) Adult wings and eyes (inset) of *w* zld*^{294} *FRT19A/ubi-mRFPnls w*^{1118} *hsFLP FRT19A* that experienced identical heatshock conditions above and left to grow to adulthood. Clones are not marked in wing, but are in the eye to some extent (inset). Scale Bar: 100um in imaginal disc images. All wing discs imaged at the same magnification. All adult wings imaged at the same magnification. All confocal images are single slices.

Chapter 4: Conclusion/Future Directions

Summary

I have detailed in this PhD thesis the discovery of *taranis* being the first regeneration-specific patterning factor identified in any model organism, where posterior to anterior fate changes occur when the levels of *taranis* is reduced during regeneration and that taranis is dispensable during unperturbed wing development. The identification of a regeneration-specific patterning factor came initially as a surprise, but now it is clear that such mechanisms should be the case due to regeneration being a unique context, where developmental mechanisms are being modulated/reactivated by wound-induced signals that promote wound-healing and regenerative growth. I further demonstrated that *taranis* acts as a protective factor to prevent inappropriate cell fate changes induced by pro-regenerative signals, and therefore *taranis* ensures that the regenerating tissue faithfully restores form and function to the damaged imaginal disc.

In chapter 3, I report the identification of Zelda as a potential upstream activator of *taranis* function, and the potential of Zelda being important for re-establishing patterning during regeneration due to the observation that a strong reduction of Zelda levels results in regenerated wings having a number of additional patterning defects in addition to posterior to anterior fate changes. This would be significant due to the current dearth of known processes that Zelda could function

in a similar way to its canonical role of regulating the maternal to zygotic transition, where it activates a number of zygotic transcripts necessary for patterning the early embryo. More work is needed in order to establish Zelda as a potential mediator of this “regenerative growth to repatterning transition”, but exciting results are emerging that could not be incorporated into this thesis due to their preliminary nature.

In the following appendices, I will detail a number of experimental paths I took that do not yet merit inclusion into this thesis, but are promising projects for new members of the lab to pick up after I am gone. The first appendix is about my efforts to answer the question of what Taranis does at the molecular level during regeneration, which remains wide-open. To accomplish this goal, I gave a valiant effort in purifying an epitope-tagged taranis in order to generate a polyclonal antibody against taranis so I can perform ChIP and other molecular biology techniques to characterize Taranis protein function. However, this project did not result in a lot of success, due to a combination of protein purification being challenging in my hands and that Taranis being an intrinsically disordered protein, which are notoriously difficult to purify. In the second appendix, I detailed three side projects that I started in order to answer questions that came-up at different points in my graduate school career. I first mention the differential regenerative phenotypes of various “wild-type” lines, and call for the need for genetic background controls in all experiments involving imaginal disc regeneration. I also point to the potential for this knowledge to identify novel

genes in these background which could be modifiers of regeneration. The second side-project was investigating the role of losing cell fate and patterning during regeneration, and to investigate the functional reason why a transient loss in cell fate and patterning is necessary for regeneration. Using vestigial as a model, I obtain data that suggests that loss of vgQE expression is important for cell survival within the blastema. However, I later found that overexpression of Vg results in cell death in both undamaged and regenerating tissue, which means that more sophisticated tools, or a different approach, are needed in order for this project to continue. Finally, I describe relatively recent results in lineage tracing wing discs that have their entire posterior compartment ablated with *rpr*. I find that ablating the P compartment results in mostly duplications, rather than true regeneration of the missing compartment. I also attempt to find the origin of the posterior to anterior fate changes in taranis mutants, and find evidence that these are indeed P to A transformations, and not transgressions of the AP boundary. This last project has great potential in identifying genes essential for duplication after damage, which is an area that has been poorly investigated to date.

Finally, in the rest of this conclusion/future directions chapter I will discuss the potential roles of *taranis* and its homologs during regeneration-related phenomena in *Drosophila* and Lepidotpterans, regeneration in other model systems and the potential for Sertad proteins having a role in virtually all regeneration model organisms, and the potential role protective factors may have in neurodegenerative disease.

Transdetermination

The identification of *taranis* as a protective factor to prevent cell fate changes that are induced simply by the ectopic activation of the JNK signaling pathway was significant since it showed that cell fate can be altered under “normal” regenerative conditions. However, there is a large body of work describing the phenomenon of transdetermination, which can be characterized as “regeneration gone wrong” where depending on the position of the injury on an imaginal disc (known as “weak spots”), the regenerating tissue will form the tissue that belongs to a different imaginal disc entirely (Worley et al., 2012). Such examples include leg regenerating wing tissue, eyes and antennae regenerating leg tissue, etc. It has been reported that transdetermination can also be induced by ubiquitous expression of Wg in various imaginal discs (Maves and Schubiger, 1995) *in situ*, in addition to cutting and transplantation. It is known that Transdetermination is a form of cell fate change during regeneration that requires JNK signaling through downregulation of the polycomb group proteins (Lee et al., 2005), but JNK signaling has not been shown to be sufficient to induce transdeterminations in damaged regenerating discs. Indeed, Lee et al., 2005 used the *hsFLP act>STOP>wg* model of inducing transdeterminations via ubiquitous overexpression of Wg. However, it is not clear if these are true regenerative transdetermination events since damage has not been induced in this model. The role of JNK signaling is also muddied in the fact that JNK signaling is also essential for regenerative growth, and cell division is essential for transdetermination (McClure and Schubiger, 2007; Schubiger, 1973). Therefore,

suppression of transdetermination in a JNK impaired tissue could simply be the off-target result of halted proliferation, not JNK signaling activating some sort of “transdetermination pathway”. Therefore, the role of JNK signaling in transdetermination is unclear. Given that transdetermination is a JNK-induced cell fate change (Lee et al., 2005; Worley et al., 2018), much like the JNK-induced P to A transformations at a large scale (Schuster and Smith-Bolton, 2015), it is tempting to speculate that taranis is involved in transdetermination as well. Indeed, a recent genetic screen identified the *Df(3R)EXEL7329* deficiency, a deficiency that deletes *taranis*, *belphegor*, and *gilgamesh* among a couple others, as having an increased rate of notum to wing transdeterminations after *eiger*-induced ablation (Worley et al., 2018). This data suggests that *taranis* may also play a critical role in preventing transdetermination in addition to AP patterning errors during true regeneration. Zelda may be involved in transdetermination as well, since transdetermination and regeneration share many of the same signals (Khan et al., 2016a; Worley et al., 2018), however the discussion below will mostly focus on *taranis*.

It is currently unknown how *taranis* may be able to prevent cell fate changes during transdetermination. One possibility is that in *tara/+* discs, *engrailed* becomes misregulated by the excess JNK signaling downstream of Eiger, which results in P to A transformations at the weak spot. This would induce an ectopic boundary at the apposition of the newly induced anterior tissue with the adjacent posterior cells. Since the weak spot is in a position where such an ectopic

boundary results in a new wing field, an ectopic wing will form. This would be mostly consistent with the Boundary Zone Model proposed by Hans Meinhardt (Meinhardt, 1983). It also explains how such a positional discontinuity/abnormality is formed without grafting or making a very large cut in the disc. This can be easily tested by examining the discs that may be undergoing transdetermination for P to A transformations via examining Ptc and Ci staining, and En staining to see if En is becoming silenced before transdetermination manifests. Reduction of *en* levels should suppress the *tara*^{1}/+ transdetermination phenotype.

An alternative hypothesis is that in addition to *engrailed*, *taranis* is also able to protect the *vestigial* locus directly from being ectopically activated by JNK signaling independent from positional information. This could be tested for by examining the expression of Vg, or the activity of its enhancers via *vgBE-lacZ* and *vgQE-lacZ*, and this ectopic Vg activity is found in the weak spot that does not have a P to A transformation. Consistent with this, the transdetermined wings should only have either anterior or just posterior structures. Reduction of the dose of *vg* should also suppress the *tara*/+ transdetermination phenotype. This hypothesis is attractive because it is in violation of both classic models of regeneration/transdetermination in imaginal discs: The Boundary Zone Model (Meinhardt, 1983) and the Polar Coordinate Model (French et al., 1976). This new model, which I am naming “The Guardian Model”, simply posits that wound-induced signaling is able to directly alter the expression of a number of essential

cell fate specification genes such as *engrailed* and *vestigial*, depending on the context. It would be interesting to see how the embryological manipulation experiments of the late 1960s to the early 1980s can be rationalized into this new model, provided the second hypothesis is correct.

Potential Deep Conservation of the role of TRiP-Br/Sertad Proteins during Regeneration

The fact that all regenerating animals experience signaling that they normally don't experience as adults/juveniles after injury points to a need for a protective mechanism to prevent unwanted side-effects of this signaling such as cell fate changes, excessive fibrosis, or tumor formation (Eming et al., 2014; Khan et al., 2016a; Seifert and Muneoka, 2018; Tanaka, 2016). Therefore, homologs of *taranis* may fit this role in other models of regeneration. However, other proteins may have evolved to perform this function in other species as well. Intriguingly, the homologs of *taranis* (or *taranis* itself), the Trip-Br/Sertad proteins, were either present (but not significantly upregulated relative to undamaged) or upregulated during regeneration. These include regenerating spinal cord of zebrafish (upregulated) (Hui et al., 2014a), as well as the regenerating tail of *Xenopus tropicalis* (present) (Love et al., 2011) and the regenerating axolotl limb (upregulated) (Voss et al., 2015). Transcriptomes from the *Drosophila* midgut also have *taranis* transcripts upregulated during midgut regeneration (Chakrabarti et al., 2012), which is a form of homeostatic regeneration (Jiang et al., 2016). These data point to the exciting potential that *taranis* and its homologs

may be important for regeneration in multiple systems in addition to its role in imaginal disc regeneration. However, functional data is still lacking after 3 years, which is understandable due to the slower experimental timescale for other model systems for regeneration. Bioinformatic searches for Zelda is problematic due to it not being obviously conserved among species outside of Panarthropoda (Ribeiro et al., 2017). However, many known pioneer factors may be able to function in a similar way as Zelda in other contexts, and there is a plethora of zinc-finger transcription factors that could potentially substitute for it in other species. Therefore this discussion will focus on *taranis* and other Sertad proteins.

Since the publication of the initial *taranis* paper, a number of regeneration transcriptome studies have come out for other non-model or “emerging” model organisms that have implications of both deep evolutionary conservation of *taranis*’s homologs being involved in regeneration. Upon mining these transcriptomes, I found a number of Sertad mRNA present or upregulated within the blastema of these organisms. The first study was performed in the African Spiny Mouse *Acomys cahirinus* (Gawriluk et al., 2016), an exciting emerging model that can regenerate its back skin after autotomy and completely regenerate 4-8mm hole punch wounds in their ear pinnae (Gawriluk et al., 2016; Seifert et al., 2012). They compared this regeneration transcriptome and compared it to the regeneration-incompetent *Mus musculus* ear hole punch transcriptome. Excitingly, within this dataset, there were three different Sertad mRNAs upregulated within the *Acomys* blastema, and all three were significantly

up compared to the *Mus* injured ear tissue, with variations on when this upregulation was apparent (Gawriluk et al., 2016). Among the three, Sertad3 had the most exciting dynamic expression pattern, where it peaked at the time when the blastema forms and is maintained at relatively high levels when the blastema is proliferating (Gawriluk et al., 2016; Ashley Seifert personal communication). It would be interesting to see what tissues express Sertad3 and if they differ from the tissues expressing of Sertad2 and Sertad4. Indeed, it would be interesting if there is a bias to which progenitors express which Sertad protein. It would also be very interesting to see if tissue-specific knockout of Sertad3 in *Acomys* results in fate transformations much like what is seen in the regenerating imaginal discs mutant for *taranis* (Schuster and Smith-Bolton, 2015). However, transgenesis is *Acomys* has still yet to be established, so this experiment may take some time to perform. An alternative experiment would be to see if overexpressing Sertad3 in the regeneration-incompetent ear wound of *Mus* would be able to rescue certain aspects of the regenerative response, or in combination with growth factor administration.

Another open question of *taranis* and its homologs is when its function was co-opted into a regenerative program. Do all regeneration-competent animals use Sertad proteins during regeneration? Is this function conserved? A way to answer this question would be to investigate *taranis*/*sertad* function in a diverse array of phyla at critical evolutionary nodes. Before 2018, the only transcriptomes that show *sertad* family transcripts in their regeneration datasets are in

vertebrates and *Drosophila* (see above), which is a very narrow view of the diversity of life on the planet. Excitingly, there has been some recent headway in looking at other regeneration transcriptomes in emerging model organisms. *Nematostella vectensis* is a cnidarian, which are the sister group to the Bilaterians (Layden et al., 2016). They are emerging as a model system to identify extremely conserved developmental processes and how they arose early in animal evolution. In theory, conserved mechanisms found in *Nematostella* are indeed very ancient, which is referred to as Deep Homology (Shubin et al., 2009). They are known to regenerate their entire body after amputation, including tentacles and pharynx (Layden et al., 2016). A recent study obtained regeneration transcriptomes over the entire course of regeneration (0-144 hours post amputation) and during the first 240 hours of embryonic development and also developed a database so search for candidates (Warner et al., 2018). In this database, Sertad2 and Sertad4 were both present during regeneration and development of *Nematostella*. Their embryonic expression pattern was low during the blastula and gastrula stages, then was up in the stages that were undergoing organogenesis. During regeneration, Sertad2 and Sertad4 mRNA levels remained relatively constant, peaking at the wound healing stages then dropping down to undamaged levels. This regeneration pattern is inconsistent with the kinetics of *taranis* transcription that occur during the late stages of blastema growth and repatterning (Schuster and Smith-Bolton, 2015), but a relatively stable expression pattern isn't necessarily indicative of a lack of function. Indeed, many developmentally important genes are rather stable in their

expression kinetics and do not change much over time once they are activated such as the PcG or TrxG proteins (Kassis et al., 2017), or Mad (Smad) (Campbell and Tomlinson, 1999a). Another likely possibility is that Taranis/Sertad proteins are post-transcriptionally modified, and may respond to pro-regenerative signals at the level of PTMs such as phosphorylation/dephosophorylation. Indeed, it is known that Sertad1 is phosphorylated and that PP2A-mediated dephosphorylation is critical for Sertad1 function in cultured mammalian cells (Zang et al., 2009), and Taranis is found to be at a higher molecular weight than predicted on Western blots, suggesting that it is post-translationally modified in the adult *Drosophila* brain (Afonso et al., 2015). The mere presence of Sertad proteins during regeneration suggests that they may have a function, and it would be interesting to knock-out *sertad2* and/or *sertad4* to see if there is a regeneration-specific patterning defect, or if there is a developmental defect as well.

Butterfly Eye Spots

Due to the homologs of *taranis*, the Trip-Br/Sertad proteins, being found in virtually all metazoans, from *Nematostella* to *Homo sapiens*, we expect that similar mechanisms cell fate protective mechanisms are in play in other regenerative contexts in a wide variety of species. It is up to the regenerative biology community to identify the breadth of roles that the Sertad proteins have in various regenerative phenomena. I will detail one hypothesis in regards to an order within holometabolous insects, the *Leptidoptera* (butterflies and moths) and

a potential role for JNK induced cell fate changes and the potential ability of *taranis* in this these species. In *Lepidoptera*, perhaps the most striking developmental feature is the vast complexity of wing color patterns found in ~140,000 different species of butterflies and moths within this order. These colors are derived from signals found in the late larval and pupal wings, and can be made of either pigment or structural color (Dinwiddie et al., 2014; Parchem et al., 2007; Protas and Patel, 2008). One particular pattern on various species of Lepidopterans is the eyespot, which functions to deflect predators into attacking the non-essential wing instead of attacking the essential body parts within the center (Prudic et al., 2014). The development of these eyespots have garnered great interest among developmental biologists, due to them being a classic example of cooption of previously used developmental gene regulatory networks found in the developing wing imaginal disc of the larvae (Monteiro, 2015). It has been shown by pioneering experiments by H. Frederik Nijhout, Vernon French, and Paul Brakefield done on the developmental organizing region of the eyespot, the focus, that ectopic eyespots form when cautery-induced damage is performed on pupal wings of various butterfly species (Brakefield and French, 1995; French and Brakefield, 1992; Nijhout, 1985; Nijhout and Grunert, 1988). Damage induces a focus, which is associated with wound-induced Wg expression, along with other eyespot-associated genes such as pMad, Dll, Sal, and En (Monteiro et al., 2006). Since a developing focus expresses En (Brunetti et al., 2001; Keys et al., 1999), and ectopic En is observed after damage (Monteiro et al., 2006); it is tempting to speculate that damage could also induce

a similar JNK-En-Tara pathway, leading to a new eyespot. It will be important to determine the functional role of En during normal development of the butterfly wing, which has yet to be done despite other developmentally important molecules being investigated (Monteiro et al., 2013; Özsu et al., 2017; Stoehr et al., 2013). Of course, JNK signaling and Tara reagents will need to be developed as well. One would expect Taranis to not be expressed in the pupal wing, yet expressed in the larval wing disc, since damage to larval imaginal discs in *Precis coenia* fail to induce ectopic eyespots (Nijhout and Grunert, 1988), implicating a potential protective context during larval wing development that is lost after metamorphosis. Bringing it back to *Drosophila*: It is currently not known when the developing wing loses its ability to upregulate *tara* expression in order to perform its protective function. One would expect *tara* to not be induced past the regenerative refractory stage in late 3rd instar wing imaginal discs much like many essential signaling proteins have a reduced/altered expression in these regeneration-incompetent discs (Harris et al., 2016; Smith-Bolton et al., 2009) as well as in the pupal wings of *Drosophila*, which are only able to undergo simple wound healing (Weavers et al., 2016). However, if *tara* has stage-specific functions in response to damage, we may still see *tara* expression reacting to tissue damage. I believe that this potential project can be a great project for a future Smith-Bolton lab member that is interested in branching-out into emerging model organisms and wants to answer evolutionary questions in imaginal disc regeneration, which has yet to be addressed by anyone in the field. Introduction of butterflies into the lab should be relatively strait forward for a *Drosophila* lab.

Neurodevelopment, neurophysiology and neurodegeneration

It is known that *taranis* is also function in neurons and during neurodevelopment. Indeed, *taranis* was initially identified in a screen for modifiers of the polyhomeotic extra sex combs phenotype. Sex combs are derived from sensory organ precursors (Kopp, 2011), so they may be sensitive to *tara* levels simply due it being required for SOP formation in the sex combs. Transcripts of both *tara* isoforms are enriched in the embryonic (Calgaro et al., 2002) and larval (Manansala et al., 2013) nervous systems, which also pointed to a neural function. Indeed, in the developing larval brain, *taranis* is essential for proper neuroblast proliferation patterns through E2F/Dp (Manansala et al., 2013). Intriguingly, Zelda is also highly expressed in embryonic (Pearson et al., 2012) and larval nervous systems and is essential for proper asymmetric cell division of neuroblasts in the larval brain (Reichardt et al., 2018). This suggests that the Zelda→Taranis connection may be found in different cell types. It would be interesting to see if Zelda activates *taranis* expression in neuroblasts.

On the same day that my *taranis* story was published online, another *taranis* paper was published detailing the role of taranis and circadian rhythm-independent sleep, where it functions with CyclinA/cdk1 in the neurons within the pars lateralis region of the adult brain to promote sleep in *Drosophila* (Afonso et al., 2015), thus connecting a role of *taranis* in the adult brain. Taranis is expressed in almost every neuron of the *Drosophila* brain (Afonso et al., 2015), which likely points out other roles of Taranis. It would be interesting to see if

Taranis preserves cell fate in the face of regenerative signals after needle injury in the adult Drosophila brain, which regenerates its neurons after such an injury (Fernández-Hernández et al., 2013). There is also another connection with sleep that I believe will be a very fruitful line of investigation, specifically in regards to neurodegeneration. In a *Drosophila* model for amyloid-β (Aβ42) induced Alzheimer's Disease, sleep is severely disrupted much like happens in human patients (Song et al., 2017). The authors found that Aβ42 induces JNK signaling in the PDF neurons, which results in aberrant arborization of the PDF neuron's axons in the pars intercerebralis region of the brain and therefore results in aberrant sleep patterns in this model (Song et al., 2017). Due to my discovery that Taranis is essential for protecting regenerating imaginal disc cells from the detrimental side-effects of JNK signaling (Schuster and Smith-Bolton, 2015), and that *taranis* is also essential for sleep (Afonso et al., 2015), it would be tempting to speculate that *taranis* might be important for protecting neurons from JNK signaling that occurs in these neurons, and perhaps other neurons to prevent neurodegeneration. In fact, the devastating neurodegenerative disorder known as Amyotrophic Lateral Sclerosis (ALS) is thought to be caused by excessive stress signaling results in JNK activation and death of motor neurons (Shenouda et al., 2018; Taylor et al., 2016). *Drosophila* models of ALS do exist, and intriguingly a recent RNAi screen showed that decreasing the levels of certain chromatin remodelers suppress or enhance the pathological symptoms of this devastating disease in the fly model (Berson et al., 2017). A simple experiment to test for a potential beneficial role of Taranis/Sertad proteins would be to

overexpress Taranis or its homologs in the motor neurons of ALS models (mice and/or flies) and see if this can protect these animals from neurodegeneration and suppress the pathogenic phenotype. This approach may be feasible, since Sertad1 has functions in the brain of mice. Indeed, mice that have *sertad1* knocked-out exhibit behavioral symptoms of depression (Hu et al., 2017), and therefore may have functions in other neurons in other contexts. Mouse neurons that have *sertad1* knocked-out also have higher rates of cell death *in vitro* (Biswas et al., 2010), also pointing to a function of Sertad proteins in preventing neurodegeneration. Sertad2 is also known to respond to ER stress in human and mouse visceral fat-derived adipocytes through GATA3 (Qiang et al., 2016b, 2016a), which points to a potential general role of Sertad proteins being important for responding to stress signaling, and may be essential for resolving the stress-induced unwanted side-effects and is open for the potential to be dysregulated in disease.

Closing Remarks

In conclusion, I have shown that the extremely understudied Sertad proteins, which Taranis is a co-founding member, are worth investigating in other model systems. Sertad proteins likely have roles during regeneration in a diverse array of phyla, and should be a fruitful target for functional studies. In addition to regeneration, I speculate that *taranis* may also be involved in regeneration-related processes such as transdetermination and the formation of butterfly eyespots after wounding. It may also be likely that Zelda, or other pioneer

transcription factors, are also involved in these processes that use *taranis*/*sertad* function. Finally, I go into the potential of protective factors to be essential for preventing devastating degenerative diseases (e.g. neurodegenerative disease such as ALS), which are viewed as the principle therapeutic targets of regenerative medicine and therefore the most likely application of regeneration research. It is my hope that my discoveries, and discoveries that are built off of my original findings will result in fundamental insights in development, regeneration, and disease.

Appendix A: Generation of Tools for the Biochemical Characterization of Taranis

Introduction

Proteins in the Trip-Br/Sertad family are an enigmatic group of transcriptional co-factors and/or scaffolding proteins found in most metazoans. They all share structural homology with each other where they have a conserved domain known as the SERTA domain (Serta standing for the first three proteins discovered with the domain: SEI-1, RBT1, and Taranis), which is thought to be important for protein-protein interactions primarily through CDK4 (Hirose et al., 2003; Li et al., 2004; Sugimoto et al., 1999). Sertad proteins also have a C-terminal PHD-Bromodomain binding domain, which is thought to be important for binding to chromatin remodelers (Calgaro et al., 2002; Hsu, 2001), a C-terminal acidic transactivation domain, and an N-terminal CyclinA-binding domain.

The Sertad proteins were initially identified as transcriptional coregulators that modulate the activity of the cell cycle in cultured mammalian cells by binding to E2F/Dp (Hayashi et al., 2006; Hsu, 2001; Sim et al., 2004) thus modulating E2f-dependent transcription, and various Cyclin/cdk complexes to control cell cycle progression (Li et al., 2004; Sim et al., 2004, 2006a, 2006b; Sugimoto et al., 1999). Subsequent analysis revealed interactions with other transcription factors such as p53 (Lee et al., 2015; Watanabe-Fukunaga et al., 2005), p300/CBP

(Hirose et al., 2003), cJun (Tategu et al., 2008), PCAF/Gcn5 (Lai et al., 2007), Smad1 (Peng et al., 2013), I-mfa (Kusano et al., 2011), and pparɣ (Liew et al., 2013). However, recent findings have challenged the notion that the Trip-Br/SERTAD proteins are solely transcriptional cofactors and regulators of the cell cycle, and that some Sertad proteins are also found in the cytoplasm. Indeed, Nedd4-1 (an E3 ubiquitin ligase), which is a major component for the proteasomal machinery, has been implicated in SERTAD function (Hong et al., 2014; Jung et al., 2013; Shrestha et al., 2017). Sertad1/p34^{SEI-1} has been shown to directly interact with Nedd4-1 and is essential for Nedd4-1's ability to ubiquitinate PTEN (Hong et al., 2014; Jung et al., 2013; Shrestha et al., 2017). Sertad1/p34^{SEI-1} also binds directly to XIAP (Hu et al., 2017; Jung et al., 2015) to ubiquitinate adenyl cyclase to induce its proteasomal degradation both in vitro and in vivo (Hu et al., 2017). PP2A is another cytoplasmic protein that is known to interact with Sertad1/p34^{SEI-1} (Zang et al., 2009). PP2A might function to allow for a dephosphorylated Sertad1/p34^{SEI-1} to translocate into the nucleus to induce E2F-dependent transcription after an unknown signaling pathway induces this dephosphorylation of Sertad1/p34^{SEI-1}.

Despite a decent amount of studies done in regards to in vitro biochemistry, and cell biological roles in mammalian cell lines, in particular immortalized cancer cell lines, the biological (*in vivo*) roles of the Sertad proteins in animal models is not well understood. Sertad1/p34^{SEI-1} is important for pancreatic beta cell proliferation by preventing p21 accumulation downstream of KLF10 (Wu et al., 2015),

SERTAD1 mutants also exhibit neurological disorders such as depression (Hu et al., 2017). It was also shown to be important for neuronal cell death in response to the prion protein amyloid beta (Biswas et al., 2010) *in vitro*. Sertad1/p34^{SEI-1} was also found to be expressed in embryonic mouse hearts, and is able to bind with Smad1to enhance Smad1-dependent transcription in cardiomyoctes (Peng et al., 2013). However, the functional relevance of this interaction was not investigated. Perhaps the most surprising result was that Sertad1/p34^{SEI-1} is induced in the innate immune response in response to viral infection in vampire bats (Glennon et al., 2015).

Sertad2 is another Sertad protein whose biological function in vivo is becoming unraveled. Sertad2 was found to be essential in thermogenesis and fat metabolism through the transcription factor Pparɣ (Liew et al., 2013). It was further demonstrated that it is induced by the obesity-induced ER stress pathway in brown (Qiang et al., 2016a) and white adipocytes of visceral fat in mice (Qiang et al., 2016b). Sertad2 was also found to be upregulated in human tumors, and is sufficient to transform mouse fibroblasts to a tumor-like phenotype (Cheong et al., 2009).

Among the Sertad proteins, Sertad3/Rbt1, Sertad4/Cdca4, and Sertad5 have the least well characterized in vivo functions. Sertad3/RBT1 has only been shown to be amplified in tumors and promotes tumor growth (Darwish et al., 2007).

Cdca4/Sertad4 Is expressed in a number of embryonic (Bennetts et al., 2006) and adult tissues (Hayashi et al., 2006) in mice. Despite having a number of interesting expression patterns, Cdca4 has yet to be knocked-out in vivo. Therefore, its function in tissues is still unknown. Sertad5 is completely uncharacterized in both cultured cells and in animal models, so its role in any biological process is a mystery.

Drosophila has two Sertad proteins in its genome, *CG2865* (Guest et al., 2011; Lee et al., 2003) and *taranis* (Calgaro et al., 2002; Fauvarque et al., 2001). The biological function of *CG2865* is not known, but it has been found to be upregulated in salivary glands undergoing steroid and radiation-induced apoptosis (Guest et al., 2011) and in an RNAi screen for cell cycle regulators in S2R+ cells (Guest et al., 2011), which may point to a role in compensatory proliferation and/or AiP. On the other hand, *taranis* function has been studied to some extent by other labs. Taranis was initially identified in a forward genetic screen for suppressors of the extra sex combs phenotype of *polyhomeotic* (*ph*) (Fauvarque et al., 2001), and was later shown to be able to dominantly modify polycomb group (PcG) and trithorax group (trxG) mutations. Taranis is able to suppress various PcG members such as *Polycomb* (*Pc*) and *ph* and enhanced trithorax group mutations such as *trithorax* (*trx*), *brahama* (*brm*), and *osa* (Calgaro et al., 2002). The biochemical basis of this genetic interaction is still not known, but recent genetic evidence suggests that Tara recruits Pc to certain loci in *Drosophila* embryos and larval salivary glands (Dutta et al., 2017). However,

Pc and Tara do not physically interact, nor do they co-localize at the same loci thus putting doubt in those claims (Dutta et al., 2017). The first in vivo evidence for a role of *taranis* was that it was essential for proper neuroblast proliferation patterns in the larval brain (Manansala et al., 2013). This phenotype was largely through E2f/Dp, much like what is found in studies on cultured mammalian cells with other Sertad proteins (Hayashi et al., 2006; Hsu, 2001; Manansala et al., 2013; Sim et al., 2004). It was recently shown that taranis is required for sleep independent of circadian rhythm via an interaction with CyclinA/cdk1 in a subset of neurons in the pars lateralis region of the adult *Drosophila* brain (Afonso et al., 2015).

We've recently identified a mechanism where *taranis* acts as a protective factor that prevents inappropriate cell-fate changes that are induced by JNK signaling during the regeneration of wing imaginal disc (Schuster and Smith-Bolton, 2015) (See Chapter 2). Intriguingly, *taranis* is required for posterior cell fate only during regeneration. It functions to stabilize the levels of the posterior selector gene *engrailed* (*en*), which was destabilized by early JNK signaling. This prevents *en* from entering an autoregulatory silencing loop mediated by *ph*. This pathway was determined purely by genetics and analysis of gene expression patterns, but the molecular mechanism has yet to be determined. Indeed, we hypothesize that Tara binds to the *en* locus directly, perhaps by displacing the AP-1 transcription factor off of the *en* enhancer/PRE. In order to test this hypothesis, we needed to generate reagents to assess protein binding to the *en* locus. The simplest way to

test this hypothesis is to perform Chromatin Immunoprecipitation (ChIP) of Tara at the *en* locus during regeneration and in undamaged conditions while also looking at the binding of Jun at the same locus in wild type and $tara^{1}$/+ regenerating discs. As a first step to test this hypothesis, I wanted to generate a ChIP-quality rabbit polyclonal antibody against Tara. However, due to recent findings that other Sertad proteins have cytoplasmic functions, we don't know if Tara functions as a transcriptional cofactor or if it exerts its protective function in the cytoplasm. Therefore the biochemical mechanism of Tara in regenerating wing imaginal discs is still unknown, and my current hypothesis on how Tara acts during regeneration has a decent probability of being incorrect. Thus, it is essential to generate the tools to investigate Tara protein function. In this chapter, I will detail my efforts to purify both full-length Tara and portions of the Tara protein to generate an epitope for further antibody generation and the pitfalls experienced during this two year period of my PhD.

Results

Taranis does not function through E2F1/Dp to protect cell fate

The vertebrate homologs of *taranis*, the Trip-Br/Sertad proteins have been shown to physically interact with Dp of the E2F/Dp complex to promote cell cycle progression in human and mouse cell lines (Hayashi et al., 2006; Hsu, 2001; Sim et al., 2004), and *tara* is known to genetically interact with both E2f1 and Dp in larval neuroblasts in *Drosophila* (Manansala et al., 2013). Therefore one could

consider the Tara-Dp/E2f interaction as the “canonical” mode of action for Tara and the other Sertad proteins. Therefore, I hypothesized that Tara might be functioning through the E2f/Dp complex during regeneration. This hypothesis is attractive due to the blastema having enhanced E2f activity, as assayed by PCNA-GFP (Smith-Bolton et al., 2009). To test to see if Tara functions through E2f1/Dp during regeneration, which would simplify preliminary biochemical analysis by simply studying E2f/Dp directly, I tested to see if heterozygosity for *E2f1*^{rM729} (Duronio et al., 1995) and *Dp*^{a1} (Royzman et al., 1997) mutants were able to induce P to A transformations during regeneration. I found that neither *E2f1*^{rM729}/+, nor *Dp*^{a1}/+ mutants were able to significantly increase the amount of P to A transformations compared to *w*^{1118} (Fig. 14A-B). To rule out a possibility that *Dp*^{a1} might not be a strong enough allele to cause a P to A transformation phenotype, *Dp*^{a1}/+*; tara*^{1}/+ mutant flies were generated and tested for the ability of *Dp*^{a1}/+ to enhance the *tara*^{1}/+ transformation phenotype. *Dp*^{a1} was unable to enhance *tara*^{1}-induced P to A transformations (Fig. 14A-B). Therefore, Tara likely does not interact with E2f/Dp during regeneration in order to carry out its protective function. In addition to E2F/Dp, Tara is also known to interact with Cyclin A (CycA) in the adult brain to control sleep (Afonso et al., 2015). A role for CycA is not known for imaginal disc regeneration, so as a first pass experiment, I stained for CycA protein in undamaged and regenerating discs at R24 and R48 (Fig. 14C-E) to see if CycA expression levels correlate with *tara-lacZ* expression (Fig.3A-C, Fig. 10A-C). I found that CycA is expressed at low levels in undamaged 3rd instar wing imaginal disc epithelial cells, and is enriched in what

is likely the myoblasts near the notum (Fig. 14C). Surprisingly, CycA levels were not upregulated within the blastema during regeneration, nor is it clear that CycA is expressed in the disc proper at all (Fig. 14D-E), which suggests that CycA is not co-regulated with Tara expression and therefore is an unlikely binding partner of Tara in this context. Of course, a more robust test would be to see if *CycA* mutants can phenocopy the *tara* phenotype. While this does not completely rule-out Taranis interacting with other E2fs or Cyclin A, this data was convincing enough for us to move on to the possibility that a “non-canonical” mechanism of Taranis function is at play, and that reagents to assess Taranis protein directly are desperately needed.

Taranis protein trap lines produce nonfunctional proteins

Before attempting to generate new reagents to study Taranis function, we wanted to test to see if any available reagents could suffice to examine Tara protein function. Tara, being an understudied protein, does not have a wealth of reagents to investigate protein function. There are two publically available protein trap lines generated through a large-scale GFP protein trapping project (Buszczak et al., 2007) that were predicted to be inserted within the intron of the *taranis* gene whose expression pattern and functionality were uncharacterized. The first test was to assess whether these protein trapped GFP::Tara lines have retained functionality, I crossed each line with the deficiency line that deletes the entire taranis locus, *Df(3R)ED10639* and assessed when the transheterozygous animal die during development (Fig. 15A). As a positive control,

tara^{1}*/Df(3R)ED10639* larvae die sometime in the first larval instar, since homozygous 2nd instar larvae were never found. The *tara*^{1} allele is the strongest known allele of *tara*, with *tara*^{L4} being considered the same strength by some (Calgaro et al., 2002). The *tara*^{1} allele is likely a genetic null, but the lack of molecular characterization of homozygous mutants so far still leaves a small possibility that it is a strong hypomorph. The GFP trap line *tara*^{YD0165} is also either a strong hypomorph or null, since we never see *tara*^{YD0165}*/Df(3R)ED10639* larvae in the second instar much like *tara*^{1}*/Df(3R)ED10639* larvae. However, we found that the second GFP trap line *tara*^{YB0035} might be either a weak hypomorph, or a non-mutant due to *tara*^{YB0035}*/Df(3R)ED10639* animals surviving to adulthood with no outwardly visible defects. However, the line was never able to lose the TM6B balancer despite 3-4 years of propagating the stock, which suggests that the *tara*^{YB0035} allele is subviable. This is likely due to the homozygous adults being infertile, or sub-fertile. Other combinations of hypomorphic *tara* alleles with *tara*^{1} do result in viable adults, which have defective sleep patterns (Afonso et al., 2015). Thus it is not surprising that this allele is at least partially defective in some contexts. As a control for hypomorphic allele phenotypes: we tested another known allele of *tara*, *tara*^{03881}*,* which is clearly a hypomorph since we find escaper *tara*^{03881}*/Df(3R)ED10639* larvae in the wandering third instar. Most animals die at the pupal stage, but some larvae died earlier in the 3rd instar. Looking at the approximate insertion sites of these two GFP traps, I found that they were located in areas that would trap a different combination of alternative isoforms of the *taranis* gene, *tara-α* and *tara-β* (Fig. 15B). The YB0035 insertion

was found to be in the intron downstream of the first exon of *tara-α*, yet upstream of the *tara-β* start site. This would be predicted to just trap *tara-α* and not *tara-β* and is therefore should just reflect the expression pattern of Tara-α. Conversely, the YD0165 insertion is inserted downstream of the *tara-β* start site but before the second exon that is shared between both isoforms (Fig. 15B). This could result in one of two scenarios: this would either trap the Tara-β protein alone, or more likely, trap both isoforms. This second hypothesis is favored due to the $tara^{YD0165}$ allele has a stronger phenotype when crossed with the *Df(3R)ED10639* deficiency compared to the $tara^{YB0035}$ allele (Fig. 15A).

Due to t*ara*^{YD0165} and $tara^{YB0035}$ likely being mutant alleles of *taranis* based on crosses with the deficiency line, I was concerned that these mutants will not give a functional protein that will be sufficient to perform molecular and biochemical analysis of the Tara protein. Consistent with this, I found that both $tara^{YD0165}$/+ and $tara^{YB0035}$/+ resulted in strong P to A transformations in adult regenerated wings (Fig. 15C-F). This confirmed that these GFP::Tara fusion proteins are non-functional. We did find GFP expression in undamaged and regenerating wing discs in both lines (Fig. 15G-L), suggesting that they do not undergo nonsense mediated decay. Much like what was found with *tara-lacZ* expression during regeneration, both lines exhibited ubiquitous and low expression of GFP::Tara in undamaged 3rd instar discs (Fig.15G, J), no upregulation at R24 (Fig. 15H, K) and was upregulated at R48 (Fig. 15I, L). However, the degree of GFP::Tara upregulation was not as drastic as was found with *tara-lacZ* (compare Fig. 10C to

Fig. 15I and Fig. 15L), and some R48 discs did not have obvious upregulation in the blastema compared to the undamaged notum (data not shown). This can be explained by a number of possible scenarios. This could simply be a consequence of differential dynamics between mRNA expression and protein translation where *tara* mRNA is transcribed at or shortly before R48, but might be translated a few hours later. Another possibility is that the nonfunctional GFP::Tara fusion proteins are targeted for degradation soon after their translation and folding, and the observed GFP fluorescence in the discs that do have upregulated GFP::Tara are simply a snapshot of Tara::GFP not being fully degraded. A simple test of this would be to observe Tara::GFP expression 6-12h later than the last time point examined. Intriguingly, both lines had different subcellular localization of the GFP::Tara. GFP::Tara was found to be expressed in both nucleus and cytoplasm in $tara^{YD0165}$/+ regenerating discs (Fig. 15G-I) compared to the strictly nuclear localization and lower GFP levels in the $tara^{YB0035}$/+ regenerating discs (Fig. 15J-L). This could be explained simply due to the Tara-α protein has a predicted NLS sequence in its N-terminus (data not shown), whereas the Tara-β protein does not (data not shown). Therefore, $tara^{YD0165}$ GFP protein trap would be expected to reflect both the cytoplasmic localization of Tara-β and the nuclear localization of Tara-α. These data taken together convinced us that these protein trap lines are inappropriate reagents to study protein function. Therefore, we elected to make our own Tara reagents. We believed that the most prudent move would be to generate a polyclonal antibody

against Taranis, with generating CRISPR edited tagged Tara lines with smaller epitopes than GFP as a backup project.

Problems with the current polyclonal antibody against Taranis

On the same day of the publication of my first *taranis* story (Schuster and Smith-Bolton, 2015), another lab published a study on Taranis's role in sleep in the adult *Drosophila* brain (Afonso et al., 2015). There they demonstrated that taranis was required for maintaining sleep, independent of circadian rhythm. They generated a rabbit polyclonal antibody using an epitope that was generated near the N-terminus of Tara, which I will call Tara$^{S68\text{-}H234}$. Unfortunately, they left all of the biochemical work to a biotech company, so the actual methodology of generating this antibody is not shown. They subsequently demonstrated that Tara physically and genetically interacts with Cyclin A (CycA), and that this complex functions through cdk1 in a subset of CycA^{+} neurons of the pars lateralis region of the brain. However, this antibody appears to have a number of problems. While the antibody does detect endogenous Tara, it has additional faint bands that may either be degradation products, as the authors suggested, but could also simply be non-specific binding of proteins that are closely associated with Tara. They also mentioned that the antibody did not work for immunostaining, which strongly suggests that the epitope is hidden when the Tara protein is in its native configuration. Therefore this antibody is not going to work with chromatin immunoprecipitation (ChIP), which is the primary reason why we want to generate a Tara antibody ourselves. An additional concern of

their methodology was reliance on the *tara*^{YB0035} protein trap line to assess Tara localization. As shown above, this is not a good strategy since *tara*^{YB0035}/+ animals have a strong *tara*/+ regeneration phenotype (Fig. 15D-F). Due to these problems, we elected to generate our own antibody against Tara.

Cloning and purification attempts of Taranis

In-depth biochemical characterization of any protein requires the generation of a specific antibody against your protein of interest at the bare minimum, with a purified full-length protein in the native conformation being the gold standard for biochemical analysis of protein function *in vitro*. Animals transgenic for epitope-tagged fusion proteins offer an adequate secondary approach, but is hampered by the need to grind-up whole tissues which makes obtaining the required minimum amount of material to perform even the most basic biochemical experiment technically challenging. This also eliminates the ability to perform *in vitro* experiments with defined components, which will complicate the interpretation of biochemical results. Therefore, I elected to generate a polyclonal antibody against the full-length Tara protein, or fragments of the protein. These results are summarized in Table 1. The examples given here are the best attempts given for each construct. To generate a fusion protein, I needed to clone part, or all of the *tara* sequence into an epitope tagging vector. With the exception of GST::Tara$^{N6\text{-}A860}$ that was generated via traditional restriction cloning, all constructs were generated via Gibson Assembly (Gibson et al., 2009) into the pET28a vector (Table 1). After successful cloning of each insert into the

vector, each line was tested for successful induction of the protein via IPTG in BL21(DE3) *E.coli* cells. Every construct tested was able to be expressed in E. coli, but all fusion proteins were found in the insoluble aggregates known as inclusion bodies, regardless of induction temperature (Table 1, Fig. 16A, data not shown). Therefore Tara is a robustly insoluble protein in *E.coli* under the experimental conditions I have tested (which are not exhaustive), which required purification under denaturing conditions instead of the more strait forward purification of soluble proteins. The requirement of purifying the Tara fusion proteins eliminated the usefulness of the GST::Tara$^{N6\text{-}A860}$ protein, due to GST not being able to bind to glutathione beads when denatured (data not shown). However, the His tag is known to be able to bind to Ni-NTA beads under denaturing conditions, so the His-tagged Tara proteins were brought through purification protocols under denaturing conditions. I first attempted to purify full-length Tara (Tara^{FL}), however this protein was unable to bind the beads under all conditions tested, including a dual-tagged Tara with his tags at both ends of the protein (6xHis::Tara^{FL}::6xHis), which just eluted contaminants (Fig. 16B). Due to full-length Tara being impossible to purify under all conditions tested, I generated and attempted to purify fragments of the Tara protein. Each fragment was a half of the full-length Tara, one ending at the Serta domain (Tara$^{M1\text{-}K480}$) and the other starting at the Serta domain (Tara$^{Y432\text{-}S912}$). Both proteins were found to be insoluble (Fig. 16A, data not shown), so both were attempted to be purified under denaturing conditions. 6xHis::Tara$^{M1\text{-}K480}$::6xHis was able to bind to the beads to a noticeable degree but not by much and washed out considerably in the first

wash, but eluted effectively from the column. (Fig. 16C). Unfortunately, some contaminants were still found in the eluates. More experiments are needed to be done to enhance binding to the column and to minimize contaminants. I then tried to purify the C-terminal fragment of Tara, Tara$^{Y432-S912}$. 6xHis::Tara$^{Y432-S912}$::6xHis was able to bind to the column a little bit better than the N-terminal fragment, but still bound poorly compared to successful purifications done by others (Fig. 16D). Despite this weak binding, 6xHis::Tara$^{Y432-S912}$::6xHis did not wash-out as much and was able to elute off the column in a defined band (Fig. 16D). Of course, these eluates also contained some contaminating proteins, which means that more optimization is needed. In conclusion, Taranis is a very difficult protein to purify under a number of conditions with my hands. More work, especially with optimizing binding conditions, is required to successfully generate a pure epitope that will allow for the generation of a rabbit anti-Tara polyclonal antibody.

Taranis is predicted to be a highly disordered protein

Taranis is a very difficult protein to express and purify under most conditions, however it is unclear at first glance why this is the case. To get an understanding of the nature of the Taranis protein, I took a bioinformatics approach to see if there are any predicted structural abnormalities found in Tara protein. I used two programs that predict the relative structural stability and disorder based on the primary amino acid sequence of a protein (Dosztanyi et al., 2005; Prilusky et al., 2005). Foldindex calculates the likelihood a sequence of amino acids will fold into

a secondary structure (Prilusky et al., 2005), and IUPred predicts how disordered an amino acid sequence will be (Dosztanyi et al., 2005). I elected to look at the sequence of the Tara-β isoform of Taranis, which differs only in the first couple amino acids when compared to Tara-α and is thought to be functionally redundant with each other (Calgaro et al., 2002). I found that Tara is predicted to mostly be composed of unstructured stretches of amino acids, with the exception of a central region of structured amino acids likely to be the Serta domain, and a couple of longer stretches in the N-terminal region and the C-terminal region (Fig. 17A), which is consistent with the domain map provided by Calgaro et al., 2002. Looking at the tendency of a protein sequence to be disordered, Tara is enriched in mostly disordered amino acids stretches with relatively ordered sequences in the central and C-terminal regions of the protein (Fig. 17B). Therefore, Taranis is predicted to be a mostly unstructured, if not an intrinsically disordered protein. Taranis likely functions as a cofactor, so these disordered regions might become ordered when bound to another protein.

As a control to make sure that these bioinformatic programs can discriminate between well-structured proteins and intrinsically disordered proteins I used the sequences of known proteins that are known to be structured and disordered, respectively. As a control for a structured protein, I used the amino acid sequence of dGAPDH1 from the *Drosophila* genome browser and tested the sequence for foldability and tendency to be disordered. I found that dGAPDH1 is predicted to be a very well structured protein and has very little predicted

disorder in its sequence (Fig. 17C-D), as was expected. To control for a known intrinsically disordered protein, I used the amino acid sequence of a recently discovered Tardigrade intrinsically disordered protein, CAHS94063, that is essential for the Tardigrade's remarkable ability to survive desiccation (Boothby et al., 2017). As expected, the sequence of CAHS94063 is mostly composed of unstructured amino acid sequence (except for a small region in the N-terminus of the protein) and is highly disordered (Fig. 17E-F). Therefore these programs are able to accurately predict, to adequate degree, on how unstructured/disordered a protein is based on primary amino acid sequence.

Looking at the Tara data shown above (Fig. 17A-B), along with the results from the purification attempts of the Tara proteins and the inability of the Afonso antibody to recognize the Tara protein in its native conformation, I can make inferences on what I believe would be the most exposed region Tara will have *in vivo*. Tara is unable to bind the beads when the His tag is on either the N-terminus or the C-terminus of $Tara^{FL}$ under the currently tested conditions (Fig. 16B). Only when the center of the protein is exposed in the Tara N-terminal and C-terminal protein fragments is when Tara can bind to the beads in the column. Therefore, the N-terminus and C-terminus are likely both folded internally in the three dimensional structure. The N-terminus is also where the epitope of the Afonso antibody is generated against (Afonso et al., 2015) which cannot bind the native Tara protein. Therefore this region is also hidden in the 3D structure. The Serta domain is thought to be a protein-protein interaction domain, so it is likely

to be exposed when Tara is not binding to another protein, but might be partially or completely hidden when Tara is bound to another protein. The very C-terminal amino acids that have any appreciable predicted structure are thought to be in the PHD-Bromodomain binding domain and the C-terminal activation domain (Calgaro et al., 2002). Due to it being another protein-protein interaction domain, it is likely not going to be exposed at all times much like the Serta domain. Therefore, the region of Tara that is most likely to be exposed is the sequence in between the Serta domain and the PHD-Bromodomain binding domain. There is a stretch of around 50 amino acids, from pro650 to Ile700 that has a reasonable foldindex (Fig. 17A) and is only predicted to have moderate to low disorder tendency (Fig. 17B). Therefore future efforts in attempting to purify Tara should either focus on the $Tara^{Y432\text{-}S912}$ or generating a new peptide that corresponds to the $Tara^{P650\text{-}I700}$ region.

Discussion

This project was met with limited success due to a number of hurdles, and ultimately failed to generate a worthwhile epitope for generating a polyclonal antibody against Taranis after two years of work. There could be many reasons why this did not work. One reason may simply be technical, and more optimizations should be attempted. The second reason is likely intrinsic to the protein. Tara is much larger than any Sertad protein known to exist (Bennetts et al., 2006), and it is predicted to be very disordered with little appreciable secondary/tertiary structure (Fig. 17A-B). This makes purification of the protein in

its native conformation very difficult without co-expressing a chaperone that endogenously folds this disordered protein, or its co-factor.

Despite these difficulties in the purification of Taranis, other groups have been able to purify one of its mammalian homologs Sertad1/p34-SEI1 with great success (Hu et al., 2017). This study used a different buffer formulation and a different bacterial growth medium that I used, therefore it would be necessary to repeat these purification attempts using the Hu et al., 2017 protocol. However, there may simply be need to optimize the buffers in a systematic way to get the optimum purification conditions that are specific for Tara. There is also a need to optimize flow rate of the column.

Due to the attempts at purifying an epitope tagged Taranis being largely unsuccessful, an alternative approach to assessing Tara protein function may be needed. One way to do this is to use CRISPR/CAS9 gene editing to make an epitope tagged Tara in the endogenous locus (Baena-Lopez et al., 2013; Gratz et al., 2015). I suspect that P-element insertions within the taranis locus typically result in mutant proteins, or result in a decrease in transcription of the gene. Therefore “scarless” modification of the genome to make a tagged Tara appears to be the most prudent method to generate a tagged Tara *in vivo* (Baena-Lopez et al., 2013; Gratz et al., 2015).

Another way to generate an epitope-tagged Taranis in the endogenous locus is to use a recently developed strategy that takes advantage of MiMIC insertions and using Recombination Mediated Cassette Exchange (RMCE) to switch a GFP that is flanked by splice acceptor and donor sites into the MiMIC insertion (Nagarkar-Jaiswal et al., 2015). This would result in a potential fusion protein between the new MiMIC sequence and the gene it is inserted in. This will theoretically make a GFP tagged Taranis just by performing simple crosses. There are two MiMIC intronic insertion lines within the taranis locus which are homozygous viable (data not shown), which means that this experiment is feasible. Of course, I am highly skeptical of this working due to it requiring the use of the large epitope of GFP or RFP in the same approximate position as the previously generated protein trap lines that have strong *tara* mutant phenotypes (Fig. 15). It will nonetheless be worthwhile to attempt this due to the protocol just requiring crosses between different lines. In conclusion, despite the large amount of pitfalls found on this part of the Taranis project, there are numerous routes to overcome these hurdles for an ambitious grad student or postdocs in the future.

Materials and Methods

Ablation and regeneration experiments

Ablation experiments were carried out as previously described (Smith-Bolton et al., 2009) with a few modifications: induction of cell death was caused by overexpressing *rpr*, and animals were raised at 18^{o}C until 7 days after egg lay

(AEL) (early 3rd instar) before the temperature was shifted to 30ºC for 24 hours in a circulating water bath. For undamaged controls, animals with the same genotype as the experimental animals were kept at 18ºC and dissected at 9-10 days AEL, which is mid-late 3rd instar. Mock ablated animals are the siblings of the flies in the ablation experiments that experienced the same thermal conditions, but they inherited the *TM6B, tubGAL80* containing chromosome instead of the ablation chromosome. For adult wings, control undamaged animals were kept at 18ºC until after eclosion.

Fly Stocks

The following Drosophila stocks were used: *w^{1118}; rnGAL4, UAS-rpr, $tubGAL80^{ts}$/TM6B, tubGAL80* (Smith-Bolton et al., 2009), *w^{1118}* (Hazelrigg et al., 1984) (Referred to as "Wild-type" in Chapter 2), *$tara^{1}$* (Fauvarque et al., 2001), *$tara^{YD0165}$* and *$tara^{YB0035}$* (Buszczak et al., 2007) (obtained from the Flytrap Project via Lynn Cooley), *$E2f1^{rM729}$* (Duronio et al., 1995), and *Dp^{a1}* (Royzman et al., 1997). All fly stocks are available from The Bloomington Drosophila Genetic Stock Center unless stated otherwise.

Adult wings

Wings were mounted on glass slides in Gary's Magic Mount (Canada balsam (Sigma) dissolved in methyl salicylate (Sigma)). Images of individual wings were taken with an Olympus SZX10 dissection microscope with an Olympus DP21

camera using the CellSens Dimension software (Olympus). All images were taken at the same magnification (5X).

To quantify the P-to-A transformation phenotype in adult wings, all wings that reached to or past the tip of abdomen were considered fully regenerated and selected for quantification. The wings were scored for five anterior markers within the posterior compartment. These five markers included socketed bristles on the posterior margin, ectopic vein material on the posterior margin, an ectopic anterior crossvein (ACV) in the posterior wing blade, distal costa-like bristles on the alar lobe, and an anterior-like shape characterized by a narrower proximal and wider distal posterior compartment. The frequency of each marker was calculated independently for each genotype. In addition, these wings were scored on a scale of 0-5 markers to assess the strength of the P-to-A transformation in each wing. For all experiments, at least 3 replicates from independent egg lays were performed. Statistics were calculated and graphs were produced in Microsoft Excel. To calculate the Average Transformation Score, the final scores of each wing was averaged in each replicate. These averages were averaged to each replicate to get the scores listed on the graph. This allowed us to calculate SEM and perform a Student's t-test to assess statistical significance compared to Wild-type.

Immunohistochemistry

Dissections, fixing and staining were done as previously described (Smith-Bolton et al., 2009). Wing imaginal discs were mounted in Vectashield (Vector Labs). Antibodies used were mouse anti-Nub (1:200), which was a gift from Steve Cohen (Averof and Cohen, 1997) and was later deposited in the DSHB, mouse anti-βgal (1:100) (DSHB), rat anti-DECAD2 (1:100), mouse anti-CycA (DSHB). The Developmental Studies Hybridoma Bank (DSHB) was created by the NICHD of the NIH and is maintained at the University of Iowa, Department of Biology, Iowa City, IA 52242.

AlexaFluor secondary antibodies (Molecular Probes) were used at 1:1000. TO-PRO-3 iodide (Molecular Probes) was used as a DNA counterstain at 1:500. Specimens were imaged with either an LSM510 or LSM700 Confocal Microscope (Carl Zeiss). Images were compiled using ZEN Black software (Carl Zeiss), Photoshop (Adobe) or ImageJ (U.S. National Institutes of Health). All confocal images are maximum intensity projections from z-stacks unless otherwise stated.

Average fluorescence intensity was measured in ImageJ using images that were stained in parallel and imaged under identical confocal settings. The trace tool was used to circle the correct zone for quantification, and the measure tool was used to calculate average fluorescence intensity within the selected area and the area of the selection zone.

Cloning

All 6xHis tagged constructs were generated via Gibson Assembly, using the Gibson Assembly Kit (New England Biolabs) following the manufacturer's instructions, and were propagated in NEB5α E.coli strain. The Tara-β coding sequence found in the DGRC clone RE26467 was amplified using primers that overlapped with at least 15 nucleotides of the target region in the Tara-β CD and flanking the Eco53KI site within the MCS of the pET28a vector. PCR conditions required the use of Pfu Ultra DNA Polymerase (Aligent) with an extension time of 2 min per kb of insert. The primers for each construct were as follows:

For(pET28a-TaraFL)Gib1:

5'-GGATCCGAATTCGAGATGTGCACTGAGGTGAATTC-3'

Rev(pET28a-TaraFL)Gib1:

5'-AGCTTGTCGACGGAGCTAACTACCGACCATG-3'

Rev(pET28a-TaraFL-NoStop)Gib3:

5'-AGCTTGTCGACGGAGACTACCGACCATGTG-3'

For(pET28a-SERTA)Gib4:

5'-GGATCCGAATTCGAGTACAAGGACACGCGC-3'

Rev(pET28a-SERTA)Gib4:

5'-TTGTCGACGGAGCTTGGCCTCTGCTTC-3'

pET28a was linearized (blunt cut) with Eco53kI overnight and gel purified with the Quiagen Gel Purification Kit (Qiagen) alongside the amplified inserts. A target concentration of 20 ng/uL for insert and 10 ng/uL for vector was needed in order to have a successful assembly reaction. Insert and vector were mixed with the Gibson Assembly Master Mix and incubated for 1 hour at 50^{o}C in a S1000 Thermocycler (BioRad). The assembly reaction was transformed into NEB5α according to the manufacturer's instructions. Potential transformants were cultured in 5mL LB overnight at 37^{o}C, miniprepped and tested for presence of the insert by digesting with EcoRI plus EcoRV, and/or XhoI plus BamHI and running out the products on a 0.7% agarose gel stained with GelRed (GoldBio, Inc.). All successful clones were validated by Sanger Sequencing in the UIUC Core Sequencing Facility. Successful clones were subsequently transformed into BL21(DE3) chemically competent E.coli (New England Biolabs) for further induction and purification attempts.

The GST::Tara$^{N6\text{-}A860}$ construct was generated by traditional restriction cloning. Briefly, RE26467 and pGEX-3X was digested with EcoRI for 1 hour. The pGEX-3X linearized fragment and the ~2kb fragment derived from RE26467 were gel purified, mixed, and treated with T4 DNA ligase (New England Biolabs) overnight at 4^{o}C. The ligation reaction was transformed into DH5α chemically competent E.coli (generated by the University of Illinois at Urbana-Champaign Cell Media Facility), and potential clones were mini-prepped and screened for presence of insert and proper orientation by performing diagnostic digests using XhoI plus

BamHI. Note that all restriction enzymes are from New England Biolabs. All successful inserts were validated by Sanger Sequencing in the UIUC Core Sequencing Facility. Successful clones were subsequently transformed into BL21(DE3) chemically competent *E.coli* (New England Biolabs) for further induction and purification attempts.

Protein Expression

Glycerol stocks and/or colonies of BL21(DE3) cells were used to inoculate 25mL LB media supplemented with antibiotic (100µg/mL ampicillin for pGEX-3X and 50µg/mL for pET28a derived plasmids), which was incubated on a shaker overnight at 37^{o}C. The overnight culture was then poured into 500mL LB plus antibiotic and were further incubated on the shaker at 37^{o}C until the culture reached an OD_{600} of around 0.7, which took about 1.5-2hrs. Once the cells reached the appropriate concentration, IPTG was added to the media to a final concentration of 0.4-0.5mM to induce protein expression. The induced cells were incubated at various temperatures and times depending on the experiment: 3hrs at 37^{o}C, 5hrs at 30^{o}C, or 25^{o}C/18^{o}C overnight. The 18^{o}C overnight condition is generally considered the best condition for producing soluble protein.

Purification

All Taranis constructs failed to produce any soluble protein, therefore denaturing conditions was necessary to purify the $Tara^{FL}$, $Tara^{M1\text{-}K480}$ and $Tara^{Y432\text{-}S912}$ proteins. Purification was performed as described by the Qiaexpressionist with a

few modifications. Detailed protocols and optimizations can be found within my lab notebook. Due to none of the conditions working very well, particularly with binding the beads on the column and eluting proteins with contaminants, many buffer combinations tweaking with NaCl concentration and divalent salt composition of the buffer was tested with limited success. I will present the most recently developed protocol that led to partial purification of Tara$^{M1\text{-}K480}$ and Tara$^{Y432\text{-}S912}$, but failed with Tara^{FL} (Fig.16). Briefly, induced cells were spun down and the supernatant containing the media was discarded. Cells were washed and resuspended with PBS, then were transferred to a 50mL conical. The culture was spun down again at 4^{o}C to pellet the washed cells. The supernatant was again discarded, and the pellet weighed. For the His-tagged proteins, 10-15mL lysis buffer (100mM HEPES 500mM NaCl 10mM imidazole 10% glycerol w/v 1% Triton X-100 5mM β-mercaptoethanol 1mg/mL lysozyme supplemented with protease inhibitors (Complete mini tablet(s) or 1mM AEBSF) pH 8.0) was added to the bacteria for lysis. Lysis was encouraged with iterative snap freeze-thaw cycles, followed by sonication to lyse the remaining cells and to fragment the DNA. The crude lysate was then spun down at 14xg's at 4^{o}C for 30min to separate the soluble fraction (supernatant) from the insoluble fraction containing inclusion bodies (pellet). The uninduced, induced, crude, supernatant, and pellet fractions were ran on a 6% SDS-PAGE gel for 1.5hrs to assay for successful induction and solubility of the Taranis protein fragment. Due to all Taranis fusion proteins always being found in inclusion bodies (pellet), denaturing conditions was necessary for further purification of 6xHis::Tara fusion

proteins. The inclusion body solubilization buffer (U_H buffer) is composed of freshly made 8M urea 50mM HEPES 50mM NaCl pH 7.94. (Note that better success at destroying inclusion bodies apparently requires ~20 passages through a 24 gauge needle, which I should do next time I attempt to purify Taranis). Dissolved inclusion bodies were then filter sterilized to remove cellular debris. Filtered pellet fractions were loaded on to 20mL EconoPac Columns (BioRad) with 1 bed volume (750µL) of U_H buffer pH 7.94 equilibrated Ni NTA agarose beads (Goldbio). Beads plus pellet fraction were incubated at room temperature while being agitated on a nutator for 3-4 hours. After incubation, 2-3 washes with 6mL/wash U_H buffer with a pH step gradient decreasing to a pH 6.3 for the last wash was brought through each column. Each experiment I did the washes slightly differently $Tara^{FL}$ purification did not use a pH gradient for the washes; U_H buffer was pH 6.33 for both washes. $Tara^{M1\text{-}K480}$ had three washes decreasing from pH 7.44 for wash 1, pH 7.04 for wash 2, and pH 6.31 for wash 3. $Tara^{Y432\text{-}S912}$ had three washes decreasing from pH 7.91 for wash 1, pH 7.01 for wash 2, and pH 6.31 for wash 3. Columns were then eluted four times with 750µL/elution U_H buffer pH 5.90 to elute monomeric proteins, and four more times with U_H buffer pH 4.50 for aggregates. All Tara fusion proteins eluted in the monomeric fractions, if at all.

All steps on this protocol required taking a 50µL aliquot from a fraction and mixing it with 50-200µL 2xLaemmli sample buffer (62.5mM Tris-HCl pH 6.8, 2% SDS, 25% glycerol, 0.01% bromophenol blue, 5% β-mercaptoethanol) made per

the instructions in the BioRad Electrophoresis Guide Manual. All lanes on SDS-PAGE gel were loaded with 10uL sample diluted to the same degree in the 2xLaemmli buffer as the rest of the samples in that experiment.

Figures and Table

Table 1. Summary of constructs and purification attempts

Fusion Protein	Vector	Induction temperatures tested	Solubility	Able to Bind Beads	Purity
GST::Tara$^{N6-A860}$	pGEX-3X	25°C, 30°C, 37°C	partial	Partially, along with other proteins	Very Impure with degradation products
6xHis::Tara$^{M1-S912}$	pET28a	18°C, 25°C, 30°C, 37°C	None	No	Not at all
6xHis::Tara$^{M1-S912}$::6xHis	pET28a	18°C, 37°C	None	No	Not at all
6xHis::Tara$^{M1-K480}$::6xHis	pET28a	37°C	None	Yes. Modestly	Partial
6xHis::Tara$^{Y432-S912}$::6xHis	pET28a	18°C	None	Yes. Modestly	Partial
6xHis::Tara$^{Y432-S912}$	pET28a	Not tested	Not tested	Not Tested	Not tested

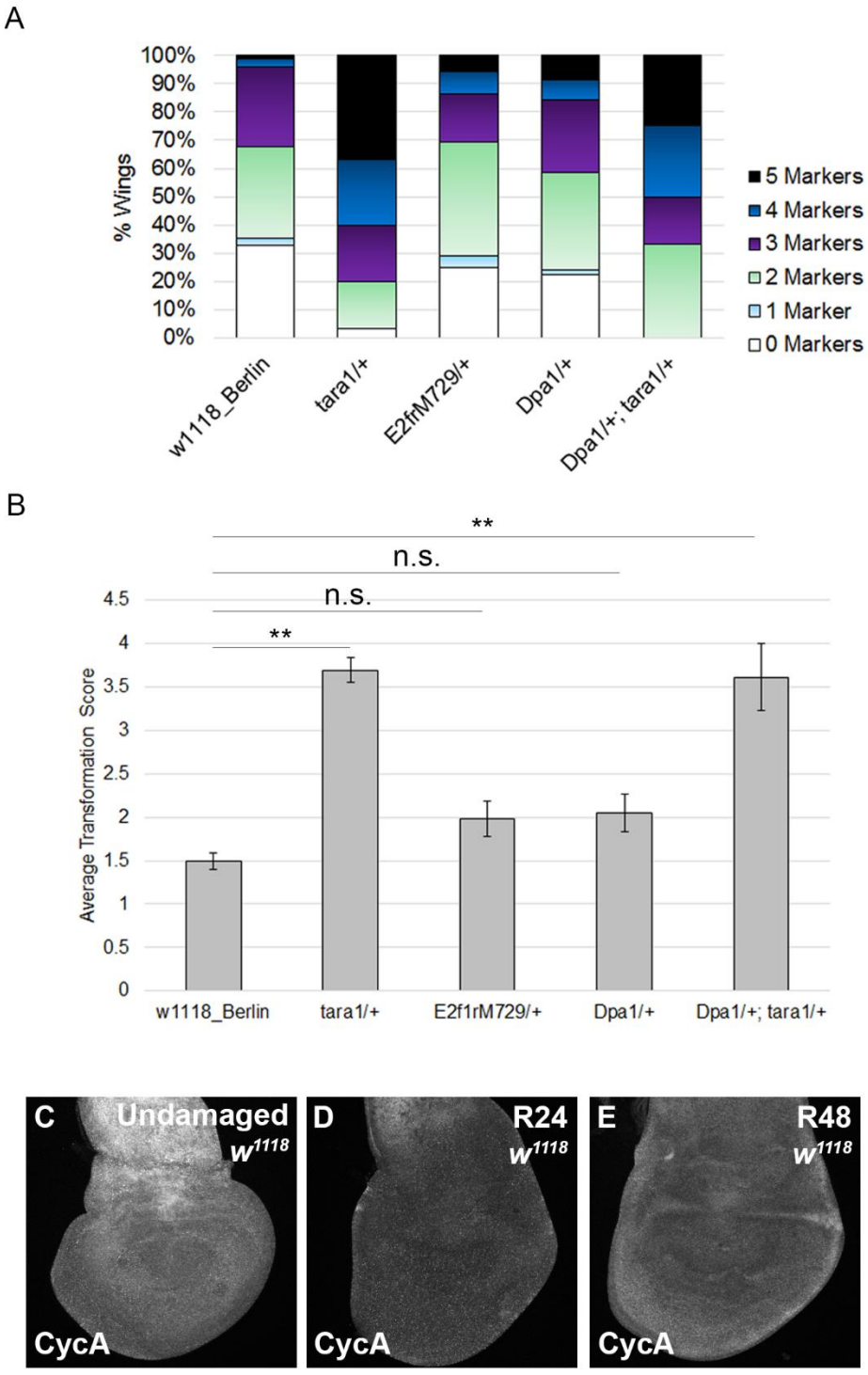

Figure 14. Taranis does not function through E2F1/Dp and CycA to protect cell fate. A) Quantification of extent of P-to-A transformation of regenerated wings that were $w^{1118}{}_{Berlin}$ (n=67), $tara^{1}$/+ (n=90) $E2f1^{rM729}$/+ (n=52), Dp^{a1}/+ (n=58), and Dp^{a1}/+; $tara^{1}$/+ (n=24). B) Average P to A

Fig. 14 (con't)

transformation score of adult fully regenerated wings that were $w^{1118}{}_{Berlin}$ (n=67), $tara^{1}$/+ (n=90) $E2f1^{rM729}$/+ (n=52), Dp^{a1}/+ (n=58), and Dp^{a1}/+; $tara^{1}$/+ (n=24). C) Undamaged 3rd instar w^{1118} wing disc stained for CycA. CycA is expressed uniformly and at low levels in the epithelium, and is expressed at high levels in the myoblasts in the notum. D) R24 w^{1118} regenerating wing disc stained for CycA. CycA is not upregulated within the blastema. E) R48 w^{1118} regenerating wing disc stained for CycA. CycA is not upregulated in the blastema. Error bars: SEM. ** $p<0.01$, n.s.: not significant ($p>0.05$).

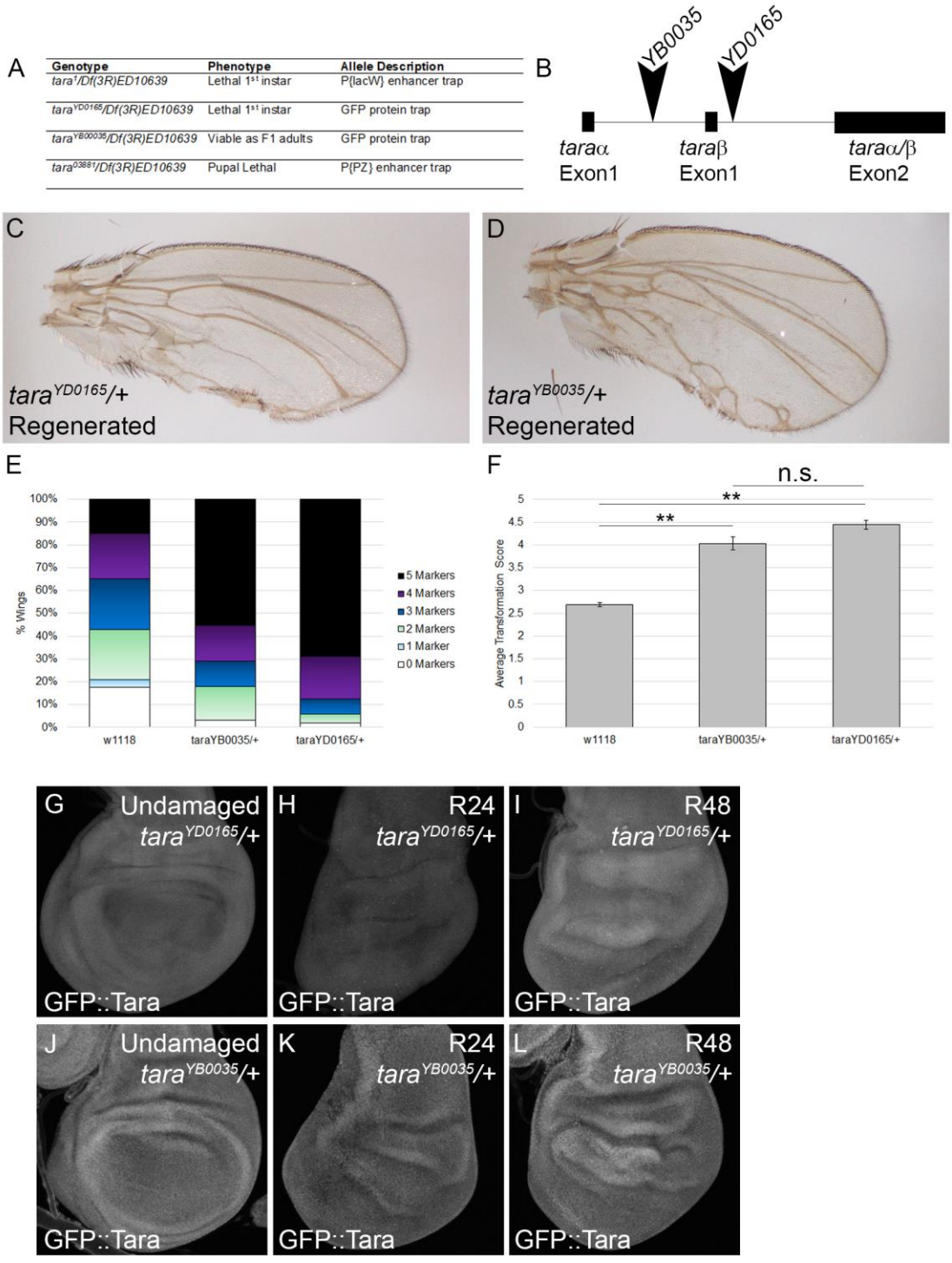

Figure 15. Taranis protein trap lines produce nonfunctional proteins. A) Allelic series crossing various *tara* mutant/reporter lines with a deficiency line that takes out the entire tara locus, *Df(3R)ED10639*. Phenotypic outcome assessed was lethality of non-Tb larvae.

Fig. 15 (con't)

B) Schematic of the *taranis* gene showing the approximate insertion site of the P-element containing the GFP protein traps. The *YD0035* insertion is found in the intron downstream of the *tara-α* exon 1 but is upstream of the *tara-β* exon 1. It is predicted to trap the *tara-α* isoform. The *YD0165* insertion is located shortly downstream of the *tara-β* exon 1 and is predicted to trap both isoforms. C) Example of a $tara^{YD0165}$/+ adult regenerated wing with massive P to A transformations. D) Example of a $tara^{YB0035}$/+ adult regenerated wing with P to A transformations. E) P-to-A transformation quantification of w^{1118} (n=86), $tara^{YB0035}$/+ (n=183), and $tara^{YD0165}$/+ (n=151). F) Corresponding Average Transformation Scores of w^{1118}, $tara^{YB0035}$/+, and $tara^{YD0165}$/+. Both GFP trap lines are significantly more transformed than w^{1118} control. G) Undamaged $tara^{YD0165}$/+ regenerating wing discs visualizing GFP::Tara expression. Note that the GFP is present in both the cytoplasm and nucleus (has a lack of obvious nuclear shape). GFP::Tara is ubiquitously expressed. H) R24 $tara^{YD0165}$/+ regenerating wing discs visualizing GFP::Tara expression. No upregulation of Tara::GFP at this timepoint. I) R48 $tara^{YD0165}$/+ regenerating wing discs visualizing GFP::Tara expression. Upregulation of Tara::GFP at this timepoint is present in most discs. J) Undamaged $tara^{YB0035}$/+ regenerating wing disc visualizing GFP::Tara expression. GFP::Tara is ubiquitously expressed with a nuclear localization. K) R24 $tara^{YB0035}$/+ regenerating wing disc visualizing GFP::Tara expression. No upregulation of Tara::GFP at this timepoint. L) R48 $tara^{YB0035}$/+ regenerating wing disc visualizing GFP::Tara expression. GFP::Tara is upregulated in the blastema of most discs. ** $p<0.01$. Error Bars: SEM.

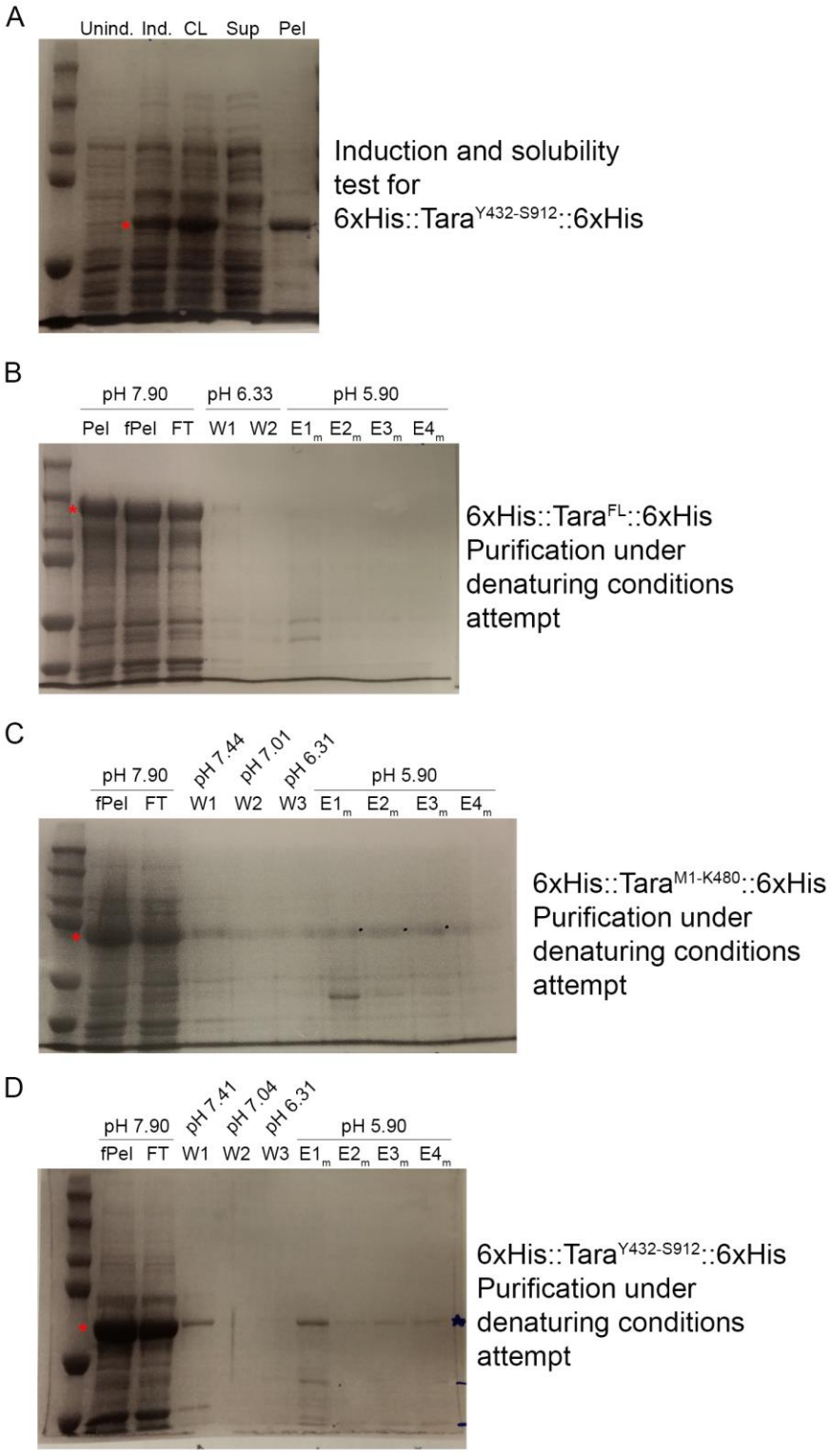

Figure 16. Purification attempts of 6xHis-tagged Taranis. A-D) 6% SDS-PAGE gels stained with 0.1% Coomassie Blue. Ladder always oriented to the far left lane. Red asterisks marks

Fig. 16 (con't)

6xHis::Tara fusion protein on each gel. A) Induction and solubility fractionation test of 6xHis::Tara$^{Y432\text{-}S912}$:6xHis induced at 18^{o}C. 6xHis::Tara$^{Y432\text{-}S912}$:6xHis is found primarily in the pellet fraction (inclusion bodies). B) Purification attempt of 6xHis::Tara^{FL}::6xHis under denaturing conditions (8M urea). 6xHis::Tara^{FL}::6xHis does not bind well to beads and only elutes contaminants. C) Purification attempt of 6xHis::Tara$^{M1\text{-}K480}$::6xHis under denaturing conditions (8M urea). In this experiment, there was a decreasing pH wash gradient before the elution. Note that the fusion protein was able to bind to beads a bit, and washed out considerably in the first wash, but eluted effectively from the column. Some contaminants were still found in the eluates. D) Purification attempt of 6xHis::Tara$^{Y432\text{-}S912}$::6xHis under denaturing conditions (8M urea). Some binding was found, with less wash-out of fusion protein. Fusion protein found in the eluates as well with some contaminants. All steps done under denaturing conditions use the U_H buffer: 8M urea 50mM NaCl 50mM HEPES pH varies depending on step. Abbreviations: Unind: Uninduced, Ind: Induced, CL: Crude Lysate, Sup: Supernatant, Pel: Pellet, fPel: Filtered Pellet, FT: Flow Through, W: Wash, E_m: Elution (monomers).

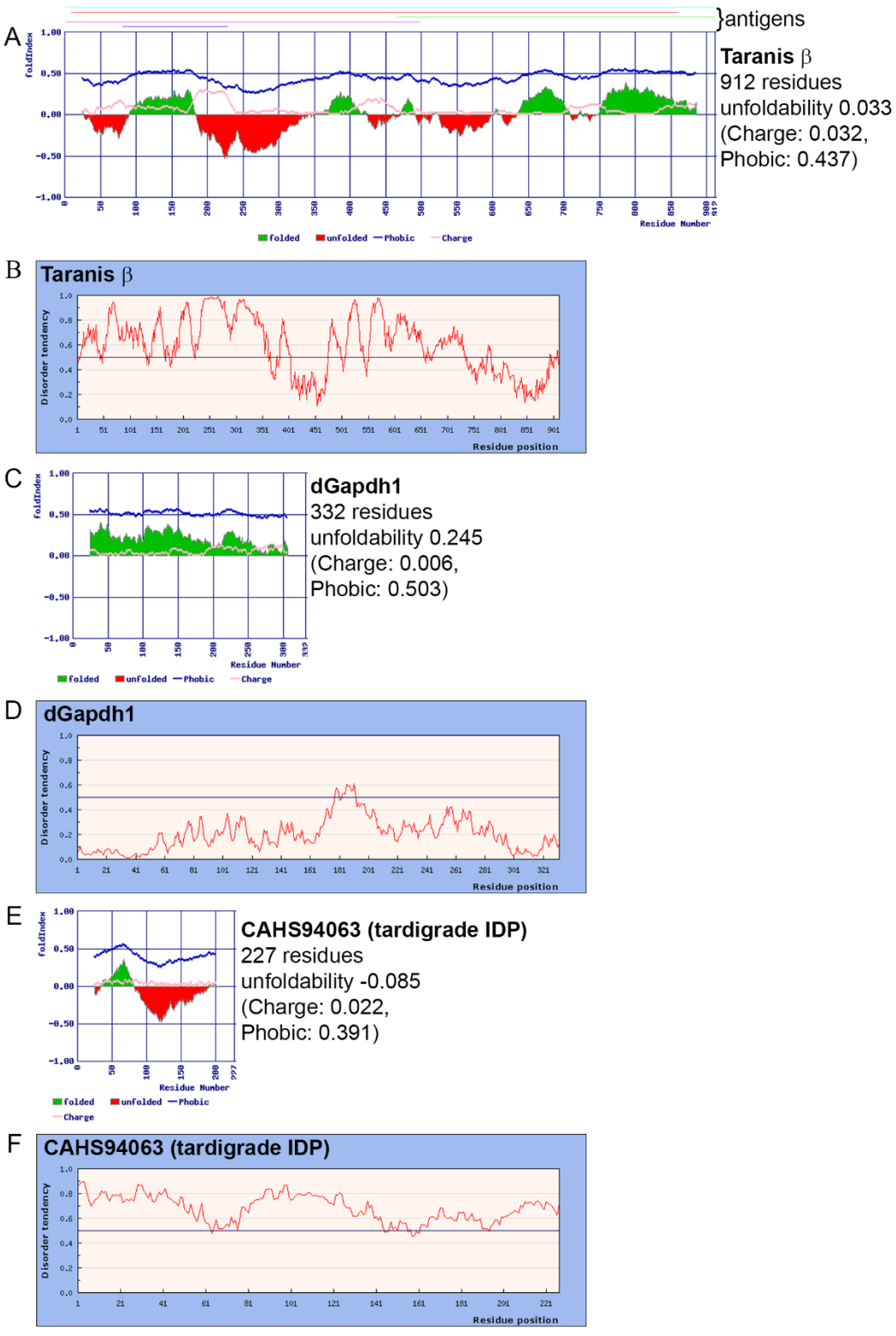

Figure 17. Taranis is predicted to be a highly disordered protein. A) Foldability index graph of Tara-β protein. Red indicates predicted disordered region, while green indicates predicted

Fig. 17 (con't)

regions that are relatively structured. Colored lines above represent each epitope intended to be generated in, or mentioned in this study. Tara$^{N6\text{-}A860}$ (red), Tara$^{M1\text{-}S12}$ (Tara^{FL}) (cyan), Tara$^{M1\text{-}K480}$ (magenta), Tara$^{Y432\text{-}S912}$ (green), Tara$^{S68\text{-}H234}$ (The Alfonso peptide) (Blue). B) Disorder tendency graph of the Tara-β protein. A higher value (closer to1.0) indicates a predicted disordered structure. Low values (closer to 0.0) indicates relatively ordered structure. C) Foldability index graph of dGAPDH protein as a control for a well folded/ordered protein. D) Disorder tendency graph of dGAPDH. E) Foldability index graph of CAHS94063, which is a bona-fide intrinsically disordered protein from the tardigrade *Hypsibius dujardini.* F) Disorder tendency graph of CAHS94063.

Appendix B: Miscellaneous Experiments

Introduction

In this chapter, I will be going over some miscellaneous results that will be helpful for future Smith-Bolton lab members trying to design experiments. This will also act as a springboard for new projects that I believe are worth pursuing. I also am putting some data here to establish me as the discoverer of certain processes. There are a number of interesting experiments mentioned here that don't necessarily fit in a complete story, or used to be a story before critical information was revealed. Many experiments were done simply to satisfy my curiosity. I hope that this chapter will be of great use for anyone who reads it.

Results and Discussion

Imaginal disc regeneration is profoundly influenced by genetic background

A major challenge of the genetic ablation system the Smith-Bolton lab relies on is the fact that the default "Wild-type" line we use, w^{1118}_{Berlin}, is very variable from experiment to experiment and is very sensitive to food quality and ambient temperature (data not shown). This often results in irreproducibility of exciting results, especially in regards to extent regeneration experiments and pupariation rates. This was partially remedied by generating isogenic w^{1118} lines by crossing w^{1118}*; ScO/CyO* and w^{1118}*; TM3/TM6B* lines with each other, then crossing

individual males that are *w^{1118}; CyO/+; TM6B/+* with females of the *w^{1118}; Sp; Dr/SM6::TM6B* stock. Males that were *w^{1118}; +; +/SM6::TM6B* were backcrossed with the fusion balancer line, then intercrossed to generate the lines *w$^{1118}_{iso2}$* and *w$^{1118}_{iso3}$*. The line *w$^{1118}_{iso3a}$* is *w$^{1118}_{iso3}$* cleaned up again by crossing to the fusion balancer line again. Experiments using these lines resulted in cleaner results in regards to regenerative growth and developmental delay, but resulted in a slightly higher P to A transformation rate (compare *w^{1118}* data in Chapter 2 to this chapter). This inspired me to investigate whether other wild type lines had similar regeneration phenotypes, or if genetic background contributes to regeneration phenotypes. It is well known that other systems have different phenotypic penetrance of many different alleles depending on the genetic background (Chow, 2016; Nadeau, 2001), with many alleles that have profound phenotypes in one background disappear in a different background. This is particularly important to know, even in *Drosophila* that exhibits a large degree of robustness in development, since in sensitized backgrounds and phenotypically plastic traits, the underlying genetic variation will manifest (Félix and Barkoulas, 2015; Kitano, 2004). *Drosophila* is particularly important to control for this, due to it having a large degree of interspecific genetic variation even compared to humans (Nevo, 1978). For the rest of the text, I will just refer to *w$^{1118}_{iso3}$* or *w$^{1118}_{iso3a}$* as *w^{1118}* for simplicity, since they have similar phenotypes. The specific isogenized *w^{1118}* line used in the experiment will be indicated within the figure. To test to see if different wild type lines have different regeneration phenotypes, I tested two commonly used wild type fly lines, *OregonR* and *CantonS* and compared them to

w^{1118}. Intriguingly, I found that both *OregonR* and *CantonS* regenerate poorly compared to w^{1118} (Fig. 18A). *CantonS* was by far the most variable, having a bimodal peak at <25%-25% regenerated and at 100% regenerated. This odd behavior is likely due to the fact that *CantonS* supplied by the Bloomington Stock Center was found to be contaminated with a P-element of unknown origin or location (Personal communication, Flybase/Bloomington Stock Center). A likely explanation for *OregonR* and *CantonS* not regenerating as well as w^{1118} is that they do not delay pupariation as long as w^{1118} (Fig. 18B). Looking at the discs at R24 and assessing regenerating pouch size by staining for Nubbin further confirms this for at least *OregonR*, since they do not have a significant difference in pouch size at R24 (Fig. 18C). However, *CantonS* has a significantly larger pouch size, but this may be due to cellular debris retaining some Nubbin immunoreactivity, since there seems to be more apoptotic debris as seen by cleaved Dcp-1 staining (data not shown). Finally, looking at the adult fully regenerated wings and assessing for the P to A transformation frequency, *OregonR* has significantly less P to A transformation features than w^{1118}, but *CantonS* did not show a statistically significant difference despite trending on the low end of transformations (Fig. 18D-E). It is interesting to note that the $tara^{1}$ and $tara^{L4}$ mutants, in addition to the DrosDel lines were all generated in the w^{1118} background (Calgaro et al., 2002; Fauvarque et al., 2001; Ryder et al., 2007), but most EMS-induced alleles are found on non-w^{1118} backgrounds such as *OregonR*.

Since w^{1118} regenerates better and has more P to A transformations compared to *OregonR* and *CantonS*, this suggested that other genetic backgrounds may have an effect on regeneration. In addition to mutants, RNAi lines from the VDRC and the TRiP have been used by the lab with variable success (Brock et al., 2017; Khan et al., 2017; Skinner et al., 2015; Smith-Bolton et al., 2009). It is not surprising that RNAi alone has a subtle effect, since UAS-RNAi transgenes must also be expressed with *rpr*. Therefore only the cells that survive ablation are able to express the RNAi transgene. This is stochastic, variable, and is unclear if it even works in some cases with *rpr*-mediated ablation. There has been speculation that some positive results of RNAi experiments could be the result of "shadow RNAi" (Bosch et al., 2016), but that hypothesis has never been tested directly. Therefore, it is possible that some positive hits for impaired or improved regeneration could be explained by a background effect. To test to see if the genetic background can influence regeneration in lines that express RNAi, crossed the *attP* insertion control line provided by the TRiP project, y^1v^1*; attP40* with the ablation line and compared its regeneration phenotypes to w^{1118}. Surprisingly, I found that *attP40*/+ animals regenerated poorly compared to w^{1118} (Fig. 18F). However, they did not differ in their ability to delay pupariation after tissue damage (Fig. 18G), suggesting that it could be a disc-autonomous difference in growth. Examining the P to A transformation frequency also revealed that the *attP40* background is more resistant to random mistakes in posterior cell fate compared to w^{1118} (Fig. 18H-I). I suspect that it is not the *attP40* insertion itself, rather somewhere else in its background that is affecting

regeneration. This is due to the majority of the 100% regenerated wings of *attP40/+* flies belonging to males that did not inherit the y^1v^1 chromosome (data not shown), which suggests that the causative locus may reside somewhere on the X. However, this observation needs to be confirmed. The fact that the *attP40* background regenerates poorly compared to w^{1118} is somewhat concerning, since it could adversely affect the interpretation of RNAi experiments. Indeed, it could introduce false positive and false negative results in various RNAi experiments. As a result of the *attP40* background having relatively poor regenerative ability, RNAi experiments that show enhanced regeneration are therefore much more profound than initially thought. The fact that *attP40/+* regenerates poorly compared to w^{1118} is precisely why I elected to use the *attP40* background in my *UAS-zldRNAi* experiments in Chapter 3 (Fig. 12).

It is perhaps not that surprising that genetic background in RNAi insertion lines may affect experiments, since a subset of the VDRC KK lines are known to have a hippo phenotype independent of the shRNA expressed (Vissers et al., 2016), and hippo signaling is essential for imaginal disc regenerative growth (Grusche et al., 2011; Repiso et al., 2013; Sun and Irvine, 2011, 2013). Therefore, it is imperative that the investigator use the proper genetic background control, or at least the closest approximation in order to minimize the number of false positives and false negatives in their experiments. In particular, w^{1118} appears to regenerate better than all of the other wild type lines tested so far, which means that w^{1118} has a modifier locus that is likely located on the X chromosome that

increases the regenerative ability of the wing disc both extrinsically and intrinsically at the expense of creating more cell fate errors. However, this may also lead to new discoveries using quantitative trait loci mapping, which takes advantage of such natural variation. Indeed, a recent report studying heart regeneration in neotanal mice found a large amount of regenerative ability depending on the genetic background, and identified a gene that induces polyploidization in cardiomyocytes, which reduces the regenerative ability in mice and zebrafish (Patterson et al., 2017). Therefore, it would be interesting to investigate the regenerative abilities of all commonly used wild type lines, and to perform either a QTL analysis, or a genome-wide association study to identify candidate genes that segregate with the regenerative phenotypes.

Vestigial gain of function experiments during regeneration

The transcription factor Vestigial is considered to be absolutely essential for wing development in *Drosophila*. It is both necessary and sufficient for wing identity and growth of the wing, and is heralded as the “wing selector gene” by some, but not others (Baena-López and García-Bellido, 2003; Halder et al., 1998; Williams et al., 1991). Therefore it came to great surprise that the activity of the two major enhancers controlling vestigial expression during development, the boundary enhancer (*vgBE*) (Williams et al., 1994) and the quadrant enhancer (*vgQE*) (Kim et al., 1996), are profoundly altered during regeneration (Fig. 9K-T), much more than what was realized when examining the expression of the Vg protein in *eiger*-ablated discs (Smith-Bolton et al., 2009). The expression of *vgBE-lacZ* was

largely maintained at low levels along the DV boundary of regenerating discs, which is not surprising since notch signaling is also maintained for the majority of regenerative growth as assessed by Dl staining (Fig, 9F-J). However the quadrant enhancer, as assessed by *vgQE-lacZ*, which is essential for wing growth and recruits non-wing tissue into the wing primordium (Zecca and Struhl, 2007b, 2007a) has its activity completely abolished from R0 to sometime after R24 (Fig. 9P-R). Only beginning to return by R48, and is restored by R72 (Fig. 9S-T). Despite this loss of *vgQE* activity, the expression of Nubbin remains throughout regeneration (Khan et al., 2016b; Smith-Bolton et al., 2009), thus suggesting that wing identity is not completely lost, and that the loss of *vgQE-lacZ* is not simply a result of a completely ablated wing. Due to this striking loss of *vgQE*-lacZ expression, the obvious question was why did *vgQE* activity disappear? Uncovering why this transient loss of cell fate happens during regeneration has implications for the regulation of dedifferentiation during regeneration in vertebrate limbs and hearts. To test this hypothesis, we employed the use of a FLP-out construct where a GFP under the control of the low-expressing ubiquitous promoter of *αTubulin* (*αTub*) is flanked by *FRT* sites, with the entire *vestigial* cDNA being fused to the 3' FRT site after the *gfp* sequence (Zecca and Struhl, 2007b). Upon activation of FLPase by heatshock (hsFLP), the *FRT-gfp-FRT* site will be excised in random cells, thus allowing for vestigial to be ectopically activated at more physiological levels in GFP^- cells (Fig. 19A) (Zecca and Struhl, 2007b, 2007a). This was considered important since it has been shown that expressing *vg* under the control of GAL4/UAS

results in impaired growth and patterning during normal wing development (Baena-Lopez and Garcia-Bellido, 2006), but is considered to be non-physiological (Zecca and Struhl, 2007b). Inducing heat shock (37^{o}C) for 20 min at A0 (d7AEL at 18^{o}C), then bringing the *αTub>gfp>vg/+* animals through the ablation-regeneration protocol resulted in efficient generation of GFP^{-}, and presumably Vg^{+} cells in mock ablated (*αTub>gfp>vg/TM6B tubGAL80* siblings) wing discs and regenerating wing discs at R24 (Fig. 19B-C), with the mock ablated wing pouches having smaller clones than those found outside of the pouch (Fig. 19B, data not shown). However, the number of clones appeared to decrease as time passed, with R48 discs having very few clones that were typically smaller than at R24 (Fig. 19D). This phenomenon strongly resembled what is seen in cell competition, where unfit cells are actively eliminated by their healthier neighbors through apoptotic cell death (Amoyel and Bach, 2014; Di Gregorio et al., 2016). Indeed, I found that the *αTub>vg* clones did occasionally contain cleaved Dcp-1 (Dcp-1*) in cells adjacent to GFP^{+} cells at R24 and R48, but not within the pouch of mock ablated wings (Fig. 19B-D). However, this proved to be difficult to quantify due to the transient nature of finding apoptotic cells, the presence Dcp-1* positive cellular debris being present around the regenerating tissue, and the negatively marked clones being difficult to discern at folds in the epithelium. The generation of a positively marked (e.g. GFP or mCherry) clones expressing ectopic Vestigial should solve the third problem of difficulty of unambiguously identifying the true size and shape of a clone. This requires the generation of new transgenic lines.

The hypothesis of the Vg-overexpressing cells were less fit than the Vg-negative blastema cells, and thus the regeneration blastema needing to keep Vg levels low to ensure that the blastema was composed of the fittest cells to regenerate the wing was an attractive hypothesis due to the observation that dMyc levels were higher in the regeneration blastema than in the uninjured parts of the wing disc, and in undamaged wings that did not experience ablation (Smith-Bolton et al., 2009), and that clones with elevated dMyc levels result in cells that are able to out-compete wild type cells in a process called “supercompetition”(Amoyel and Bach, 2014; Di Gregorio et al., 2016). Unfortunately, I was unable to identify any changes in expression of the markers of cell competition (including dMyc, yorkie/hippo signaling components, JNK signaling reporters, innate immune proteins cactus and relish, and flower isoforms (Amoyel and Bach, 2014; Di Gregorio et al., 2016) within the *αTub>vg* clones during regeneration (data not shown), which suggests that cell competition is likely not being altered in the Vg-expressing clones at any measurable degree.

The alternative hypothesis to cell competition is that the loss of *vg* activity is required for cell survival during regeneration. Which is the opposite to what is thought to be the case during normal development, where loss of *vg* function results in cell death (Kim et al., 1996; Williams et al., 1991). To test this hypothesis, a more brute force approach was employed with simply overexpressing Vg by crossing *UAS-EGFP; UAS-vg* with the ablation line and examining the number and distribution of dead/dying cells and comparing it to a

wild type *UAS-EGFP/+* control. Looking at R0 discs, which is when GAL4/UAS activity will be at its peak, I was unable to quantify the number or extent of apoptotic cells in *UAS-EGFP/+* and *UAS-EGFP/+; UAS-vg/+* discs due to the vast amount of cellular debris floating around the entire epithelium (Fig. 19E-F) and being unable to identify single apoptotic cells within a mass of dead $GFP^{+}Dcp1^{*+}$ cells near the ablation site. It was also unclear how to distinguish cells that have been ablated versus cells that are dying due to *UAS-vg*. Similar results and difficulties in interpretation was also found in R24 discs (Fig. 19G-H). Therefore, lineage tracing methods such as G-TRACE (Evans et al., 2009) are required to unambiguously identify cells that are contributing to regeneration from cells that were ablated. As a control, *UAS-EGFP* and *UAS-EGFP; UAS-vg* flies were crossed with w^{1118}*; rnGAL4 GAL80*^{ts}*/TM6B, GAL80* to see if transient overexpression of vg results in an increase in cell death during normal development. Surprisingly, rn^{ts}*>EGFP, vg* wing discs had an increase in number of apoptotic cells compared to rn^{ts}*>EGFP* wing discs (Fig. 19G-I), yet the size of the *rn* domain was not significantly different between *vg* overexpressing discs and controls (Fig. 19J). Therefore, in contrary to previous reports (Baena-Lopez and Garcia-Bellido, 2006; Khan et al., 2013), overexpression of *vg* results in an increase in cell death, yet likely not growth during normal development. This result marked the end of my investigation of the role of *vestigial* during regeneration, since the cell death phenotype is not regeneration specific, at least when vestigial levels are above the physiological range. While the role of the loss of *vgQE* expression is likely to be profoundly interesting once it is elucidated, the

amount of new reagents that are required to test new hypotheses about Vestigial's role will take a large part of a PhD to complete. Therefore the *vg* project will be shelved until a fresh pair of hands is willing to tackle the project.

Ablation of the Posterior Compartment to Determine Compartment of Origin of the Posterior to Anterior Fate Transformations.

In the initial study on *taranis* during imaginal disc regeneration, a major question was what developmental compartment was the origin of the ectopic Ptc expressing cells (as well as the corresponding En-silenced tissue). There were two possibilities: 1) Ectopic Ptc and En silencing was reflecting a true posterior to anterior fate transformation and the anterior tissue found in the posterior compartment of $tara^{1}$/+ regenerated discs originated from cells in the posterior compartment. 2) The Ptc-expressing cells in the posterior compartment were anterior cells that transgressed the AP compartment boundary into the posterior compartment and maintained their anterior fate within the posterior compartment, or were anterior cells that transgressed, were reprogrammed to posterior cells, but had unstable epigenetic status as posterior cells and reverted to anterior cells in the posterior compartment. This second hypothesis was a formal possibility due to work done by Salvador Herrera and Gines Morata (Herrera and Morata, 2014) where ablation of the entire posterior compartment by driving the expression of the proapoptotic protein Hid transiently via *hhGAL4* (hh^{ts}>*hid*) while co-expressing a lineage tracer (UAS-FLP act>stop>lacZ) to label cells that experienced *hid* expression yet survived and contributed to the compensatory

proliferation of posterior compartment. They found that upon ablating the posterior compartment, cells from the anterior compartment (lineage-negative cells) contributed to regenerating the posterior compartment and were reprogrammed into En-expressing posterior cells and vice versa. It was further claimed in a later publication that taranis might function to facilitate transgressions of the compartment boundary (Morata and Herrera, 2016), yet no data was shown to support this speculation. Indeed, our data suggested that the ectopic anterior cells were due to a cell fate change within the posterior compartment (and therefore not a transgression) by the following two lines of evidence: 1) The ectopic Ptc and En silencing occurred late in regeneration, where ectopic anterior cells and corresponding En silencing became visible only 60-72 hours after damage (Fig. 2G-P; Fig. 6A-J). Whereas transgressions of the AP boundary were shown to occur almost immediately during and after damage (Herrera and Morata, 2014). 2) By performing a rudimentary form of lineage tracing by taking advantage of the long perdurance of βgal after transcription is terminated, I found that in *en-lacZ/+; Df(3R)ED10639/+* regenerated discs that ectopic Ptc^{+} cells in the posterior compartment were co-expressing en-lacZ (Fig. 6O-P), thus confirming that these cells were of posterior compartment origin before transforming into an anterior compartment fate (Schuster and Smith-Bolton, 2015). However, this form of lineage tracing has some limitations (mentioned above) and the question remained open.

Therefore, to further confirm the origin of ectopic anterior cells in the posterior compartment in *tara*^{1}/+ mutants, I attempted to repeat the major experiment done in Herrera and Morata, 2014 with some changes. Due to Hid not being efficient at ablating wing disc tissue, there was never any missing positional information after apoptosis induction, leading to a compensatory proliferation response (Herrera and Morata, 2014; Herrera et al., 2013) instead of a true regenerative response that occurs after *rpr* overexpression, *eiger* overexpression, or physical fragmentation that results in a massive loss of positional information (Bergantiños et al., 2010; Bosch et al., 2005; Khan et al., 2016a; Smith-Bolton et al., 2009). Therefore, I opted to use *rpr* as my apoptotic driver under the spatial control of *hhGAL4*, which is expressed in the entire posterior compartment (Tabata and Kornberg, 1994; Tanimoto et al., 2000) and temporal control of *tubGAL80*^{ts} (*hh*^{ts}*>rpr*) to be able to induce a true regenerative response after damage. In addition, I wanted to perform lineage tracing of the *hh* domain after ablation, so I used a FLP-out GFP cassette known as *ubi>stop>stinger* to permanently label the *hh* lineage with GFP. To confirm that this method is able to label the *hh*-lineage, I crossed *hhGAL4* to the *ubi>stop>stinger* (note that *stinger* is version of GFP) cassette containing flies and looked at the expression of the canonical Hh signaling components Ptc and Ci (Briscoe and Thérond, 2013) in 3rd instar larvae. As expected, the FLP-out GFP cassette efficiently labels the entire posterior compartment in the disc proper and the peripodial membrane (Fig.20A), which are off-register with each other, and Ptc was expressed at high levels at the AP boundary and at lower levels the rest of the anterior compartment, and Ci

was also restricted to the anterior compartment (Fig. 20A). Notably, I found that the *hhGAL4*-lineage was restricted to the posterior compartment and did not cross the AP boundary to any significant extent. This is in contrast to what I found with examining the lineage with GTRACE, which does have massive transgressions of the AP boundary, but this was due to cell death-induced by the *UAS-RedStinger* transgene (data not shown).

To ablate the posterior compartment using hh^{ts}>*rpr*, I elected to follow essentially the same procedure we perform for rn^{ts}>*rpr* (Brock et al., 2017; Khan et al., 2017; Schuster and Smith-Bolton, 2015; Smith-Bolton et al., 2009) where we induce ablation after 7 days AEL at 18^{o}C (early 3rd instar) where we shift them to 30^{o}C for 24 hours to induce rpr expression, then let them recover at 18^{o}C until needed. There were some interesting differences between rn^{ts}>*rpr* and hh^{ts}>*rpr*. The recovery period after damage in the hh^{ts}>*rpr* animals lasted for much longer than rn^{ts}>*rpr*, and I never was able to obtain adults since they died in the early-mid pupal stage before differentiation of the adult cuticle (data not shown). This treatment also effectively ablated almost the entire posterior compartment, and indeed resulted in a massive tissue loss unlike hh^{ts}>*hid* ablated animals (data not shown). Surprisingly, when observing the *hh*-lineage at R96 (approximately when regeneration should be completed), I found that in the majority of damaged discs (n=8/9), there was a small pocket of *hh*>GFP lineage^{+} cells surrounded by anterior tissue (Ptc^{+}Ci^{+}) on both sides of the disc with Ptc being highly expressed adjacent to the *hh*>GFP lineage^{+} cells (Fig. 20B). The anterior tissue was lineage

negative so likely originated from the anterior compartment, and on both sides of the disc appeared to have regenerated and discs morphologically appeared almost normal (Fig. 20B). The same phenomenon was observed in the majority of the discs (n=9/11) in the *tara*^{1}/+ background (Fig. 20C). There was also GFP negative tissue found in some discs (Fig. 20B-C), much like what was found in Herrera and Morata, 2014, but it is unclear if this lineage-negative tissue is from remodeling of unablated posterior cells or are indeed anterior to posterior transgressions.

The observation that anterior tissue is compensating for the posterior tissue's inability to effectively regenerate the entire posterior half is reminiscent of a classic phenomenon of duplication. Imaginal discs have been known for a long time to differentially respond to damage depending on the nature of the cut (Worley et al., 2012). For example, wing discs that are cut by removing ¼ of the disc, the ¾ fragment regenerates the missing tissue after culturing in an adult female abdomen (Bryant, 1975). However, the remaining ¼ fragment instead of regenerating the entire disc, duplicates itself by just regenerating the tissue already present (Bryant, 1975). The opposite is seen in the leg disc, where ¼ fragments regenerate the missing portion of the disc, whereas the ¾ fragment duplicates (Schubiger, 1971; Schubiger and Nöthiger, 1966). This was extensively studied in the 1970s and 1980s, and some of the first theoretical models of positional information were derived from these studies of duplication vs. regeneration in the imaginal discs (French et al., 1976; Meinhardt, 1983). It

has also been shown recently when ablating portions of the notum using *pnr^{ts}>rpr*, results in duplication of notum structures (Martín et al., 2017). Ablating the entire wing and hinge, while leaving the notum using *sd^{ts}>rpr* also result in the duplication of the notum (Martín et al., 2017). Intriguingly, my data of ablating the posterior compartment is contrary to published reports in both the classic (Bryant, 1975; Karlsson, 1981) and modern literature (Herrera and Morata, 2014; Martín et al., 2017). Both Peter Bryant and Jane Karlsson found that by cutting wing discs along the approximate AP boundary that posterior fragments duplicated, and anterior fragments regenerated the missing positional information (Bryant, 1975; Karlsson, 1981). Morata and colleagues have also recently claimed that ablating the posterior compartment results in regeneration, not duplication (Martín et al., 2017) unlike their data by ablating the notum with *rpr*. However, they made this claim by using their previous discovery that hhts>hid mediated ablation results in regeneration (Herrera and Morata, 2014), however *sd^{ts}>hid* also results in what they refer to “regeneration” whereas *sd^{ts}>rpr* results in duplication. Since they did not ablate the posterior compartment with *rpr*, they cannot make such a bold claim. On the contrary, my data suggests that the anterior compartment duplicates in most situations, but may be able to regenerate in rare instances (Fig.20D-E). It could be a function of the amount of surviving posterior compartment cells after ablation, but this remains to be tested. It would be a very interesting project to study how the *hh^{ts}>rpr* discs duplicate rather than regenerate, and to see what factors are involved in duplication versus regeneration. Can you manipulate a disc to duplicate or regenerate depending on

what factors are expressed/missing? The observation that imaginal discs duplicate and regenerate depending on the cut has been known for almost 50 years, yet the molecular mechanisms are not well understood. Uncovering the factors important for duplication versus regeneration would likely identify factors involved in positional information, since duplicating discs are thought to duplicate due to not having enough positional information to regenerate the complete structure (French et al., 1976; Meinhardt, 1983).

While the observation that many *hh^{ts}>rpr* ablated discs duplicate is fascinating, it did not answer my initial question: which compartment do the ectopic anterior cells originate from? The duplicated discs in both backgrounds did not exhibit obvious ectopic Ptc in the posterior compartment, likely due to the posterior compartment not undergoing true regeneration. Indeed, it is unclear how much regenerative growth is happening in the *hh>GFP lineage* relative to the duplicating anterior compartment and if the P-lineage is experiencing any pro-regenerative signals. Luckily, there were rare instances where the ablated posterior compartment appeared to be regenerating, or has yet to duplicate in the wild-type (n=1/9) and *tara^{1}*/+ (n=2/11) backgrounds (Fig. 20D-E). To confirm that the anterior cells found in the posterior compartment were cell fate changes and not migrating anterior cells, I examined the expression of Ptc in R96 *tara^{1}*/+ discs that regenerated instead of duplicated. Examining Ptc expression in the regenerating *hh^{ts}>rpr; tara^{1}*/+ discs, I found that ectopic Ptc was found mostly in the *hh*>GFP lineage^{+} cells (Fig. 20E arrowheads) which is consistent with a true

posterior to anterior fate change. There was one rare example of a Ptc^{+} cell found in the lineage-negative zone (Fig. 20E arrow). This cell appears long and thin with weak Ptc staining, which is different from the robustly-expressing and globular morphology of the traditional ectopic Ptc found in the original *taranis* study using *rn^{ts}>rpr* (Schuster and Smith-Bolton, 2015) and in the ectopic Ptc found in the *hh*>GFP lineage^{+} cells. Therefore it is unclear if this is an experimental artifact, notum-specific Ptc that is normally present in the posterior compartment, a double fate change (A to P to A), or is a rare intermediate where a migrating anterior cell has yet to shut-off the anterior-specific genetic program and adopting the posterior compartment signature.

Given this limited numbers of true regenerators versus duplicators, it is hard to make any solid conclusions. More numbers will be necessary before any solid conclusion can be drawn. Due to the propensity of *hh^{ts}>rpr* wing discs to duplicate rather than regenerate (Fig. 20B-C), and that observations in *hh^{ts}>rpr* may not be directly comparable to *rn^{ts}>rpr*, another experimental paradigm might want to be adopted in order to definitively determine the origin of the ectopic anterior cells. One way to do this is to use a second binary transgenic system, such as *LexA^{LHG}/LexO* (Yagi et al., 2010) to lineage trace the posterior compartment (eg *hhLexA^{LHG}, LexO-FLP, ubi>stop>stinger*) while simultaneously ablating the entire pouch using *rnGAL4 GAL80^{ts} UAS-rpr*. Alternatively, a lexA/lexO-based genetic ablation system could be employed, and using *hhGAL4*-mediated lineage tracing would also work. This genetic combination may more

effectively determine the lineage of the posterior compartment after tissue damage, and would be able to determine the compartment of origin of the ectopic anterior cells in the posterior compartment. Despite this experimental shortcoming described above, the conclusion of the ectopic anterior cells in the posterior compartment of *tara*^{1}/+ regenerating discs are posterior to anterior fate changes will likely hold due to existing data suggesting that they are indeed fate changes do exist (Schuster and Smith-Bolton, 2015), and the statistically weak data above still supports to the original conclusion of a fate change nonetheless. I am particularly excited about seeing what exciting discoveries that will follow my observation that wing discs that have ablated their posterior compartment typically duplicate, rather than regenerate.

Materials and Methods

Ablation and regeneration experiments

Ablation experiments were carried out as previously described (Smith-Bolton et al., 2009) with a few modifications: induction of cell death was caused by overexpressing *rpr*, and animals were raised at 18^{o}C until 7 days after egg lay (AEL) (early 3rd instar) before the temperature was shifted to 30^{o}C for 24 hours in a circulating water bath. For undamaged controls, animals with the same genotype as the experimental animals were kept at 18^{o}C and dissected at 9-10 days AEL, which is mid-late 3rd instar. Mock ablated animals are the siblings of the flies in the ablation experiments that experienced the same thermal

conditions, but they inherited the *TM6B, tubGAL80* containing chromosome instead of the ablation chromosome. For adult wings, control undamaged animals were kept at 18ºC until after eclosion.

Mitotic clone induction and overexpression during normal development

For induction of Vg overexpressing clones, y^1 w^{1118} *hsFLP/+; αTub>gfp>vg/+* larvae were heat shocked at 37ºC for 20 min on d7AEL, just prior to ablation. After heat shock, vials were placed in an ice water bath for 1 min before shifting the larvae to 30ºC for 24 hours to induce *rpr* expression and ablate the wing pouch. Larvae were then allowed to recover at 18ºC until the desired time point.

Fly Stocks

The following Drosophila stocks were used: w^{1118}*; rnGAL4, UAS-rpr, tubGAL80*^{ts}*/TM6B, tubGAL80* (Smith-Bolton et al., 2009), w^{1118} (referred to as Wild type" in Chapter 2), w^{1118}*; UAS-rpr tubGAL80*^{ts}*; hhGAL4/TM6B, tubGAL80* was generated from a *hhGAL4* containing progenitor (BL67046). The GFP lineage tracing chromosome was generated by recombining *UAS-FLP* with *ubi>stop>Stinger* on the second chromosome. w^{1118} (Hazelrigg et al., 1984), *OregonR*, *CantonS*, y^1v^1*; attP40* (Markstein et al., 2008) is a genetic background control for RNAi experiments, *tara*^{1} (Fauvarque et al., 2001), and *UAS-vg*^{K}. The y^1 w^{1118} *hsFLP; αTub>gfp>vg* (Zecca and Struhl, 2007b, 2007a) line was a kind

gift from Gary Struhl. All fly stocks are available from The Bloomington Drosophila Genetic Stock Center unless stated otherwise.

Adult wings

Wings were mounted on glass slides in Gary's Magic Mount (Canada balsam (Sigma) dissolved in methyl salicylate (Sigma)). Images of individual wings were taken with an Olympus SZX10 dissection microscope with an Olympus DP21 camera using the CellSens Dimension software (Olympus). All images were taken at the same magnification (5X).

To quantify the P-to-A transformation phenotype in adult wings, all wings that reached to or past the tip of abdomen were considered fully regenerated and selected for quantification. The wings were scored for five anterior markers within the posterior compartment. These five markers included socketed bristles on the posterior margin, ectopic vein material on the posterior margin, an ectopic anterior crossvein (ACV) in the posterior wing blade, distal costa-like bristles on the alar lobe, and an anterior-like shape characterized by a narrower proximal and wider distal posterior compartment. The frequency of each marker was calculated independently for each genotype. In addition, these wings were scored on a scale of 0-5 markers to assess the strength of the P-to-A transformation in each wing. For all experiments, at least 3 replicates from independent egg lays were performed. Statistics were calculated and graphs

were produced in Microsoft Excel. To calculate the Average Transformation Score, the final scores of each wing was averaged in each replicate. These averages were averaged to each replicate to get the scores listed on the graph. This allowed us to calculate SEM and perform a Student's t-test to assess statistical significance compared to Wild-type.

Extent Regeneration and Pupariation Rate experiments were performed as previously described (Brock et al., 2017; Khan et al., 2017; Skinner et al., 2015; Smith-Bolton et al., 2009).

Immunohistochemistry

Dissections, fixing and staining were done as previously described (Smith-Bolton et al., 2009). Wing imaginal discs were mounted in Vectashield (Vector Labs). Antibodies used were mouse anti-Ptc (1:50) (Capdevila et al., 1994) (DSHB), rat anti-Ci (1:100) (Motzny and Holmgren, 1995) (DSHB), mouse anti-Nub (1:200), was a gift from Steve Cohen (Averof and Cohen, 1997), mouse anti-βgal (1:100) (DSHB), rabbit anti-cleaved Dcp-1 (Cell Signaling), and rat anti-DECAD2 (1:100) (DSHB). The Developmental Studies Hybridoma Bank (DSHB) was created by the NICHD of the NIH and is maintained at the University of Iowa, Department of Biology, Iowa City, IA 52242.

AlexaFluor secondary antibodies (Molecular Probes) were used at 1:1000. TO-PRO-3 iodide (Molecular Probes) was used as a DNA counterstain at 1:500. Specimens were imaged with either an LSM510 or LSM700 Confocal Microscope (Carl Zeiss). Images were compiled using ZEN Black software (Carl Zeiss), Photoshop (Adobe) or ImageJ (U.S. National Institutes of Health). All confocal images are maximum intensity projections from z-stacks unless otherwise stated.

Average fluorescence intensity was measured in ImageJ using images that were stained in parallel and imaged under identical confocal settings. The trace tool was used to circle the correct zone for quantification, and the measure tool was used to calculate average fluorescence intensity within the selected area and the area of the selection zone. The Student's t-test was performed to assess significance.

To count the number of apoptotic cells in maximum intensity projections of wing discs that were *rn^{ts}>EGFP* and *rn^{ts}>EGFP, vg*: the cell counter tool in ImageJ was used to count the number of Dcp-1* positive cells within the *rn* domain. The number of Dcp-1* positive cells per disc was averaged in a population of 16 discs per genotype. SEM was calculated, with significance determined by the student's t-test. This method was difficult to use on regenerating discs, so it was not employed.

Figures

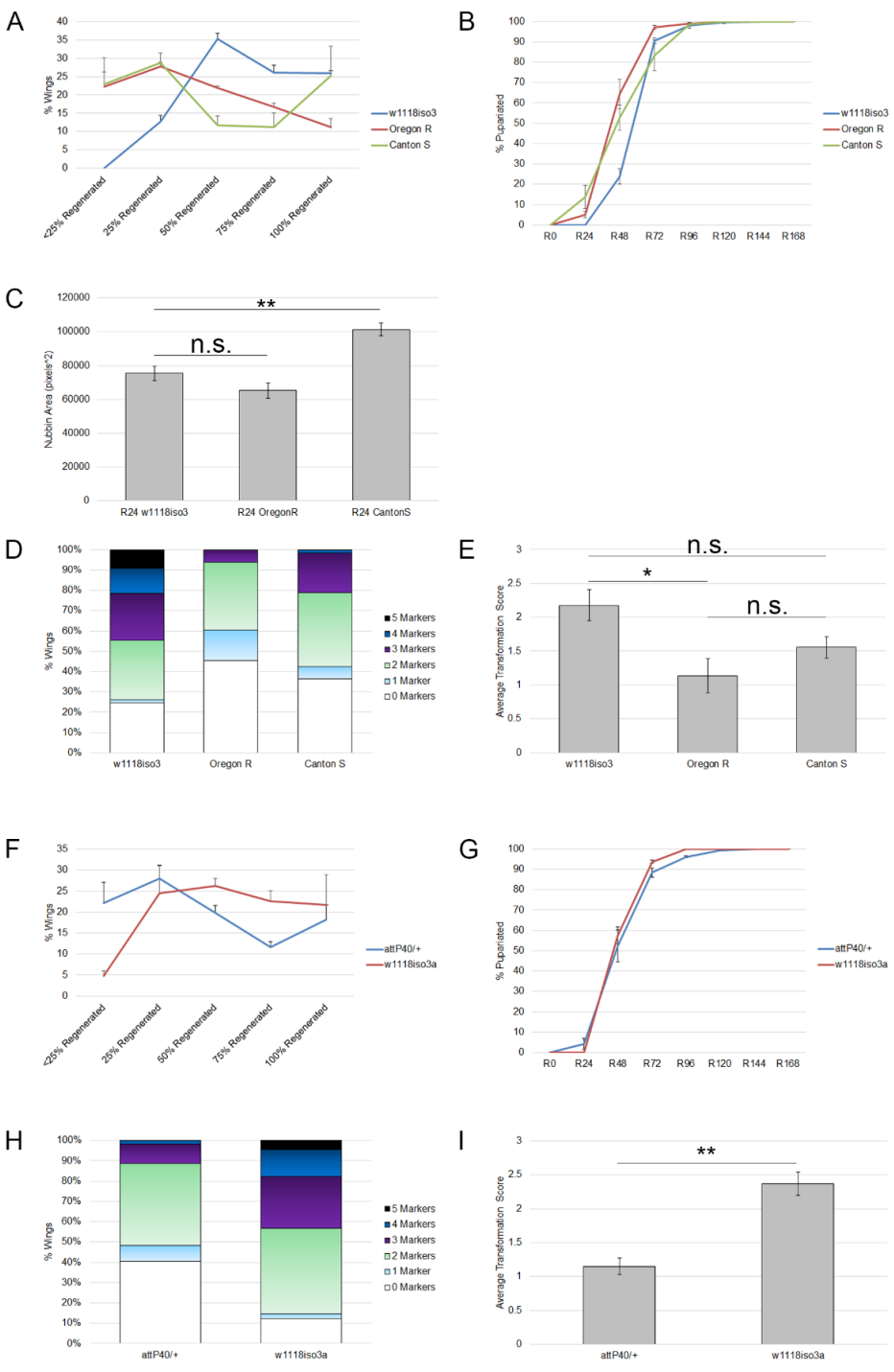

Figure 18. Genetic background has a profound effect on regenerative ability. A) Extent regeneration semi-quantitative measurements of w^{1118}_{iso3}, *OregonR*, and *CantonS* adult

Fig. 18 (con't)

regenerated wings. B) Pupariation rates of regenerating w^{1118}_{iso3}, *OregonR*, and *CantonS* larvae. C) Area of Nubbin-positive pouch in R24 w^{1118}_{iso3}, *OregonR*, and *CantonS* regenerating wing imaginal discs. D) Quantification of extent of P-to-A transformation of adult fully regenerated wings that were w^{1118}_{iso3}, *OregonR*, and *CantonS*. E) Average P to A transformation score of adult fully regenerated wings that were w^{1118}_{iso3}, *OregonR*, and *CantonS.* F) Extent regeneration semi-quantitative measurements of *attP40/+* and w^{1118}_{iso3a} adult regenerated wings. G) Pupariation rates of regenerating *attP40/+* and w^{1118}_{iso3a} *larvae.* H) Quantification of extent of P-to-A transformation of adult fully regenerated wings that were *attP40/+* and w^{1118}_{iso3a}. I) Average P to A transformation score of adult fully regenerated wings that were *attP40/+* and w^{1118}_{iso3a}. Error Bars: SEM. * $p<0.5$, ** $p<0.01$, n.s.: not significant ($p>0.05$).

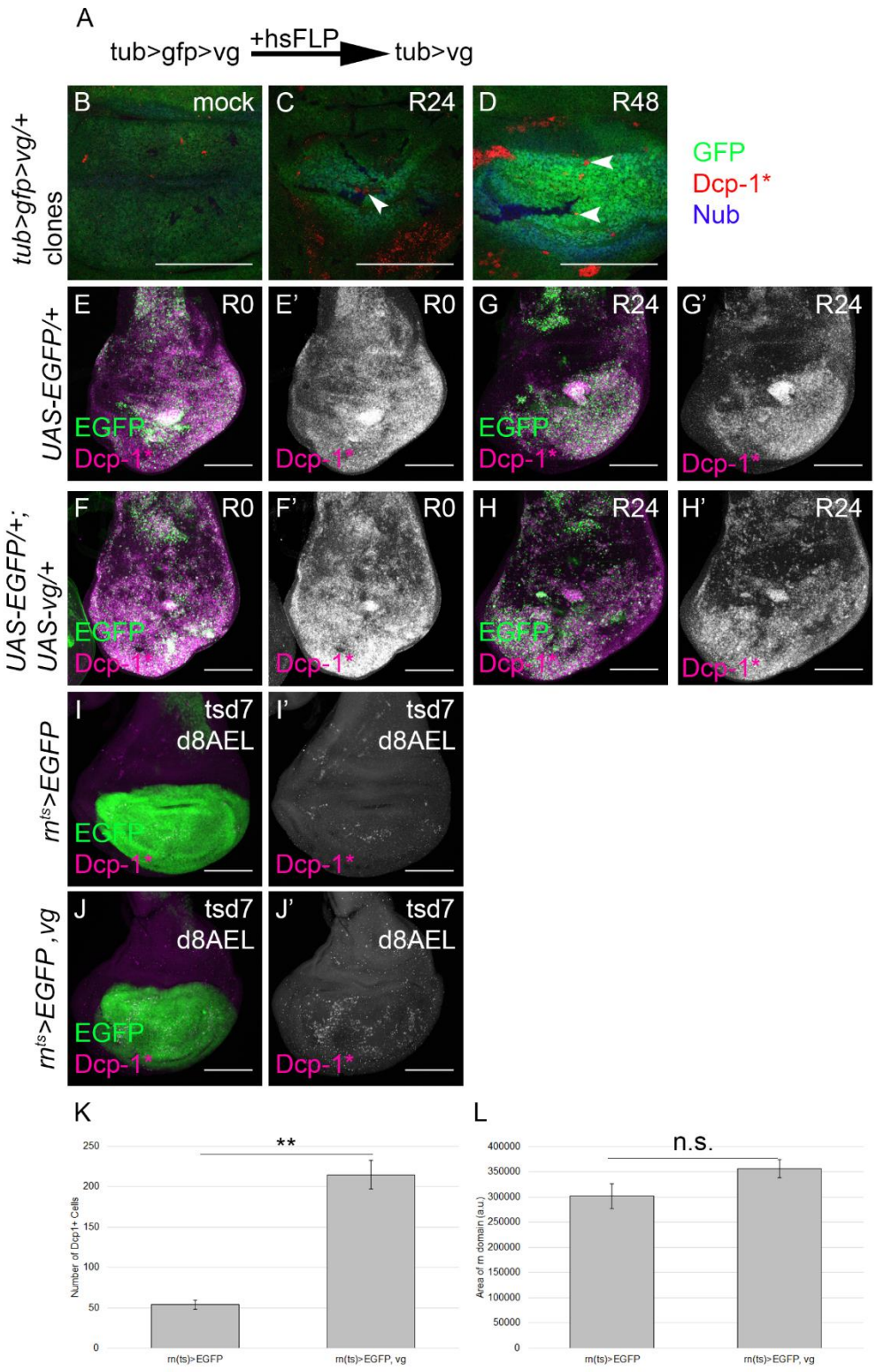

Figure 19. Vestigial gain of function experiments. A) Diagram of how the *αTub>gfp>vg* FLP-out system works. Heat shock was performed just prior to thermal shifts on d7AEL for 20 min at

Fig. 19 (con't)

37°C. B-D) Single confocal slices of *αTub>gfp>vg/+* wing discs that were subjected to a 20 min heat shock on d7AEL just prior to the thermal shift (A0). Stained for GFP (green), Dcp-1* (red), and Nubbin (blue). B) Mock ablated *αTub>gfp>vg/+* 3rd instar wing disc. C) R24 *αTub>gfp>vg/+* wing disc showing a GFP negative clone that have some Dcp-1* positive cells near wild type tissue (arrowhead). D) R48 *αTub>gfp>vg/+* wing disc showing a GFP negative clone that have some Dcp-1* positive cells near wild type tissue (bottom arrowhead). A second, very small, GFP negative clone can be seen that is entirely composed of Dcp-1* staining (top arrowhead). The relative lack of clones, and clones that are smaller than clones that were visualized earlier implies that *αTub>vg* clones are actively being eliminated from the tissue. E) Maximum projection of R0 *UAS-EGFP/+* wing disc stained for Dcp-1* (magenta) and visualizing EGFP expression (green). E') Dcp-1* staining alone. F) Maximum projection of R0 *UAS-EGFP/+; UAS-vg/+* wing disc stained for Dcp-1* (magenta) and visualizing EGFP expression (green). F') Dcp-1* staining alone. G) Maximum projection of R24 *UAS-EGFP/+* wing disc stained for Dcp-1* (magenta) and visualizing EGFP expression (green). G') Dcp-1* staining alone. H) Maximum projection of R24 *UAS-EGFP/+; UAS-vg/+* wing disc stained for Dcp-1* (magenta) and visualizing EGFP expression (green). H') Dcp-1* staining alone. I-J) Undamaged wing discs that were subject to a 24 hour thermal shift at d7AEL to transiently overexpress transgenes in the *rn* domain. Discs were dissected, fixed, and stained immediately after the thermal shift. I) *UAS-EGFP/+; rnGAL4 GAL80^{ts}/+* (*rn^{ts}>EGFP*) wing discs stained for Dcp-1* (magenta) and visualizing EGFP expression (green). I') Dcp-1* staining alone. J) *UAS-EGFP/+; rnGAL4 GAL80^{ts}/UAS-vg* (*rn^{ts}>EGFP, vg*) wing discs stained for Dcp-1* (magenta) and visualizing EGFP expression (green). J') Dcp-1* staining alone. K) Quantification of the number of Dcp-1* positive cells within the *rn* domain in *rn^{ts}>EGFP* (n=16 discs) *and rn^{ts}>EGFP, vg* (n=16) wing discs. L) Quantification of the area of the *rn* domain in *rn^{ts}>EGFP* (n=16 discs) and *rn^{ts}>EGFP, vg* (n=16) wing discs. Scale bar: 100μm. Error Bars: SEM. ** $p<0.01$. n.s.: not significant ($p>0.05$).

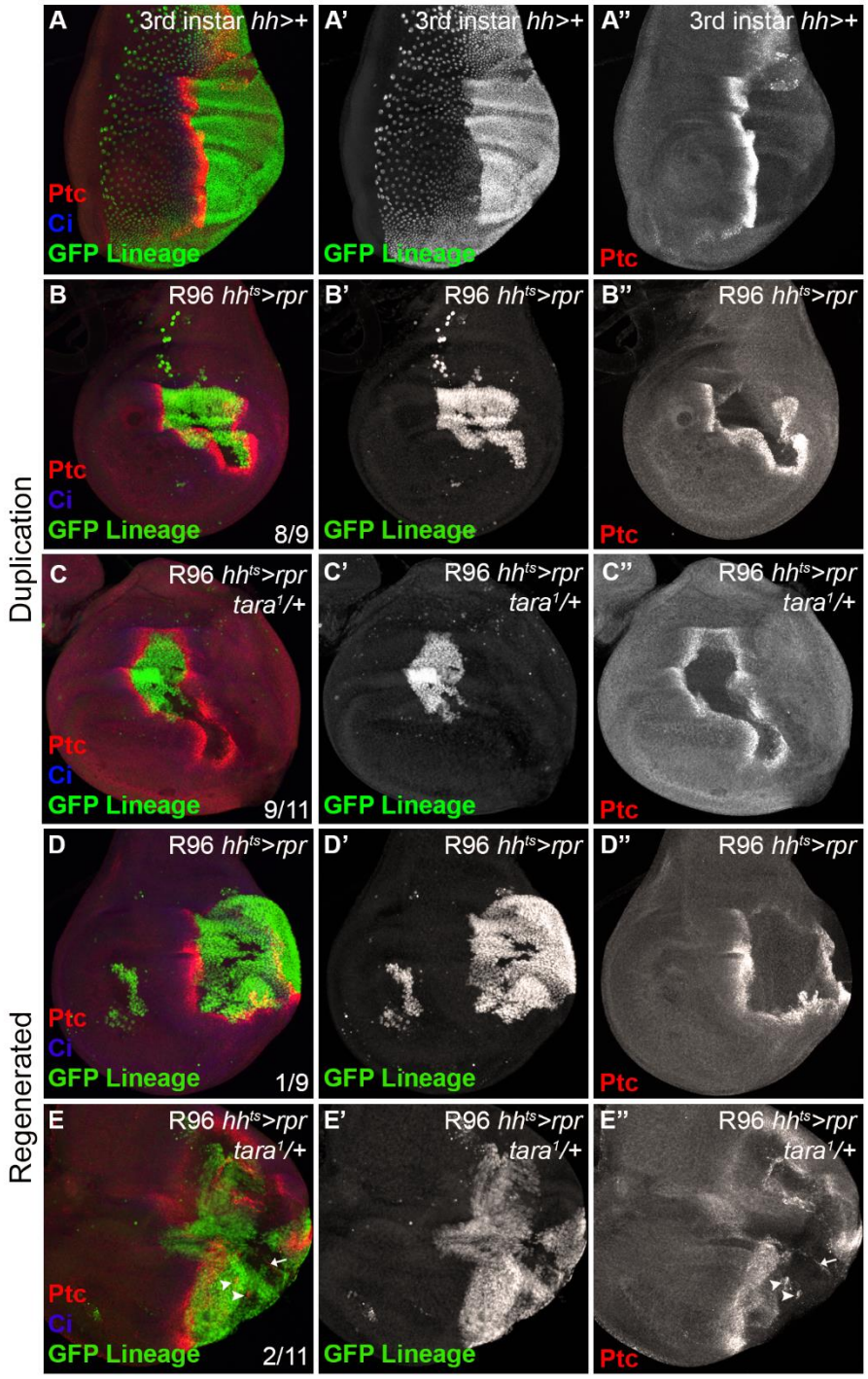

Figure 20. Ablation of the posterior compartment results in duplications. A) Undamaged 3rd instar wing disc of *w*^{1118}*; UAS-FLP ubi>stop>Stinger/+; hhGAL4/+* stained for Ptc (red), Ci (blue-note that 633 channel is weak in these experiments), and visualizing GFP (green). GFP (stinger)

Fig. 20 (con't)

is marking the *hhGAL4* lineage. Note that the peripodial membrane (large GFP^+ nuclei) is not in register with the disc proper posterior compartment. A') GFP Lineage. A'') Ptc staining. B) R96 *w^{1118}; UAS-rpr GAL80^{ts}/UAS-FLP ubi>stop>Stinger; hhGAL4/+* wing disc that underwent duplication of the anterior compartment rather than traditional regeneration. Note that the posterior compartment is labeled by the GFP lineage and is encircled by anterior Ptc^+Ci^+ tissue. B') GFP lineage. B'') Ptc staining. C) R96 *w^{1118}; UAS-rpr GAL80^{ts}/UAS-FLP ubi>stop>Stinger; hhGAL4/tara^1* wing disc that underwent duplication of the anterior compartment rather than traditional regeneration. C') GFP lineage. C'') Ptc Staining. D) Rare R96 *w^{1118}; UAS-rpr GAL80ts/UAS-FLP ubi>stop>Stinger; hhGAL4/+* that regenerated a portion of the posterior compartment that is not encircled by anterior tissue, but may be in an intermediate step before duplication. D') GFP lineage. D'') Ptc Staining. E) Rare R96 *w^{1118}; UAS-rpr GAL80^{ts}/UAS-FLP ubi>stop>Stinger; hhGAL4/tara^1* wing disc that regenerated the posterior compartment from the surviving hhGAL4 lineage. Ectopic Ptc can be found within the GFP^+ hhGAL4 lineage (arrowheads) or outside of the hhGAL4 lineage (GFP-) (arrow). E') GFP lineage. E'') Ptc Staining.

References

1. Adams, D.S., Masi, A., and Levin, M. (2007). H+ pump-dependent changes in membrane voltage are an early mechanism necessary and sufficient to induce Xenopus tail regeneration. Development *134*, 1323–1335.

2. Adler, P.N., and Bryant, P.J. (1977). Participation of lethally irradiated imaginal disc tissue in pattern regulation in Drosophila. Dev. Biol. *60*, 298–304.

3. Afonso, D.J.S., Liu, D., Machado, D.R., Pan, H., Jepson, J.E.C., Rogulja, D., and Koh, K. (2015). TARANIS Functions with Cyclin A and Cdk1 in a Novel Arousal Center to Control Sleep in Drosophila. Curr. Biol. *25*, 1717–1726.

4. del Álamo Rodríguez, D., Terriente Felix, J., and Díaz-Benjumea, F.J. (2004). The role of the T-box gene optomotor-blind in patterning the Drosophila wing. Dev. Biol. *268*, 481–492.

5. Almuedo-Castillo, M., Crespo, X., Seebeck, F., Bartscherer, K., Salò, E., Adell, T., Steller, H., and Morata, G. (2014). JNK Controls the Onset of Mitosis in Planarian Stem Cells and Triggers Apoptotic Cell Death Required for Regeneration and Remodeling. PLoS Genet. *10*, e1004400.

6. Álvarez-Fernández, C., Tamirisa, S., Prada, F., Chernomoretz, A., Podhajcer, O., Blanco, E., and Martín-Blanco, E. (2015). Identification and Functional Analysis of Healing Regulators in Drosophila. PLOS Genet. *11*, e1004965.

7. Alwes, F., Enjolras, C., and Averof, M. (2016). Live imaging reveals the progenitors and cell dynamics of limb regeneration. Elife *5*.

8. Amamoto, R., Huerta, V.G.L., Takahashi, E., Dai, G., Grant, A.K., Fu, Z., and Arlotta, P. (2016). Adult axolotls can regenerate original neuronal diversity in response to brain injury. Elife *5*.

9. Amoyel, M., and Bach, E.A. (2014). Cell competition: how to eliminate your neighbours. Development *141*, 988–1000.

10. Arnold, K., Sarkar, A., Yram, M.A., Polo, J.M., Bronson, R., Sengupta, S., Seandel, M., Geijsen, N., and Hochedlinger, K. (2011). Sox2+ Adult Stem and Progenitor Cells Are Important for Tissue Regeneration and Survival of Mice. Cell Stem Cell *9*, 317–329.

11. Averof, M., and Cohen, S.M. (1997). Evolutionary origin of insect wings from ancestral gills. Nature *385*, 627–630.

12. Aza-Blanc, P., Ramírez-Weber, F.A., Laget, M.P., Schwartz, C., and Kornberg, T.B. (1997). Proteolysis that is inhibited by hedgehog targets Cubitus interruptus protein to the nucleus and converts it to a repressor. Cell *89*, 1043–1053.

13. Baena-Lopez, L.A., and Garcia-Bellido, A. (2006). Control of growth and positional information by the graded vestigial expression pattern in the wing of Drosophila melanogaster. Proc. Natl. Acad. Sci. *103*, 13734–13739.

14. Baena-Lopez, L.A., Alexandre, C., Mitchell, A., Pasakarnis, L., and Vincent, J.-P. (2013). Accelerated homologous recombination and subsequent genome modification in Drosophila. Development *140*, 4818–4825.

15. Baena-López, L.A., and García-Bellido, A. (2003). Genetic requirements of vestigial in the regulation of Drosophila wing development. Development *130*, 197–208.

16. Bedelbaeva, K., Snyder, A., Gourevitch, D., Clark, L., Zhang, X.-M., Leferovich, J., Cheverud, J.M., Lieberman, P., and Heber-Katz, E. (2010). Lack of p21 expression links cell cycle control and appendage regeneration in mice. Proc. Natl. Acad. Sci. *107*, 5845–5850.

17. Beira, J.V., Springhorn, A., Gunther, S., Hufnagel, L., Pyrowolakis, G., and Vincent, J.-P. (2014). The Dpp/TGFβ-Dependent Corepressor Schnurri Protects Epithelial Cells from JNK-Induced Apoptosis in Drosophila Embryos. Dev. Cell *31*, 240–247.

18. Bely, A.E., and Sikes, J.M. (2010). Latent regeneration abilities persist following recent evolutionary loss in asexual annelids. Proc. Natl. Acad. Sci. *107*, 1464–1469.

19. Bely, A.E., Zattara, E.E., and Sikes, J.M. (2014). Regeneration in spiralians: evolutionary patterns and developmental processes. Int. J. Dev. Biol. *58*, 623–634.

20. Bennetts, J.S., Fowles, L.F., Berkman, J.L., van Bueren, K.L., Richman, J.M., Simpson, F., and Wicking, C. (2006). Evolutionary conservation and murine embryonic expression of the gene encoding the SERTA domain-containing protein CDCA4 (HEPP). Gene *374*, 153–165.

21. Bergantiños, C., Corominas, M., and Serras, F. (2010). Cell death-induced regeneration in wing imaginal discs requires JNK signalling. Development *137*.

22. Berson, A., Sartoris, A., Nativio, R., Van Deerlin, V., Toledo, J.B., Porta, S., Liu, S., Chung, C.-Y., Garcia, B.A., Lee, V.M.-Y., et al. (2017). TDP-43 Promotes Neurodegeneration by Impairing Chromatin Remodeling. Curr. Biol. *27*, 3579–3590.e6.

23. Bilak, A., Uyetake, L., and Su, T.T. (2014). Dying Cells Protect Survivors from Radiation-Induced Cell Death in Drosophila. PLoS Genet. *10*.

24. Biswas, S.C., Zhang, Y., Iyirhiaro, G., Willett, R.T., Rodriguez Gonzalez, Y., Cregan, S.P., Slack, R.S., Park, D.S., and Greene, L.A. (2010). Sertad1 Plays an Essential Role in Developmentaland Pathological Neuron Death. J. Neurosci. *30*, 3973–3982.

25. Blair, S.S. (2007). Wing Vein Patterning in *Drosophila* and the Analysis of Intercellular Signaling. Annu. Rev. Cell Dev. Biol. *23*, 293–319.

26. Boothby, T.C., Tapia, H., Brozena, A.H., Piszkiewicz, S., Smith, A.E., Giovannini, I., Rebecchi, L., Pielak, G.J., Koshland, D., and Goldstein, B. (2017). Tardigrades Use Intrinsically Disordered Proteins to Survive Desiccation. Mol. Cell *65*, 975–984.e5.

27. Borgens, R.B. (1982). Mice regrow the tips of their foretoes. Science *217*, 747–750.

28. Bosch, J.A., Sumabat, T.M., and Hariharan, I.K. (2016). Persistence of RNAi-Mediated Knockdown in *Drosophila* Complicates Mosaic Analysis Yet Enables Highly Sensitive Lineage Tracing. Genetics *203*, 109–118.

29. Bosch, M., Serras, F., Martín-Blanco, E., and Baguñà, J. (2005). JNK signaling pathway required for wound healing in regenerating Drosophila wing imaginal discs. Dev. Biol. *280*, 73–86.

30. Bosch, M., Baguñà, J., and Serras, F. (2008). Origin and proliferation of blastema cells during regeneration of Drosophila wing imaginal discs. Int. J. Dev. Biol. *52*, 1043–1050.

31. Bosch, M., Bishop, S.-A., Baguña, J., and Couso, J.-P. (2010). Leg regeneration in Drosophila abridges the normal developmental program. Int. J. Dev. Biol. *54*, 1241–1250.

32. Brakefield, P.M., and French, V. (1995). Eyespot Development on Butterfly Wings: The Epidermal Response to Damage. Dev. Biol. *168*, 98–111.

33. Brand, A.H., and Perrimon, N. (1993). Targeted gene expression as a means of altering cell fates and generating dominant phenotypes. Development *118*, 401–415.

34. Briscoe, J., and Thérond, P.P. (2013). The mechanisms of Hedgehog signalling and its roles in development and disease. Nat. Rev. Mol. Cell Biol. *14*, 416–429.

35. Brock, A.R., Seto, M., and Smith-Bolton, R.K. (2017). Cap-n-Collar Promotes Tissue Regeneration by Regulating ROS and JNK Signaling in the Drosophila Wing Imaginal Disc. Genetics.

36. Brook, W.J., and Cohen, S.M. (1996). Antagonistic interactions between wingless and decapentaplegic responsible for dorsal-ventral pattern in the Drosophila Leg. Science *273*, 1373–1377.

37. Brunetti, C.R., Selegue, J.E., Monteiro, A., French, V., Brakefield, P.M., and Carroll, S.B. (2001). The generation and diversification of butterfly eyespot color patterns. Curr. Biol. *11*, 1578–1585.

38. Bryant, P.J. (1971). Regeneration and duplication following operations in situ on the imaginal discs of Drosophila melanogaster. Dev. Biol. *26*, 637–651.

39. Bryant, P.J. (1975). Pattern formation in the imaginal wing disc ofDrosophila melanogaster: Fate map, regeneration and duplication. J. Exp. Zool. *193*, 49–77.

40. Bryant, P.J., and Fraser, S.E. (1988). Wound healing, cell communication, and DNA synthesis during imaginal disc regeneration in Drosophila. Dev. Biol. *127*, 197–208.

41. Buszczak, M., Paterno, S., Lighthouse, D., Bachman, J., Planck, J., Owen, S., Skora, A.D., Nystul, T.G., Ohlstein, B., Allen, A., et al. (2007). The Carnegie Protein Trap Library: A Versatile Tool for Drosophila Developmental Studies. Genetics *175*.

42. Calgaro, S., Boube, M., Cribbs, D.L., and Bourbon, H.-M. (2002). The Drosophila Gene taranis Encodes a Novel Trithorax Group Member Potentially Linked to the Cell Cycle Regulatory Apparatus. Genetics *160*.

43. Calleja, M., Moreno, E., Pelaz, S., and Morata, G. (1996). Visualization of gene expression in living adult Drosophila. Science *274*, 252–255.

44. Campbell, G., and Tomlinson, A. (1999a). Transducing the Dpp morphogen gradient in the wing of Drosophila: regulation of Dpp targets by brinker. Cell *96*, 553–562.

45. Campbell, G., and Tomlinson, A. (1999b). Transducing the Dpp Morphogen Gradient in the Wing of Drosophila: Regulation of Dpp Targets by brinker. Cell *96*, 553–562.

46. Capdevila, J., Estrada, M.P., Sánchez-Herrero, E., and Guerrero, I. (1994). The Drosophila segment polarity gene patched interacts with decapentaplegic in wing development. EMBO J. *13*, 71–82.

47. de Celis, J.F., and Barrio, R. (2000). Function of the spalt/spalt-related gene complex in positioning the veins in the Drosophila wing. Mech. Dev. *91*, 31–41.

48. de Celis, J.F., Barrio, R., and Kafatos, F.C. (1996). A gene complex acting downstream of dpp in Drosophila wing morphogenesis. Nature *381*, 421–424.

49. Chakrabarti, S., Liehl, P., Buchon, N., and Lemaitre, B. (2012). Infection-Induced Host Translational Blockage Inhibits Immune Responses and Epithelial Renewal in the Drosophila Gut. Cell Host Microbe *12*, 60–70.

50. Chanas, G., Lavrov, S., Iral, F., Cavalli, G., and Maschat, F. (2004). Engrailed and polyhomeotic maintain posterior cell identity through cubitus-interruptus regulation. Dev. Biol. *272*, 522–535.

51. Chen, C.-F., Foley, J., Tang, P.-C., Li, A., Jiang, T.X., Wu, P., Widelitz, R.B., and Chuong, C.M. (2015). Development, Regeneration, and Evolution of Feathers. Annu. Rev. Anim. Biosci. *3*, 169–195.

52. Chen, C.-H., von Kessler, D.P., Park, W., Wang, B., Ma, Y., and Beachy, P.A. (1999). Nuclear Trafficking of Cubitus interruptus in the Transcriptional Regulation of Hedgehog Target Gene Expression. Cell *98*, 305–316.

53. Cheng, C., Ko, A., Chaieb, L., Koyama, T., Sarwar, P., Mirth, C.K., Smith, W.A., and Suzuki, Y. (2014). The POU Factor Ventral Veins Lacking/Drifter Directs the Timing of Metamorphosis through Ecdysteroid and Juvenile Hormone Signaling. PLoS Genet. *10*, e1004425.

54. Cheong, J., Gunaratnam, L., Zang, Z., Yang, C.M., Sun, X., Nasr, S.L., Sim, K., Peh, B., Rashid, S., Bonventre, J. V, et al. (2009). TRIP-Br2 promotes oncogenesis in nude mice and is frequently overexpressed in multiple human tumors. J. Transl. Med. *7*, 8.

55. Chera, S., Ghila, L., Dobretz, K., Wenger, Y., Bauer, C., Buzgariu, W., Martinou, J.-C., and Galliot, B. (2009). Apoptotic Cells Provide an Unexpected Source of Wnt3 Signaling to Drive Hydra Head Regeneration. Dev. Cell *17*, 279–289.

56. Chow, C.Y. (2016). Bringing genetic background into focus. Nat. Rev. Genet. *17*, 63–64.

57. Cirillo, L.A., Lin, F.R., Cuesta, I., Friedman, D., Jarnik, M., and Zaret, K.S. (2002). Opening of Compacted Chromatin by Early Developmental Transcription Factors HNF3 (FoxA) and GATA-4. Mol. Cell *9*, 279–289.

58. Classen, A.-K., Bunker, B.D., Harvey, K.F., Vaccari, T., and Bilder, D. (2009). A tumor suppressor activity of Drosophila Polycomb genes mediated by JAK-STAT signaling. Nat. Genet. *41*, 1150–1155.

59. Colombani, J., Andersen, D.S., and Léopold, P. (2012). Secreted Peptide Dilp8 Coordinates Drosophila Tissue Growth with Developmental Timing. Science (80-.). *336*.

60. Colombani, J., Andersen, D.S., Boulan, L., Boone, E., Romero, N., Virolle, V., Texada, M., and L??opold, P. (2015). Drosophila Lgr3 Couples Organ Growth with Maturation and Ensures Developmental Stability. Curr. Biol. *25*.

61. Couso, J.P., Bate, M., and Martínez-Arias, A. (1993). A wingless-dependent polar coordinate system in Drosophila imaginal discs. Science *259*, 484–489.

62. Couso, J.P., Knust, E., and Martinez Arias, A. (1995). Serrate and wingless cooperate to induce vestigial gene expression and wing formation in Drosophila. Curr. Biol. *5*, 1437–1448.

63. Currie, J.D., Kawaguchi, A., Traspas, R.M., Schuez, M., Chara, O., and Tanaka, E.M. (2016). Live Imaging of Axolotl Digit Regeneration Reveals Spatiotemporal Choreography of Diverse Connective Tissue Progenitor Pools. Dev. Cell *39*, 411–423.

64. Darwish, H., Cho, J.M., Loignon, M., and Alaoui-Jamali, M.A. (2007). Overexpression of SERTAD3, a putative oncogene located within the 19q13 amplicon, induces E2F activity and promotes tumor growth. Oncogene *26*, 4319–4328.

65. Das, S., and Durica, D.S. (2013). Ecdysteroid receptor signaling disruption obstructs blastemal cell proliferation during limb regeneration in the fiddler crab, Uca pugilator. Mol. Cell. Endocrinol. *365*, 249–259.

66. Davies, E.L., Lei, K., Seidel, C.W., Kroesen, A.E., McKinney, S.A., Guo, L., Robb, S.M., Ross, E.J., Gotting, K., and Alvarado, A.S. (2017). Embryonic origin of adult stem cells required for tissue homeostasis and regeneration. Elife *6*.

67. Delsuc, F., Brinkmann, H., Chourrout, D., and Philippe, H. (2006). Tunicates and not cephalochordates are the closest living relatives of vertebrates. Nature *439*, 965–968.

68. Di Gregorio, A., Bowling, S., and Rodriguez, T.A. (2016). Cell Competition and Its Role in the Regulation of Cell Fitness from Development to Cancer. Dev. Cell *38*, 621–634.

69. Diaz-Garcia, S., Ahmed, S., and Baonza, A. (2016). Analysis of the Function of Apoptosis during Imaginal Wing Disc Regeneration in Drosophila melanogaster. PLoS One *11*, e0165554.

70. Díaz-García, S., and Baonza, A. (2013). Pattern reorganization occurs independently of cell division during Drosophila wing disc regeneration in situ. Proc. Natl. Acad. Sci. U. S. A. *110*.

71. Diaz Quiroz, J.F., Tsai, E., Coyle, M., Sehm, T., and Echeverri, K. (2014). Precise control of miR-125b levels is required to create a regeneration-permissive environment after spinal cord injury: a cross-species comparison between salamander and rat. Dis. Model. Mech. *7*, 601–611.

72. Diep, C.Q., Ma, D., Deo, R.C., Holm, T.M., Naylor, R.W., Arora, N., Wingert, R.A., Bollig, F., Djordjevic, G., Lichman, B., et al. (2011). Identification of adult nephron progenitors capable of kidney regeneration in zebrafish. Nature *470*, 95–100.

73. DiNardo, S., and O'Farrell, P.H. (1987). Establishment and refinement of segmental pattern in the Drosophila embryo: spatial control of engrailed expression by pair-rule genes. Genes Dev. *1*, 1212–1225.

74. Dinsmore, C.E. (1996). Urodele limb and tail regeneration in early biological thought: an essay on scientific controversy and social change. Int. J. Dev. Biol. *40*, 621–627.

75. Dinwiddie, A., Null, R., Pizzano, M., Chuong, L., Leigh Krup, A., Ee Tan, H., and Patel, N.H. (2014). Dynamics of F-actin prefigure the structure of butterfly wing scales. Dev. Biol. *392*, 404–418.

76. Doherty, D., Feger, G., Younger-Shepherd, S., Jan, L.Y., and Jan, Y.N. (1996a). Delta is a ventral to dorsal signal complementary to Serrate, another Notch ligand, in Drosophila wing formation. Genes Dev. *10*, 421–434.

77. Doherty, D., Feger, G., Younger-Shepherd, S., Jan, L.Y., and Jan, Y.N. (1996b). Delta is a ventral to dorsal signal complementary to Serrate, another Notch ligand, in Drosophila wing formation. Genes Dev. *10*, 421–434.

78. Dosztanyi, Z., Csizmok, V., Tompa, P., and Simon, I. (2005). IUPred: web server for the prediction of intrinsically unstructured regions of proteins based on estimated energy content. Bioinformatics *21*, 3433–3434.

79. Ducuing, A., Keeley, C., Mollereau, B., and Vincent, S. (2015). A DPP-mediated feed-forward loop canalizes morphogenesis during *Drosophila* dorsal closure. J. Cell Biol. *208*, 239–248.

80. Dura, J.-M., Randsholt, N.B., Deatrick, J., Erk, I., Santamaria, P., Freeman, J.D., Freeman, S.J., Weddell, D., and Brock, H.W. (1987). A complex genetic locus, polyhomeotic, is required for segmental specification and epidermal development in D. melanogaster. Cell *51*, 829–839.

81. Durica, D.S., and Hopkins, P.M. (1996). Expression of the genes encoding the ecdysteroid and retinoid receptors in regenerating limb tissues from the fiddler crab, Uca pugilator. Gene *171*, 237–241.

82. Duronio, R.J., O'Farrell, P.H., Xie, J.E., Brook, A., and Dyson, N. (1995). The transcription factor E2F is required for S phase during Drosophila embryogenesis. Genes Dev. *9*, 1445–1455.

83. Dutta, P., Li, W.X., Netter, S., Charollais, J., Antoniewski, C., and Theodore, L. (2017). The SERTAD protein Taranis plays a role in Polycomb-mediated gene repression. PLoS One *12*, e0180026.

84. Eaton, S., and Kornberg, T.B. (1990). Repression of ci-D in posterior compartments of Drosophila by engrailed. Genes Dev. *4*, 1068–1077.

85. Eming, S.A., Martin, P., and Tomic-Canic, M. (2014). Wound repair and regeneration: Mechanisms, signaling, and translation. Sci. Transl. Med. *6*, 265sr6-265sr6.

86. Evans, C.J., Olson, J.M., Ngo, K.T., Kim, E., Lee, N.E., Kuoy, E., Patananan, A.N., Sitz, D., Tran, P., Do, M.-T., et al. (2009). G-TRACE: rapid Gal4-based cell lineage analysis in Drosophila. Nat. Methods *6*, 603–605.

87. Evans Anderson, H., and Christiaen, L. (2016). Ciona as a Simple Chordate Model for Heart Development and Regeneration. J. Cardiovasc. Dev. Dis. *3*, 25.

88. Fan, Y., and Bergmann, A. (2008). Distinct Mechanisms of Apoptosis-Induced Compensatory Proliferation in Proliferating and Differentiating Tissues in the Drosophila Eye. Dev. Cell *14*, 399–410.

89. Fan, Y., Wang, S., Hernandez, J., Yenigun, V.B., Hertlein, G., Fogarty, C.E., Lindblad, J.L., and Bergmann, A. (2014). Genetic Models of Apoptosis-Induced Proliferation Decipher Activation of JNK and Identify a Requirement of EGFR Signaling for Tissue Regenerative Responses in Drosophila. PLoS Genet. *10*.

90. Fauvarque, M.O., Laurenti, P., Boivin, A., Bloyer, S., Griffin-Shea, R., Bourbon, H.M., and Dura, J.M. (2001). Dominant modifiers of the polyhomeotic extra-sex-combs phenotype induced by marked P element insertional mutagenesis in Drosophila. Genet. Res. *78*, 137–148.

91. Fei, J.-F., Schuez, M., Tazaki, A., Taniguchi, Y., Roensch, K., and Tanaka, E.M. (2014). CRISPR-Mediated Genomic Deletion of Sox2 in the Axolotl Shows a Requirement in Spinal Cord Neural Stem Cell Amplification during Tail Regeneration. Stem Cell Reports *3*, 444–459.

92. Félix, M.-A., and Barkoulas, M. (2015). Pervasive robustness in biological systems. Nat. Rev. Genet. *16*, 483–496.

93. Fernández-Hernández, I., Rhiner, C., and Moreno, E. (2013). Adult Neurogenesis in Drosophila. Cell Rep. *3*, 1857–1865.

94. Fisher, R.E., Geiger, L.A., Stroik, L.K., Hutchins, E.D., George, R.M., Denardo, D.F., Kusumi, K., Rawls, J.A., and Wilson-Rawls, J. (2012). A Histological Comparison of the Original and Regenerated Tail in the Green Anole, *Anolis carolinensis*. Anat. Rec. Adv. Integr. Anat. Evol. Biol. *295*, 1609–1619.

95. Flink, I. (2002). Cell cycle reentry of ventricular and atrial cardiomyocytes and cells within the epicardium following amputation of the ventricular apex in the axolotl, Amblystoma mexicanum : confocal microscopic immunofluorescent image analysis of bromodeoxyuridine-labeled nuclei. Anat. Embryol. (Berl). *205*, 235–244.

96. Fogarty, C.E., and Bergmann, A. (2015). The Sound of Silence. In Current Topics in Developmental Biology, pp. 241–265.

97. Fogarty, C.E., Diwanji, N., Lindblad, J.L., Tare, M., Amcheslavsky, A., Makhijani, K., Br??ckner, K., Fan, Y., and Bergmann, A. (2016). Extracellular Reactive Oxygen Species Drive Apoptosis-Induced Proliferation via Drosophila Macrophages. Curr. Biol. *26*.

98. Foo, S., Sun, Y., Lim, B., Ziukaite, R., O?Brien, K., Nien, C.-Y., Kirov, N., Shvartsman, S., and Rushlow, C. (2014). Zelda Potentiates Morphogen Activity by Increasing Chromatin Accessibility. Curr. Biol. *24*, 1341–1346.

99. La Fortezza, M., Schenk, M., Cosolo, A., Kolybaba, A., Grass, I., and Classen, A.-K. (2016). JAK/STAT signalling mediates cell survival in response to tissue stress. Development.

100. French, V., and Brakefield, P.M. (1992). The development of eyespot patterns on butterfly wings: morphogen sources or sinks? Development *116*.

101. French, V., Bryant, P., and Bryant, S. (1976). Pattern regulation in epimorphic fields. Science (80-.). *193*.

102. Fukunaga, R., Han, B.W., Hung, J.-H., Xu, J., Weng, Z., and Zamore, P.D. (2012). Dicer Partner Proteins Tune the Length of Mature miRNAs in Flies and Mammals. Cell *151*, 533–546.

103. Galliot, B. (2012). Hydra, a fruitful model system for 270 years. Int. J. Dev. Biol. *56*, 411–423.

104. Galliot, B., Miljkovic-Licina, M., de Rosa, R., and Chera, S. (2006). Hydra, a niche for cell and developmental plasticity. Semin. Cell Dev. Biol. *17*, 492–502.

105. Galliot, B., Miljkovic-Licina, M., Ghila, L., and Chera, S. (2007). RNAi gene silencing affects cell and developmental plasticity in hydra. C. R. Biol. *330*, 491–497.

106. Garaulet, D.L., Foronda, D., Calleja, M., and Sánchez-Herrero, E. (2008). Polycomb-dependent Ultrabithorax Hox gene silencing induced by high Ultrabithorax levels in Drosophila. Development *135*.

107. Garelli, A., Gontijo, A.M., Miguela, V., Caparros, E., and Dominguez, M. (2012). Imaginal Discs Secrete Insulin-Like Peptide 8 to Mediate Plasticity of Growth and Maturation. Science (80-.). *336*, 579–582.

108. Garelli, A., Heredia, F., Casimiro, A.P., Macedo, A., Nunes, C., Garcez, M., Dias, A.R.M., Volonte, Y.A., Uhlmann, T., Caparros, E., et al. (2015). Dilp8 requires the neuronal relaxin receptor Lgr3 to couple growth to developmental timing. Nat. Commun. *6*.

109. Gargioli, C., and Slack, J.M.W. (2004). Cell lineage tracing during Xenopus tail regeneration. Development *131*, 2669–2679.

110. Gauron, C., Rampon, C., Bouzaffour, M., Ipendey, E., Teillon, J., Volovitch, M., and Vriz, S. (2013). Sustained production of ROS triggers compensatory proliferation and is required for regeneration to proceed. Sci. Rep. *3*, 2084.

111. Gawriluk, T.R., Simkin, J., Thompson, K.L., Biswas, S.K., Clare-Salzler, Z., Kimani, J.M., Kiama, S.G., Smith, J.J., Ezenwa, V.O., and Seifert, A.W. (2016). Comparative analysis of ear-hole closure identifies epimorphic regeneration as a discrete trait in mammals. Nat. Commun. *7*, 11164.

112. Gettings, M., Serman, F., Rousset, R., Bagnerini, P., Almeida, L., and Noselli, S. (2010). JNK Signalling Controls Remodelling of the Segment Boundary through Cell Reprogramming during Drosophila Morphogenesis. PLoS Biol. *8*, e1000390.

113. Giannios, P., and Tsitilou, S.G. (2013). The embryonic transcription factor Zelda of Drosophila melanogaster is also expressed in larvae and may regulate developmentally important genes. Biochem. Biophys. Res. Commun. *438*, 329–333.

114. Gibson, D.G., Young, L., Chuang, R.-Y., Venter, J.C., Hutchison, C.A., and Smith, H.O. (2009). Enzymatic assembly of DNA molecules up to several hundred kilobases. Nat. Methods *6*, 343–345.

115. Glennon, N.B., Jabado, O., Lo, M.K., and Shaw, M.L. (2015). Transcriptome Profiling of the Virus-Induced Innate Immune Response in Pteropus vampyrus and Its Attenuation by Nipah Virus Interferon Antagonist Functions. J. Virol. *89*, 7550–7566.

116. Gómez-Skarmeta, J.-L., del Corral, R.D., de la Calle-Mustienes, E., Ferrés-Marcó, D., and Modolell, J. (1996). araucan and caupolican, Two Members of the Novel Iroquois Complex, Encode Homeoproteins That Control Proneural and Vein-Forming Genes. Cell *85*, 95–105.

117. Gratz, S.J., Harrison, M.M., Wildonger, J., and O'Connor-Giles, K.M. (2015). Precise Genome Editing of Drosophila with CRISPR RNA-Guided Cas9. In Methods in Molecular Biology (Clifton, N.J.), pp. 335–348.

118. Grusche, F.A., Degoutin, J.L., Richardson, H.E., and Harvey, K.F. (2011). The Salvador/Warts/Hippo pathway controls regenerative tissue growth in Drosophila melanogaster. Dev. Biol. *350*, 255–266.

119. Guest, S.T., Yu, J., Liu, D., Hines, J.A., Kashat, M.A., Finley, R.L., Millar, A., Taylor, P., Bennett, K., and Boutilier, K. (2011). A protein network-guided screen for cell cycle regulators in Drosophila. BMC Syst. Biol. *5*, 65.

120. Guillen, I., Mullor, J.L., Capdevila, J., Sanchez-Herrero, E., Morata, G., and Guerrero, I. (1995). The function of engrailed and the specification of Drosophila wing pattern. Development *121*.

121. Gupta, V., Gemberling, M., Karra, R., Rosenfeld, G.E., Evans, T., and Poss, K.D. (2013). An Injury-Responsive Gata4 Program Shapes the Zebrafish Cardiac Ventricle. Curr. Biol. *23*, 1221–1227.

122. Gustavson, E., Goldsborough, A.S., Ali, Z., and Kornberg, T.B. (1996). The Drosophila engrailed and invected Genes: Partners in Regulation, Expression and Function. Genetics *142*.

123. Gutiérrez, L., Zurita, M., Kennison, J.A., and Vázquez, M. (2003). The Drosophila trithorax group gene tonalli(tna) interacts genetically with the Brahma remodeling complex and encodes an SP-RING finger protein. Development *130*.

124. Hadorn, E. (1968). Transdetermination in cells. Sci. Am. *219*, 110–4 passim.

125. Halasi, G., Søviknes, A.M., Sigurjonsson, O., and Glover, J.C. (2012). Proliferation and recapitulation of developmental patterning associated with regulative regeneration of the spinal cord neural tube. Dev. Biol. *365*, 118–132.

126. Halder, G., Polaczyk, P., Kraus, M.E., Hudson, A., Kim, J., Laughon, A., and Carroll, S. (1998). The Vestigial and Scalloped proteins act together to directly regulate wing-specific gene expression in Drosophila. Genes Dev. *12*, 3900–3909.

127. Hama, C., Ali, Z., and Kornberg, T.B. (1990). Region-specific recombination and expression are directed by portions of the Drosophila engrailed promoter. Genes Dev. *4*, 1079–1093.

128. Hamm, D.C., Bondra, E.R., and Harrison, M.M. (2015). Transcriptional activation is a conserved feature of the early embryonic factor Zelda that requires a cluster of four zinc fingers for DNA binding and a low-complexity activation domain. J. Biol. Chem. *290*, 3508–3518.

129. Hariharan, I.K., and Serras, F. (2017). Imaginal disc regeneration takes flight. Curr. Opin. Cell Biol. *48*.

130. Harland, R.M., and Grainger, R.M. (2011). Xenopus research: metamorphosed by genetics and genomics. Trends Genet. *27*, 507–515.

131. Harris, R.E., Setiawan, L., Saul, J., and Hariharan, I.K. (2016). Localized epigenetic silencing of a damage-activated WNT enhancer limits regeneration in mature Drosophila imaginal discs. Elife *5*.

132. Harrison, M.M., Li, X.-Y., Kaplan, T., Botchan, M.R., and Eisen, M.B. (2011). Zelda Binding in the Early Drosophila melanogaster Embryo Marks Regions Subsequently Activated at the Maternal-to-Zygotic Transition. PLoS Genet. *7*, e1002266.

133. Haughton, C.L., Gawriluk, T.R., and Seifert, A.W. (2016). The Biology and Husbandry of the African Spiny Mouse (Acomys cahirinus) and the Research Uses of a Laboratory Colony. J. Am. Assoc. Lab. Anim. Sci. *55*, 9–17.

134. Hay, B.A., Wolff, T., and Rubin, G.M. (1994). Expression of baculovirus P35 prevents cell death in Drosophila. Development *120*, 2121–2129.

135. Hayashi, R., Goto, Y., Ikeda, R., Yokoyama, K.K., and Yoshida, K. (2006). CDCA4 is an E2F transcription factor family-induced nuclear factor that regulates E2F-dependent transcriptional activation and cell proliferation. J. Biol. Chem. *281*, 35633–35648.

136. Hazelrigg, T., Levis, R., and Rubin, G.M. (1984). Transformation of white locus DNA in drosophila: dosage compensation, zeste interaction, and position effects. Cell *36*, 469–481.

137. Heber-Katz, E., and Gourevitch, D. (2009). The Relationship between Inflammation and Regeneration in the MRL Mouse. Ann. N. Y. Acad. Sci. *1172*, 110–114.

138. Heber-Katz, E., Zhang, Y., Bedelbaeva, K., Song, F., Chen, X., and Stocum, D.L. (2012). Cell Cycle Regulation and Regeneration. In Current Topics in Microbiology and Immunology, pp. 253–276.

139. Henry, J.J., and Tsonis, P.A. (2010). Molecular and cellular aspects of amphibian lens regeneration. Prog. Retin. Eye Res. *29*, 543–555.

140. Herrera, S.C., and Morata, G. (2014). Transgressions of compartment boundaries and cell reprogramming during regeneration in *Drosophila*. Elife *3*.

141. Herrera, S.C., Martín, R., and Morata, G. (2013). Tissue Homeostasis in the Wing Disc of Drosophila melanogaster: Immediate Response to Massive Damage during Development. PLoS Genet. *9*.

142. Hesselson, D., Anderson, R.M., Beinat, M., and Stainier, D.Y.R. (2009). Distinct populations of quiescent and proliferative pancreatic -cells identified by HOTcre mediated labeling. Proc. Natl. Acad. Sci. *106*, 14896–14901.

143. Hirose, T., Fujii, R., Nakamura, H., Aratani, S., Fujita, H., Nakazawa, M., Nakamura, K., Nishioka, K., and Nakajima, T. (2003). Regulation of CREB-mediated transcription by association of CDK4 binding protein p34SEI-1 with CBP. Int. J. Mol. Med. *11*, 705–712.

144. Hong, S.-W., Moon, J.-H., Kim, J.-S., Shin, J.-S., Jung, K.-A., Lee, W.-K., Jeong, S.-Y., Hwang, J.J., Lee, S.-J., Suh, Y.-A., et al. (2014). p34 is a novel regulator of the oncogenic behavior of NEDD4-1 and PTEN. Cell Death Differ. *21*, 146–160.

145. Hsu, S.I.-H. (2001). TRIP-Br: a novel family of PHD zinc finger- and bromodomain-interacting proteins that regulate the transcriptional activity of E2F-1/DP-1. EMBO J. *20*, 2273–2285.

146. Hu, W., Yu, X., Liu, Z., Sun, Y., Chen, X., Yang, X., Li, X., Lam, W.K., Duan, Y., Cao, X., et al. (2017). The complex of TRIP-Br1 and XIAP ubiquitinates and degrades multiple adenylyl cyclase isoforms. Elife *6*.

147. Huh, J.R., Guo, M., and Hay, B.A. (2004). Compensatory Proliferation Induced by Cell Death in the Drosophila Wing Disc Requires Activity of the Apical Cell Death Caspase Dronc in a Nonapoptotic Role. Curr. Biol. *14*, 1262–1266.

148. Hui, S.P., Sengupta, D., Lee, S.G.P., Sen, T., Kundu, S., Mathavan, S., and Ghosh, S. (2014a). Genome Wide Expression Profiling during Spinal Cord Regeneration Identifies Comprehensive Cellular Responses in Zebrafish. PLoS One *9*, e84212.

144. Hui, S.P., Sengupta, D., Lee, S.G.P., Sen, T., Kundu, S., Mathavan, S., and Ghosh, S. (2014b). Genome Wide Expression Profiling during Spinal Cord Regeneration Identifies Comprehensive Cellular Responses in Zebrafish. PLoS One *9*, e84212.

145. Igaki, T., and Miura, M. (2014). The Drosophila TNF ortholog Eiger: Emerging physiological roles and evolution of the TNF system. Semin. Immunol. *26*, 267–274.

146. Ishimaru, Y., Nakamura, T., Bando, T., Matsuoka, Y., Ohuchi, H., Noji, S., and Mito, T. (2015). Involvement of dachshund and Distal-less in distal pattern formation of the cricket leg during regeneration. Sci. Rep. *5*, 8387.

147. Iwafuchi-Doi, M., and Zaret, K.S. (2014). Pioneer transcription factors in cell reprogramming. Genes Dev. *28*, 2679–2692.

148. Iwafuchi-Doi, M., and Zaret, K.S. (2016). Cell fate control by pioneer transcription factors. Development *143*.

149. Jaszczak, J.S., Wolpe, J.B., Dao, A.Q., and Halme, A. (2015). Nitric Oxide Synthase Regulates Growth Coordination During Drosophila melanogaster Imaginal Disc Regeneration. Genetics *200*.

150. Jaszczak, J.S., Wolpe, J.B., Bhandari, R., Jaszczak, R.G., and Halme, A. (2016). Growth coordination during Drosophila melanogaster imaginal disc regeneration is mediated by signaling through the relaxin receptor Lgr3 in the prothoracic gland. Genetics *204*.

151. Jaźwińska, A., Kirov, N., Wieschaus, E., Roth, S., and Rushlow, C. (1999). The Drosophila Gene brinker Reveals a Novel Mechanism of Dpp Target Gene Regulation. Cell *96*, 563–573.

152. Jeffery, W.R. (2015a). Closing the wounds: One hundred and twenty five years of regenerative biology in the ascidian *Ciona intestinalis*. Genesis *53*, 48–65.

153. Jeffery, W.R. (2015b). Distal Regeneration Involves the Age Dependent Activity of Branchial Sac Stem Cells in the Ascidian Ciona intestinalis. Regen. (Oxford, England) *2*, 1–18.

154. Jiang, H., Tian, A., and Jiang, J. (2016). Intestinal stem cell response to injury: lessons from Drosophila. Cell. Mol. Life Sci. *73*, 3337–3349.

155. Jung, S., Li, C., Jeong, D., Lee, S., Ohk, J., Park, M., Han, S., Duan, J., Kim, C., Yang, Y., et al. (2013). Oncogenic function of p34SEI-1 via NEDD4-1-mediated PTEN ubiquitination/degradation and activation of the PI3K/AKT pathway. Int. J. Oncol. *43*, 1587–1595.

156. Jung, S., Li, C., Duan, J., Lee, S., Kim, K., Park, Y., Yang, Y., Kim, K.-I., Lim, J.-S., Cheon, C.-I., et al. (2015). TRIP-Br1 oncoprotein inhibits autophagy, apoptosis, and necroptosis under nutrient/serum-deprived condition. Oncotarget *6*, 29060–29075.

157. Kan, N.G., Junghans, D., and Belmonte, J.C.I. (2009). Compensatory growth mechanisms regulated by BMP and FGF signaling mediate liver regeneration in zebrafish after partial hepatectomy. FASEB J. *23*, 3516–3525.

158. Karami, A., Tebyanian, H., Goodarzi, V., and Shiri, S. (2015). Planarians: an In Vivo Model for Regenerative Medicine. Int. J. Stem Cells *8*, 128–133.

159. Karlsson, J. (1981). The distribution of regenerative potential in the wing disc of Drosophila. Development *61*.

160. Kashio, S., Obata, F., Zhang, L., Katsuyama, T., Chihara, T., and Miura, M. (2016). Tissue nonautonomous effects of fat body methionine metabolism on imaginal disc repair in *Drosophila*. Proc. Natl. Acad. Sci. *113*, 1835–1840.

161. Kassis, J.A., Kennison, J.A., and Tamkun, J.W. (2017). Polycomb and Trithorax Group Genes in *Drosophila*. Genetics *206*, 1699–1725.

162. Kato, K., Awasaki, T., and Ito, K. (2009). Neuronal programmed cell death induces glial cell division in the adult Drosophila brain. Development *136*, 51–59.

163. Kato, K., Forero, M.G., Fenton, J.C., and Hidalgo, A. (2011). The Glial Regenerative Response to Central Nervous System Injury Is Enabled by Pros-Notch and Pros-NFκB Feedback. PLoS Biol. *9*, e1001133.

164. Katsuyama, T., and Paro, R. (2013). Innate immune cells are dispensable for regenerative growth of imaginal discs. Mech. Dev. *130*, 112–121.

165. Katsuyama, T., Comoglio, F., Seimiya, M., Cabuy, E., and Paro, R. (2015). During *Drosophila* disc regeneration, JAK/STAT coordinates cell proliferation with Dilp8-mediated developmental delay. Proc. Natl. Acad. Sci. *112*.

166. Keys, D.N., Lewis, D.L., Selegue, J.E., Pearson, B.J., Goodrich, L. V, Johnson, R.L., Gates, J., Scott, M.P., and Carroll, S.B. (1999). Recruitment of a hedgehog regulatory circuit in butterfly eyespot evolution. Science *283*, 532–534.

167. Khan, S.J., Bajpai, A., Alam, M.A., Gupta, R.P., Harsh, S., Pandey, R.K., Goel-Bhattacharya, S., Nigam, A., Mishra, A., and Sinha, P. (2013). Epithelial neoplasia in Drosophila entails switch to primitive cell states. Proc. Natl. Acad. Sci. *110*, E2163–E2172.

168. Khan, S.J., Schuster, K.J., and Smith-Bolton, R.K. (2016a). Regeneration in Crustaceans and Insects. ELS.

169. Khan, S.J., Abidi, S.N.F., Tian, Y., Skinner, A., and Smith-Bolton, R.K. (2016b). A rapid, gentle and scalable method for dissociation and fluorescent sorting of imaginal disc cells for mRNA sequencing. Fly (Austin). *10*, 73–80.

170. Khan, S.J., Abidi, S.N.F., Skinner, A., Tian, Y., and Smith-Bolton, R.K. (2017). The Drosophila Duox maturation factor is a key component of a positive feedback loop that sustains regeneration signaling. PLOS Genet. *13*, e1006937.

171. Khattak, S., and Tanaka, E.M. (2015). Transgenesis in Axolotl (Ambystoma mexicanum). In Methods in Molecular Biology (Clifton, N.J.), pp. 269–277.

172. Kim, J., Sebring, A., Esch, J.J., Kraus, M.E., Vorwerk, K., Magee, J., and Carroll, S.B. (1996). Integration of positional signals and regulation of wing formation and identity by Drosophila vestigial gene. Nature *382*, 133–138.

173. Kitano, H. (2004). Biological robustness. Nat. Rev. Genet. *5*, 826–837.

174. Knopf, F., Hammond, C., Chekuru, A., Kurth, T., Hans, S., Weber, C.W., Mahatma, G., Fisher, S., Brand, M., Schulte-Merker, S., et al. (2011). Bone Regenerates via Dedifferentiation of Osteoblasts in the Zebrafish Fin. Dev. Cell *20*, 713–724.

175. Konstantinides, N., and Averof, M. (2014). A Common Cellular Basis for Muscle Regeneration in Arthropods and Vertebrates. Science (80-.). *343*, 788–791.

176. Kopp, A. (2011). Drosophila sex combs as a model of evolutionary innovations. Evol. Dev. *13*, 504–522.

177. Kornberg, T., Sidén, I., O'Farrell, P., and Simon, M. (1985). The engrailed locus of drosophila: In situ localization of transcripts reveals compartment-specific expression. Cell *40*, 45–53.

178. Kragl, M., Knapp, D., Nacu, E., Khattak, S., Maden, M., Epperlein, H.H., and Tanaka, E.M. (2009). Cells keep a memory of their tissue origin during axolotl limb regeneration. Nature *460*, 60–65.

179. Kroehne, V., Freudenreich, D., Hans, S., Kaslin, J., and Brand, M. (2011). Regeneration of the adult zebrafish brain from neurogenic radial glia-type progenitors. Development *138*, 4831–4841.

180. Kumar, A., Godwin, J.W., Gates, P.B., Garza-Garcia, A.A., and Brockes, J.P. (2007). Molecular Basis for the Nerve Dependence of Limb Regeneration in an Adult Vertebrate. Science (80-.). *318*.

181. Kumar, A., Gates, P.B., Czarkwiani, A., and Brockes, J.P. (2015). An orphan gene is necessary for preaxial digit formation during salamander limb development. Nat. Commun. *6*, 8684.

182. Kusano, S., Shiimura, Y., and Eizuru, Y. (2011). I-mfa domain proteins specifically interact with SERTA domain proteins and repress their transactivating functions. Biochimie *93*, 1555–1564.

183. Lai, I.-L., Wang, S.-Y., Yao, Y.-L., and Yang, W.-M. (2007). Transcriptional and subcellular regulation of the TRIP-Br family. Gene *388*, 102–109.

184. Layden, M.J., Rentzsch, F., and Röttinger, E. (2016). The rise of the starlet sea anemone *Nematostella vectensis* as a model system to investigate development and regeneration. Wiley Interdiscip. Rev. Dev. Biol. *5*, 408–428.

185. Lee, A.K., Sze, C.C., Kim, E.R., and Suzuki, Y. (2013a). Developmental coupling of larval and adult stages in a complex life cycle: insights from limb regeneration in the flour beetle, Tribolium castaneum. Evodevo *4*, 20.

186. Lee, C.-Y., Clough, E.A., Yellon, P., Teslovich, T.M., Stephan, D.A., and Baehrecke, E.H. (2003). Genome-Wide Analyses of Steroid- and Radiation-Triggered Programmed Cell Death in Drosophila. Curr. Biol. *13*, 350–357.

187. Lee, M.T., Bonneau, A.R., Takacs, C.M., Bazzini, A.A., DiVito, K.R., Fleming, E.S., and Giraldez, A.J. (2013b). Nanog, Pou5f1 and SoxB1 activate zygotic gene expression during the maternal-to-zygotic transition. Nature *503*, 360–364.

188. Lee, N., Maurange, C., Ringrose, L., and Paro, R. (2005). Suppression of Polycomb group proteins by JNK signalling induces transdetermination in Drosophila imaginal discs. Nature *438*, 234–237.

189. Lee, S., Kim, J., Jung, S., Li, C., Yang, Y., Kim, K., Lim, J.-S., Kim, Y., Cheon, C.-I., and Lee, M.-S. (2015). SIAH1-induced p34SEI-1 polyubiquitination/degradation mediates p53 preferential vitamin C cytotoxicity. Int. J. Oncol. *46*, 1377–1384.

190. Lehoczky, J.A., Robert, B., and Tabin, C.J. (2011). Mouse digit tip regeneration is mediated by fate-restricted progenitor cells. Proc. Natl. Acad. Sci. U. S. A. *108*, 20609–20614.

191. Leichsenring, M., Maes, J., Mossner, R., Driever, W., and Onichtchouk, D. (2013). Pou5f1 Transcription Factor Controls Zygotic Gene Activation In Vertebrates. Science (80-.). *341*, 1005–1009.

192. Lengner, C.J., Camargo, F.D., Hochedlinger, K., Welstead, G.G., Zaidi, S., Gokhale, S., Scholer, H.R., Tomilin, A., and Jaenisch, R. (2007). Oct4 Expression Is Not Required for Mouse Somatic Stem Cell Self-Renewal. Cell Stem Cell *1*, 403–415.

193. Lenkowski, J.R., and Raymond, P.A. (2014). Müller glia: Stem cells for generation and regeneration of retinal neurons in teleost fish. Prog. Retin. Eye Res. *40*, 94–123.

194. Lévesque, M., Villiard, É., and Roy, S. (2010). Skin wound healing in axolotls: a scarless process. J. Exp. Zool. Part B Mol. Dev. Evol. *314B*, 684–697.

195. Li, J., Melvin, W.S., Ming-Daw Tsai, A., and Muscarella, P. (2004). The Nuclear Protein p34SEI-1 Regulates the Kinase Activity of Cyclin-Dependent Kinase 4 in a Concentration-Dependent Manner†. Biochemistry *43*, 4394–4399.

196. Liang, H.-L., Nien, C.-Y., Liu, H.-Y., Metzstein, M.M., Kirov, N., and Rushlow, C. (2008). The zinc-finger protein Zelda is a key activator of the early zygotic genome in Drosophila. Nature *456*, 400–403.

197. Liew, C.W., Boucher, J., Cheong, J.K., Vernochet, C., Koh, H.-J., Mallol, C., Townsend, K., Langin, D., Kawamori, D., Hu, J., et al. (2013). Ablation of TRIP-Br2, a regulator of fat lipolysis, thermogenesis and oxidative metabolism, prevents diet-induced obesity and insulin resistance. Nat. Med. *19*, 217–226.

198. Ligoxygakis, P., Bray, S.J., Apidianakis, Y., and Delidakis, C. (1999). Ectopic expression of individual E(spl) genes has differential effects on different cell fate decisions and underscores the biphasic requirement for notch activity in wing margin establishment in Drosophila. Development *126*, 2205–2214.

199. Lin, G., Chen, Y., and Slack, J.M.W. (2013). Imparting Regenerative Capacity to Limbs by Progenitor Cell Transplantation. Dev. Cell *24*, 41–51.

200. Lindsay, S.A., and Wasserman, S.A. (2014). Conventional and non-conventional Drosophila Toll signaling. Dev. Comp. Immunol. *42*, 16–24.

201. Love, N.R., Chen, Y., Bonev, B., Gilchrist, M.J., Fairclough, L., Lea, R., Mohun, T.J., Paredes, R., Zeef, L.A., and Amaya, E. (2011). Genome-wide analysis of gene expression during Xenopus tropicalis tadpole tail regeneration. BMC Dev. Biol. *11*, 70.

202. Love, N.R., Chen, Y., Ishibashi, S., Kritsiligkou, P., Lea, R., Koh, Y., Gallop, J.L., Dorey, K., and Amaya, E. (2013). Amputation-induced reactive oxygen species are required for successful Xenopus tadpole tail regeneration. Nat. Cell Biol. *15*.

203. Manansala, M.C., Min, S., and Cleary, M.D. (2013). The Drosophila SERTAD protein Taranis determines lineage-specific neural progenitor proliferation patterns. Dev. Biol. *376*, 150–162.

204. Markstein, M., Pitsouli, C., Villalta, C., Celniker, S.E., and Perrimon, N. (2008). Exploiting position effects and the gypsy retrovirus insulator to engineer precisely expressed transgenes. Nat. Genet. *40*, 476–483.

205. Martín-Blanco, E., Gampel, A., Ring, J., Virdee, K., Kirov, N., Tolkovsky, A.M., and Martinez-Arias, A. (1998). puckered encodes a phosphatase that mediates a feedback loop regulating JNK activity during dorsal closure in Drosophila. Genes Dev. *12*, 557–570.

206. Martin, F.A., Herrera, S.C., and Morata, G. (2009a). Cell competition, growth and size control in the Drosophila wing imaginal disc. Development *136*, 3747–3756.

207. Martin, F.A., Perez-Garijo, A., and Morata, G. (2009b). Apoptosis in Drosophila: compensatory proliferation and undead cells. Int. J. Dev. Biol. *53*, 1341–1347.

208. Martín, R., Pinal, N., and Morata, G. (2017). Distinct regenerative potential of trunk and appendages of *Drosophila* mediated by JNK signalling. Development *144*, 3946–3956.

209. Maschat, F., Serrano, N., Randsholt, N.B., and Geraud, G. (1998). engrailed and polyhomeotic interactions are required to maintain the A/P boundary of the Drosophila developing wing. Development *125*.

210. Matsuda, S., Harmansa, S., and Affolter, M. (2016). BMP morphogen gradients in flies. Cytokine Growth Factor Rev. *27*, 119–127.

211. Mattila, J., Omelyanchuk, L., and Nokkala, S. (2004). Dynamics of decapentaplegic expression during regeneration of the Drosophila melanogaster wing imaginal disc. Int. J. Dev. Biol. *48*, 343–347.

212. Maves, L., and Schubiger, G. (1995). Wingless induces transdetermination in developing Drosophila imaginal discs. Development *121*, 1263–1272.

213. McClure, K.D., and Schubiger, G. (2007). Transdetermination: Drosophila imaginal disc cells exhibit stem cell-like potency. Int. J. Biochem. Cell Biol. *39*, 1105–1118.

214. McCusker, C.D., Gardiner, D.M., Dawson, C., Lucifero, D., and Madeja, Z. (2013). Positional Information Is Reprogrammed in Blastema Cells of the Regenerating Limb of the Axolotl (Ambystoma mexicanum). PLoS One *8*, e77064.

215. McLean, K.E., and Vickaryous, M.K. (2011). A novel amniote model of epimorphic regeneration: the leopard gecko, Eublepharis macularius. BMC Dev. Biol. *11*, 50.

216. Meinhardt, H. (1983). Cell determination boundaries as organizing regions for secondary embryonic fields. Dev. Biol. *96*, 375–385.

217. Meserve, J.H., and Duronio, R.J. (2015). Scalloped and Yorkie are required for cell cycle re-entry of quiescent cells after tissue damage. Development *142*.

218. Michalopoulos, G.K. (2017). Hepatostat: Liver regeneration and normal liver tissue maintenance. Hepatology *65*, 1384–1392.

219. Mito, T., and Noji, S. (2008). The Two-Spotted Cricket Gryllus bimaculatus: An Emerging Model for Developmental and Regeneration Studies. CSH Protoc. *2008*, pdb.emo110.

220. Mito, T., Inoue, Y., Kimura, S., Miyawaki, K., Niwa, N., Shinmyo, Y., Ohuchi, H., and Noji, S. (2002). Involvement of hedgehog, wingless, and dpp in the initiation of proximodistal axis formation during the regeneration of insect legs, a verification of the modified boundary model. Mech. Dev. *114*, 27–35.

221. Mokalled, M.H., Patra, C., Dickson, A.L., Endo, T., Stainier, D.Y.R., and Poss, K.D. (2016). Injury-induced ctgfa directs glial bridging and spinal cord regeneration in zebrafish. Science *354*, 630–634.

222. Monteiro, A. (2015). Origin, Development, and Evolution of Butterfly Eyespots. Annu. Rev. Entomol. *60*, 253–271.

223. Monteiro, A., Glaser, G., Stockslager, S., Glansdorp, N., and Ramos, D. (2006). Comparative insights into questions of lepidopteran wing pattern homology. BMC Dev. Biol. *6*, 52.

224. Monteiro, A., Chen, B., Ramos, D.M., Oliver, J.C., Tong, X., Guo, M., Wang, W.-K., Fazzino, L., and Kamal, F. (2013). Distal- L ess Regulates Eyespot Patterns and Melanization in Bicyclus Butterflies. J. Exp. Zool. Part B Mol. Dev. Evol. *320*, 321–331.

225. Morata, G., and Herrera, S.C. (2016). Cell reprogramming during regeneration in Drosophila : transgression of compartment boundaries. Curr. Opin. Genet. Dev. *40*, 11–16.

226. Motzny, C.K., and Holmgren, R. (1995). The Drosophila cubitus interruptus protein and its role in the wingless and hedgehog signal transduction pathways. Mech. Dev. *52*, 137–150.

227. Muneoka, K., Allan, C.H., Yang, X., Lee, J., and Han, M. (2008). Mammalian regeneration and regenerative medicine. Birth Defects Res. Part C Embryo Today Rev. *84*, 265–280.

228. Myllymaki, H., Valanne, S., and Ramet, M. (2014). The Drosophila Imd Signaling Pathway. J. Immunol. *192*, 3455–3462.

229. Nacu, E., and Tanaka, E.M. (2011). Limb Regeneration: A New Development? Annu. Rev. Cell Dev. Biol. *27*, 409–440.

230. Nacu, E., Gromberg, E., Oliveira, C.R., Drechsel, D., and Tanaka, E.M. (2016). FGF8 and SHH substitute for anterior–posterior tissue interactions to induce limb regeneration. Nature *533*, 407–410.

231. Nadeau, J.H. (2001). Modifier genes in mice and humans. Nat. Rev. Genet. *2*, 165–174.

232. Nagarkar-Jaiswal, S., DeLuca, S.Z., Lee, P.-T., Lin, W.-W., Pan, H., Zuo, Z., Lv, J., Spradling, A.C., and Bellen, H.J. (2015). A genetic toolkit for tagging intronic MiMIC containing genes. Elife *4*.

233. Nakamura, T., Mito, T., Tanaka, Y., Bando, T., Ohuchi, H., and Noji, S. (2007). Involvement of canonical Wnt/Wingless signaling in the determination of the positional values within the leg segment of the cricket Gryllus bimaculatus. Dev. Growth Differ. *49*, 79–88.

234. Narciso, C., Wu, Q., Brodskiy, P., Garston, G., Baker, R., Fletcher, A., and Zartman, J. (2015). Patterning of wound-induced intercellular Ca 2+ flashes in a developing epithelium. Phys. Biol. *12*.

235. Neumann, C.J., and Cohen, S.M. (1996). A hierarchy of cross-regulation involving Notch, wingless, vestigial and cut organizes the dorsal/ventral axis of the Drosophila wing. Development *122*, 3477–3485.

236. Nevo, E. (1978). Genetic variation in natural populations: patterns and theory. Theor. Popul. Biol. *13*, 121–177.

237. Ng, M., Diaz-Benjumea, F.J., Vincent, J.-P., Wu, J., and Cohen, S.M. (1996). Specification of the wing by localized expression of wingless protein. Nature *381*, 316–318.

238. Ni, J.-Q., Zhou, R., Czech, B., Liu, L.-P., Holderbaum, L., Yang-Zhou, D., Shim, H.-S., Tao, R., Handler, D., Karpowicz, P., et al. (2011). A genome-scale shRNA resource for transgenic RNAi in Drosophila. Nat. Methods *8*, 405–407.

239. Nien, C.-Y., Liang, H.-L., Butcher, S., Sun, Y., Fu, S., Gocha, T., Kirov, N., Manak, J.R., and Rushlow, C. (2011). Temporal Coordination of Gene Networks by Zelda in the Early Drosophila Embryo. PLoS Genet. *7*, e1002339.

240. Nijhout, H.F. (1985). Cautery-induced colour patterns in Precis coenia (Lepidoptera: Nymphalidae). J. Embryol. Exp. Morphol. *86*, 191–203.

241. Nijhout, H.F., and Grunert, L.W. (1988). Colour pattern regulation after surgery on the wing disks of Precis coenia (Lepidoptera: Nymphalidae). Development *102*.

242. Nussbaumer, U., Halder, G., Groppe, J., Affolter, M., and Montagne, J. (2000). Expression of the blistered/DSRF gene is controlled by different morphogens during Drosophila trachea and wing development. Mech. Dev. *96*, 27–36.

243. Nüsslein-Volhard, C., and Wieschaus, E. (1980). Mutations affecting segment number and polarity in Drosophila. Nature *287*, 795–801.

244. O'Brochta, D.A., and Bryant, P.J. (1987). Distribution of S-phase cells during the regeneration of Drosophila imaginal wing discs. Dev. Biol. *119*, 137–142.

245. Özsu, N., Chan, Q.Y., Chen, B., Gupta, M. Das, and Monteiro, A. (2017). Wingless is a positive regulator of eyespot color patterns in Bicyclus anynana butterflies. Dev. Biol. *429*, 177–185.

246. Page-McCaw, A., Serano, J., Santé, J.M., and Rubin, G.M. (2003). Drosophila matrix metalloproteinases are required for tissue remodeling, but not embryonic development. Dev. Cell *4*, 95–106.

247. Parchem, R.J., Perry, M.W., and Patel, N.H. (2007). Patterns on the insect wing. Curr. Opin. Genet. Dev. *17*, 300–308.

248. Passamaneck, Y.J., and Martindale, M.Q. (2012). Cell proliferation is necessary for the regeneration of oral structures in the anthozoan cnidarian Nematostella vectensis. BMC Dev. Biol. *12*, 34.

249. Patel, N.H., Martin-Blanco, E., Coleman, K.G., Poole, S.J., Ellis, M.C., Kornberg, T.B., and Goodman, C.S. (1989). Expression of engrailed proteins in arthropods, annelids, and chordates. Cell *58*, 955–968.

250. Patterson, M., Barske, L., Van Handel, B., Rau, C.D., Gan, P., Sharma, A., Parikh, S., Denholtz, M., Huang, Y., Yamaguchi, Y., et al. (2017). Frequency of mononuclear diploid cardiomyocytes underlies natural variation in heart regeneration. Nat. Publ. Gr.

251. Paul, S., Schindler, S., Giovannone, D., de Millo Terrazzani, A., Mariani, F. V., and Crump, J.G. (2016). Ihha induces hybrid cartilage-bone cells during zebrafish jawbone regeneration. Development *143*, 2066–2076.

252. Pearson, J.C., Watson, J.D., and Crews, S.T. (2012). Drosophila melanogaster Zelda and Single-minded collaborate to regulate an evolutionarily dynamic CNS midline cell enhancer. Dev. Biol. *366*, 420–432.

253. Peng, Y., Zhao, S., Song, L., Wang, M., and Jiao, K. (2013). Sertad1 encodes a novel transcriptional co-activator of SMAD1 in mouse embryonic hearts.

254. Perez-Garijo, A., Martin, F.A., Struhl, G., and Morata, G. (2005). Dpp signaling and the induction of neoplastic tumors by caspase-inhibited apoptotic cells in Drosophila. Proc. Natl. Acad. Sci. *102*, 17664–17669.

255. Perez-Garijo, A., Shlevkov, E., and Morata, G. (2009). The role of Dpp and Wg in compensatory proliferation and in the formation of hyperplastic overgrowths caused by apoptotic cells in the Drosophila wing disc. Development *136*, 1169–1177.

256. Pérez-Garijo, A., Martín, F.A., and Morata, G. (2004). Caspase inhibition during apoptosis causes abnormal signalling and developmental aberrations in Drosophila. Development *131*.

257. Pérez-Garijo, A., Fuchs, Y., and Steller, H. (2013). Apoptotic cells can induce non-autonomous apoptosis through the TNF pathway. Elife *2*, e01004.

258. Phillips, R.G., Roberts, I.J.H., Ingham, P.W., Robert, J., and Whittle, S. (1990). The Drosophila segment polarity gene patched is involved in a position - signalling mechanism in imaginal discs. Development *110*, 105–114.

259. Platzer, M., and Englert, C. (2016). Nothobranchius furzeri: A Model for Aging Research and More. Trends Genet. *32*, 543–552.

260. Porrello, E.R., Mahmoud, A.I., Simpson, E., Hill, J.A., Richardson, J.A., Olson, E.N., and Sadek, H.A. (2011). Transient Regenerative Potential of the Neonatal Mouse Heart. Science (80-.). *331*, 1078–1080.

261. Poss, K.D., Wilson, L.G., and Keating, M.T. (2002). Heart Regeneration in Zebrafish. Science (80-.). *298*, 2188–2190.

262. Prilusky, J., Felder, C.E., Zeev-Ben-Mordehai, T., Rydberg, E.H., Man, O., Beckmann, J.S., Silman, I., and Sussman, J.L. (2005). FoldIndex(C): a simple tool to predict whether a given protein sequence is intrinsically unfolded. Bioinformatics *21*, 3435–3438.

263. Protas, M.E., and Patel, N.H. (2008). Evolution of Coloration Patterns. Annu. Rev. Cell Dev. Biol. *24*, 425–446.

264. Prudic, K.L., Stoehr, A.M., Wasik, B.R., and Monteiro, A. (2014). Eyespots deflect predator attack increasing fitness and promoting the evolution of phenotypic plasticity. Proc. R. Soc. B Biol. Sci. *282*, 20141531–20141531.

265. Qiang, G., Kong, H.W., Fang, D., Mccann, M., Yang, X., Du, G., Blüher, M., Zhu, J., Chong, &, and Liew, W. (2016b). The obesity-induced transcriptional regulator TRIP-Br2 mediates visceral fat endoplasmic reticulum stress-induced inflammation.

266. Qiang, G., Whang Kong, H., Gil, V., and Wee Liew, C. (2016a). Transcription regulator TRIP-Br2 mediates ER stress-induced brown adipocytes dysfunction. Nat. Publ. Gr.

267. Ramachandran, R., Fausett, B. V., and Goldman, D. (2010). Ascl1a regulates Müller glia dedifferentiation and retinal regeneration through a Lin-28-dependent, let-7 microRNA signalling pathway. Nat. Cell Biol. *12*, 1101–1107.

268. Randsholt, N.B., Maschat, F., and Santamaria, P. (2000). polyhomeotic controls engrailed expression and the hedgehog signaling pathway in imaginal discs. Mech. Dev. *95*, 89–99.

269. Reichardt, I., Bonnay, F., Steinmann, V., Loedige, I., Burkard, T.R., Meister, G., and Knoblich, J.A. (2018). The tumor suppressor Brat controls neuronal stem cell lineages by inhibiting Deadpan and Zelda. EMBO Rep. *19*, 102–117.

270. Repiso, A., Bergantiños, C., and Serras, F. (2013). Cell fate respecification and cell division orientation drive intercalary regeneration in Drosophila wing discs. Development *140*.

271. Restrepo, S., and Basler, K. (2016). Drosophila wing imaginal discs respond to mechanical injury via slow InsP3R-mediated intercellular calcium waves. Nat. Commun. *7*, 12450.

272. Restrepo, S., Zartman, J.J., and Basler, K. (2014). Coordination of Patterning and Growth by the Morphogen DPP. Curr. Biol. *24*, R245–R255.

273. Ribeiro, L., Tobias-Santos, V., Santos, D., Antunes, F., Feltran, G., de Souza Menezes, J., Aravind, L., Venancio, T.M., and Nunes da Fonseca, R. (2017). Evolution and multiple roles of the Pancrustacea specific transcription factor zelda in insects. PLOS Genet. *13*, e1006868.

274. Rinkevich, Y., Lindau, P., Ueno, H., Longaker, M.T., and Weissman, I.L. (2011). Germ-layer and lineage-restricted stem/progenitors regenerate the mouse digit tip. Nature *476*, 409–413.

275. Roensch, K., Tazaki, A., Chara, O., and Tanaka, E.M. (2013). Progressive Specification Rather than Intercalation of Segments During Limb Regeneration. Science (80-.). *342*, 1375–1379.

276. Royzman, I., Whittaker, A.J., and Orr-Weaver, T.L. (1997). Mutations in Drosophila DP and E2F distinguish G1-S progression from an associated transcriptional program. Genes Dev. *11*, 1999–2011.

277. Ryder, E., Ashburner, M., Bautista-Llacer, R., Drummond, J., Webster, J., Johnson, G., Morley, T., Chan, Y.S., Blows, F., Coulson, D., et al. (2007). The DrosDel Deletion Collection: A Drosophila Genomewide Chromosomal Deficiency Resource. Genetics *177*, 615–629.

278. Ryoo, H.D., Gorenc, T., and Steller, H. (2004). Apoptotic Cells Can Induce Compensatory Cell Proliferation through the JNK and the Wingless Signaling Pathways. Dev. Cell *7*, 491–501.

279. Saijilafu, Zhang, B.-Y., and Zhou, F.-Q. (2013). Signaling pathways that regulate axon regeneration. Neurosci. Bull. *29*, 411–420.

280. Sandoval-Guzmán, T., Wang, H., Khattak, S., Schuez, M., Roensch, K., Nacu, E., Tazaki, A., Joven, A., Tanaka, E.M., and Simon, A. (2014). Fundamental Differences in Dedifferentiation and Stem Cell Recruitment during Skeletal Muscle Regeneration in Two Salamander Species. Cell Stem Cell *14*, 174–187.

281. Santabárbara-Ruiz, P., López-Santillán, M., Martínez-Rodríguez, I., Binagui-Casas, A., Pérez, L., Milán, M., Corominas, M., and Serras, F. (2015). ROS-Induced JNK and p38 Signaling Is Required for Unpaired Cytokine Activation during Drosophila Regeneration. PLoS Genet. *11*.

282. Satoh, A., Makanae, A., and Wada, N. (2010). The apical ectodermal ridge (AER) can be re-induced by wounding, wnt-2b, and fgf-10 in the chicken limb bud. Dev. Biol. *342*, 157–168.

283. Schnapp, E., Kragl, M., Rubin, L., and Tanaka, E.M. (2005). Hedgehog signaling controls dorsoventral patterning, blastema cell proliferation and cartilage induction during axolotl tail regeneration. Development *132*, 3243–3253.

284. Schubiger, G. (1971). Regeneration, duplication and transdetermination in fragments of the leg disc of Drosophila melanogaster. Dev. Biol. *26*, 277–295.

285. Schubiger, G. (1973). Regeneration ofDrosophila melanogaster male leg disc fragments in sugar fed female hosts. Experientia *29*, 631–632.

286. Schubiger, G., and Nöthiger, R. (1966). Developmental behaviour of fragments of symmetrical and asymmetrical imaginal discs of Drosophila melanogaster (Diptera). Development *16*.

287. Schulz, K.N., Bondra, E.R., Moshe, A., Villalta, J.E., Lieb, J.D., Kaplan, T., McKay, D.J., and Harrison, M.M. (2015). Zelda is differentially required for chromatin accessibility, transcription factor binding, and gene expression in the early Drosophila embryo. Genome Res. *25*, 1715–1726.

288. Schuster, K.J., and Smith-Bolton, R.K. (2015). Taranis Protects Regenerating Tissue from Fate Changes Induced by the Wound Response in Drosophila. Dev. Cell *34*, 119–128.

289. Seifert, A.W., and Muneoka, K. (2018). The blastema and epimorphic regeneration in mammals. Dev. Biol. *433*, 190–199.

290. Seifert, A.W., Kiama, S.G., Seifert, M.G., Goheen, J.R., Palmer, T.M., and Maden, M. (2012). Skin shedding and tissue regeneration in African spiny mice (Acomys). Nature *489*, 561–565.

291. Shah, M. V., Namigai, E.K.O., and Suzuki, Y. (2011). The role of canonical Wnt signaling in leg regeneration and metamorphosis in the red flour beetle Tribolium castaneum. Mech. Dev. *128*, 342–358.

292. Shenouda, M., Zhang, A.B., Weichert, A., and Robertson, J. (2018). Mechanisms Associated with TDP-43 Neurotoxicity in ALS/FTLD. In Advances in Neurobiology, pp. 239–263.

293. Shrestha, P., Yun, J.-H., Ko, Y.-J., Yeon, K.J., Kim, D., Lee, H., Jin, D.-H., Nam, K.-Y., Yoo, H.D., and Lee, W. (2017). NMR uncovers direct interaction between human NEDD4-1 and p34 SEI−1. Biochem. Biophys. Res. Commun. *490*, 984–990.

294. Shubin, N., Tabin, C., and Carroll, S. (2009). Deep homology and the origins of evolutionary novelty. Nature *457*, 818–823.

295. Siegrist, S.E., Haque, N.S., Chen, C.-H., Hay, B.A., and Hariharan, I.K. (2010). Inactivation of Both foxo and reaper Promotes Long-Term Adult Neurogenesis in Drosophila. Curr. Biol. *20*, 643–648.

296. da Silva, S.M., Gates, P.B., and Brockes, J.P. (2002). The newt ortholog of CD59 is implicated in proximodistal identity during amphibian limb regeneration. Dev. Cell *3*, 547–555.

297. Sim, K.G., Zang, Z., Yang, C.M., Bonventre, J. V., and Hsu, S.I.-H. (2004). TRIP-Br Links E2F to Novel Functions in the Regulation of Cyclin E Expression During Cell Cycle Progression and in the Maintenance of Genomic Stability. Cell Cycle *3*, 1296–1304.

298. Sim, K.G., Cheong, J.K., and Hsu, S.I.-H. (2006a). The TRIP-Br Family of Transcriptional Regulators is Essential for the Execution of Cyclin E-Mediated Cell Cycle Progression. Cell Cycle *5*, 1111–1115.

299. Sim, K.G., Cheong, J.K., and Hsu, S.I.-H. (2006b). The TRIP-Br Family of Transcriptional Regulators is Essential for the Execution of Cyclin E-Mediated Cell Cycle Progression. Cell Cycle *5*, 1111–1115.

300. Simkin, J., Gawriluk, T.R., Gensel, J.C., and Seifert, A.W. (2017). Macrophages are necessary for epimorphic regeneration in African spiny mice. Elife *6*.

301. Simon, H.-G., and Odelberg, S. (2015). Maintaining Eastern Newts (Notophthalmus viridescens) for Regeneration Research. In Methods in Molecular Biology (Clifton, N.J.), pp. 17–25.

302. Singer, M.A., Penton, A., Twombly, V., Hoffmann, F.M., and Gelbart, W.M. (1997). Signaling through both type I DPP receptors is required for anterior-posterior patterning of the entire Drosophila wing. Development *124*, 79–89.

303. Singh, S.P., Holdway, J.E., and Poss, K.D. (2012). Regeneration of Amputated Zebrafish Fin Rays from De Novo Osteoblasts. Dev. Cell *22*, 879–886.

304. Skeath, J.B., and Carroll, S.B. (1991). Regulation of achaete-scute gene expression and sensory organ pattern formation in the Drosophila wing. Genes Dev. *5*, 984–995.

305. Skinner, A., Khan, S.J., and Smith-Bolton, R.K. (2015). Trithorax regulates systemic signaling during Drosophila imaginal disc regeneration. Development *142*.

306. Slack, J.M.W., Beck, C.W., Gargioli, C., and Christen, B. (2004). Cellular and molecular mechanisms of regeneration in Xenopus. Philos. Trans. R. Soc. B Biol. Sci. *359*, 745–751.

307. Smith-Bolton, R. (2016). *Drosophila* Imaginal Discs as a Model of Epithelial Wound Repair and Regeneration. Adv. Wound Care *5*, 251–261.

308. Smith-Bolton, R.K., Worley, M.I., Kanda, H., and Hariharan, I.K. (2009). Regenerative Growth in Drosophila Imaginal Discs Is Regulated by Wingless and Myc. Dev. Cell *16*, 797–809.

309. Soares, L., Parisi, M., and Bonini, N.M. (2015). Axon Injury and Regeneration in the Adult Drosophila. Sci. Rep. *4*, 6199.

310. Somorjai, I.M.L., Somorjai, R.L., Garcia-Fernandez, J., and Escriva, H. (2012). Vertebrate-like regeneration in the invertebrate chordate amphioxus. Proc. Natl. Acad. Sci. *109*, 517–522.

311. Song, Q., Feng, G., Huang, Z., Chen, X., Chen, Z., and Ping, Y. (2017). Aberrant Axonal Arborization of PDF Neurons Induced by Aβ42-Mediated JNK Activation Underlies Sleep Disturbance in an Alzheimer's Model. Mol. Neurobiol. *54*, 6317–6328.

312. Sousa, S., Afonso, N., Bensimon-Brito, A., Fonseca, M., Simões, M., Leon, J., Roehl, H., Cancela, M.L., and Jacinto, A. (2011). Differentiated skeletal cells contribute to blastema formation during zebrafish fin regeneration. Development *138*.

313. Staudt, N., Fellert, S., Chung, H.-R., Jäckle, H., and Vorbrüggen, G. (2006). Mutations of the Drosophila zinc finger-encoding gene vielfältig impair mitotic cell divisions and cause improper chromosome segregation. Mol. Biol. Cell *17*, 2356–2365.

314. Stewart, S., and Stankunas, K. (2012). Limited dedifferentiation provides replacement tissue during zebrafish fin regeneration. Dev. Biol. *365*, 339–349.

315. Stoehr, A.M., Walker, J.F., and Monteiro, A. (2013). Spalt expression and the development of melanic color patterns in pierid butterflies. Evodevo *4*, 6.

316. Stronach, B. (2005). Dissecting JNK signaling, one KKKinase at a time. Dev. Dyn. *232*, 575–584.

317. Sturtevant, M.A., Roark, M., and Bier, E. (1993). The Drosophila rhomboid gene mediates the localized formation of wing veins and interacts genetically with components of the EGF-R signaling pathway. Genes Dev. *7*, 961–973.

318. Suetsugu-Maki, R., Maki, N., Nakamura, K., Sumanas, S., Zhu, J., Del Rio-Tsonis, K., and Tsonis, P.A. (2012). Lens regeneration in axolotl: new evidence of developmental plasticity. BMC Biol. *10*, 103.

319. Sugimori, S., Hasegawa, A., and Nakagoshi, H. (2016). Spalt-mediated dve repression is a critical regulatory motif and coordinates with Iroquois complex in Drosophila vein formation. Mech. Dev. *141*, 25–31.

320. Sugimoto, M., Nakamura, T., Ohtani, N., Hampson, L., Hampson, I.N., Shimamoto, A., Furuichi, Y., Okumura, K., Niwa, S., Taya, Y., et al. (1999). Regulation of CDK4 activity by a novel CDK4-binding protein, p34(SEI-1). Genes Dev. *13*, 3027–3033.

321. Sugiura, T., Wang, H., Barsacchi, R., Simon, A., and Tanaka, E.M. (2016). MARCKS-like protein is an initiating molecule in axolotl appendage regeneration. Nature.

322. Sun, G., and Irvine, K.D. (2011). Regulation of Hippo signaling by Jun kinase signaling during compensatory cell proliferation and regeneration, and in neoplastic tumors. Dev. Biol. *350*, 139–151.

323. Sun, G., and Irvine, K.D. (2013). Ajuba Family Proteins Link JNK to Hippo Signaling. Sci. Signal. *6*, ra81-ra81.

324. Sun, G., and Irvine, K.D. (2014). Control of Growth During Regeneration. pp. 95–120.

325. Sun, X., and Artavanis-Tsakonas, S. (1996). The intracellular deletions of Delta and Serrate define dominant negative forms of the Drosophila Notch ligands. Development *122*, 2465–2474.

326. Sunderland, M.E. (2010). Regeneration: Thomas Hunt Morgan's window into development. J. Hist. Biol. *43*, 325–361.

327. Sustar, A., and Schubiger, G. (2005). A Transient Cell Cycle Shift in Drosophila Imaginal Disc Cells Precedes Multipotency. Cell *120*, 383–393.

328. Suzuki, Y., Squires, D.C., and Riddiford, L.M. (2009). Larval leg integrity is maintained by Distal-less and is required for proper timing of metamorphosis in the flour beetle, Tribolium castaneum. Dev. Biol. *326*, 60–67.

329. Szabad, J., Simpson, P., and Nöthiger, R. (1979). Regeneration and compartments in Drosophila. J. Embryol. Exp. Morphol. *49*, 229–241.

330. Tabata, T., and Kornberg, T.B. (1994). Hedgehog is a signaling protein with a key role in patterning Drosophila imaginal discs. Cell *76*, 89–102.

331. Tabata, T., Tsuneizumi, K., Nakayama, T., Kamoshida, Y., Kornberg, T.B., and Christian, J.L. (1997). Daughters against dpp modulates dpp organizing activity in Drosophila wing development. Nature *389*, 627–631.

332. Taipale, J., Cooper, M.K., Maiti, T., and Beachy, P.A. (2002). Patched acts catalytically to suppress the activity of Smoothened. Nature *418*, 892–897.

333. Tanaka, E.M. (2016). The Molecular and Cellular Choreography of Appendage Regeneration. Cell *165*.

334. Tanaka, E.M., and Reddien, P.W. (2011). The Cellular Basis for Animal Regeneration. Dev. Cell *21*, 172–185.

335. Tanimoto, H., Itoh, S., ten Dijke, P., and Tabata, T. (2000). Hedgehog Creates a Gradient of DPP Activity in Drosophila Wing Imaginal Discs. Mol. Cell *5*, 59–71.

336. Tategu, M., Nakagawa, H., Hayashi, R., and Yoshida, K. (2008). Transcriptional co-factor CDCA4 participates in the regulation of JUN oncogene expression. Biochimie *90*, 1515–1522.

337. Taylor, J.P., Brown, R.H., and Cleveland, D.W. (2016). Decoding ALS: from genes to mechanism. Nature *539*, 197–206.

338. Technau, U., and Holstein, T.W. (1992). Cell sorting during the regeneration of Hydra from reaggregated cells. Dev. Biol. *151*, 117–127.

339. Thompson-Peer, K.L., DeVault, L., Li, T., Jan, L.Y., and Jan, Y.N. (2016). In vivo dendrite regeneration after injury is different from dendrite development. Genes Dev. *30*, 1776–1789.

340. Tonnarelli, B., Centola, M., Barbero, A., Zeller, R., and Martin, I. (2014). Re-engineering Development to Instruct Tissue Regeneration. pp. 319–338.

341. Tseng, A.-S., Beane, W.S., Lemire, J.M., Masi, A., and Levin, M. (2010). Induction of Vertebrate Regeneration by a Transient Sodium Current. J. Neurosci. *30*, 13192–13200.

342. Tsonis, P.A. (2006). How to build and rebuild a lens. J. Anat. *209*, 433–437.

343. Uhlirova, M., and Bohmann, D. (2006). JNK- and Fos-regulated Mmp1 expression cooperates with Ras to induce invasive tumors in Drosophila. EMBO J. *25*, 5294–5304.

344. Umetsu, D., and Dahmann, C. (2015). Signals and mechanics shaping compartment boundaries in *Drosophila*. Wiley Interdiscip. Rev. Dev. Biol. *4*, 407–417.

345. Umetsu, D., Aigouy, B., Aliee, M., Sui, L., Eaton, S., Jü, F., and Dahmann, C. (2014). Report Local Increases in Mechanical Tension Shape Compartment Boundaries by Biasing Cell Intercalations. Curr. Biol. *24*, 1798–1805.

346. Vallejo, D.M., Juarez-Carreño, S., Bolivar, J., Morante, J., and Dominguez, M. (2015). A brain circuit that synchronizes growth and maturation revealed through Dilp8 binding to Lgr3. Science *350*, aac6767.

347. Vissers, J.H.A., Manning, S.A., Kulkarni, A., and Harvey, K.F. (2016). A Drosophila RNAi library modulates Hippo pathway-dependent tissue growth. Nat. Commun. *7*, 10368.

348. Voss, S.R., Palumbo, A., Nagarajan, R., Gardiner, D.M., Muneoka, K., Stromberg, A.J., and Athippozhy, A.T. (2015). Gene expression during the first 28 days of axolotl limb regeneration I: Experimental design and global analysis of gene expression. Regeneration *2*, 120–136.

348. Vriz, S., Reiter, S., and Galliot, B. (2014). Cell Death. A Program to Regenerate. Curr. Top. Dev. Biol. *108*.

349. Wagner, D.E., Wang, I.E., and Reddien, P.W. (2011). Clonogenic neoblasts are pluripotent adult stem cells that underlie planarian regeneration. Science *332*, 811–816.

350. Wang, X., He, H., Tang, W., Zhang, X.A., Hua, X., and Yan, J. (2012). Two Origins of Blastemal Progenitors Define Blastemal Regeneration of Zebrafish Lower Jaw. Doi.Org *7*, e45380.

351. Warner, J.F., Guerlais, V., Amiel, A.R., Johnston, H., Nedoncelle, K., and Röttinger, E. (2018). NvERTx: a gene expression database to compare embryogenesis and regeneration in the sea anemone *Nematostella vectensis*. Development *145*, dev162867.

352. Watanabe-Fukunaga, R., Iida, S., Shimizu, Y., Nagata, S., and Fukunaga, R. (2005). SEI family of nuclear factors regulates p53-dependent transcriptional activation. Genes to Cells *10*, 851–860.

353. Weavers, H., Liepe, J., Sim, A., Wood, W., Martin, P., and Stumpf, M.P.H. (2016). Systems Analysis of the Dynamic Inflammatory Response to Tissue Damage Reveals Spatiotemporal Properties of the Wound Attractant Gradient. Curr. Biol. *26*, 1975–1989.

354. Weber, U., Paricio, N., and Mlodzik, M. (2000). Jun mediates Frizzled-induced R3/R4 cell fate distinction and planar polarity determination in the Drosophila eye. Development *127*.

355. Whitehead, G.G., Makino, S., Lien, C.-L., and Keating, M.T. (2005). fgf20 is essential for initiating zebrafish fin regeneration. Science *310*, 1957–1960.

356. Wijesena, N., Simmons, D.K., and Martindale, M.Q. (2017). Antagonistic BMP–cWNT signaling in the cnidarian *Nematostella vectensis* reveals insight into the evolution of mesoderm. Proc. Natl. Acad. Sci. *114*, E5608–E5615.

357. Williams, J.A., Bell, J.B., and Carroll, S.B. (1991). Control of Drosophila wing and haltere development by the nuclear vestigial gene product. Genes Dev. *5*, 2481–2495.

358. Williams, J.A., Paddock, S.W., Vorwerk, K., and Carroll, S.B. (1994). Organization of wing formation and induction of a wing-patterning gene at the dorsal/ventral compartment boundary. Nature *368*, 299–305.

359. Wittlieb, J., Khalturin, K., Lohmann, J.U., Anton-Erxleben, F., and Bosch, T.C.G. (2006). Transgenic Hydra allow in vivo tracking of individual stem cells during morphogenesis. Proc. Natl. Acad. Sci. *103*, 6208–6211.

340. Worley, M.I., Setiawan, L., and Hariharan, I.K. (2012). Regeneration and Transdetermination in *Drosophila* Imaginal Discs. Annu. Rev. Genet. *46*, 289–310.

341. Worley, M.I., Setiawan, L., and Hariharan, I.K. (2013). TIE-DYE: a combinatorial marking system to visualize and genetically manipulate clones during development in Drosophila melanogaster. Development *140*.

342. Worley, M.I., Alexander, L.A., and Hariharan, I.K. (2018). CtBP impedes JNK- and Upd/STAT-driven cell fate misspecifications in regenerating Drosophila imaginal discs. Elife *7*.

343. Wu, M.-J., Wu, W.-C., Chang, H.-W., Lai, Y.-T., Lin, C.-H., Yu, W.C.Y., and Chang, V.H.S. (2015). KLF10 affects pancreatic function via the SEI-1/p21Cip1 pathway. Int. J. Biochem. Cell Biol. *60*, 53–59.

344. Wu, Z., Ghosh-Roy, A., Yanik, M.F., Zhang, J.Z., Jin, Y., and Chisholm, A.D. (2007). Caenorhabditis elegans neuronal regeneration is influenced by life stage, ephrin signaling, and synaptic branching. Proc. Natl. Acad. Sci. *104*, 15132–15137.

345. Wuestefeld, T., Pesic, M., Rudalska, R., Dauch, D., Longerich, T., Kang, T.-W., Yevsa, T., Heinzmann, F., Hoenicke, L., Hohmeyer, A., et al. (2013). A Direct In Vivo RNAi Screen Identifies MKK4 as a Key Regulator of Liver Regeneration. Cell *153*, 389–401.

346. Yagi, R., Mayer, F., Basler, K., Tabata, T., Kooperberg, C., Leeuwen, F. van, Gottschling, D., O'Neill, L., Turner, B., Delrow, J., et al. (2010). Refined LexA transactivators and their use in combination with the Drosophila Gal4 system. Proc. Natl. Acad. Sci. *107*, 16166–16171.

347. Yanik, M.F., Cinar, H., Cinar, H.N., Chisholm, A.D., Jin, Y., and Ben-Yakar, A. (2004). Neurosurgery: Functional regeneration after laser axotomy. Nature *432*, 822–822.

348. Yoo, S.K., Pascoe, H.G., Pereira, T., Kondo, S., Jacinto, A., Zhang, X., and Hariharan, I.K. (2016). Plexins function in epithelial repair in both Drosophila and zebrafish. Nat. Commun. *7*.

349. Zang, Z.J., Gunaratnam, L., Cheong, J.K., Lai, L.Y., Hsiao, L.-L., O'Leary, E., Sun, X., Salto-Tellez, M., Bonventre, J. V, and Hsu, S.I.-H. (2009). Identification of PP2A as a novel interactor and regulator of TRIP-Br1. Cell. Signal. *21*, 34–42.

350. Zecca, M., and Struhl, G. (2007b). Control of Drosophila wing growth by the vestigial quadrant enhancer. Development *134*, 3011–3020.

351. Zecca, M., and Struhl, G. (2007a). Recruitment of cells into the Drosophila wing primordium by a feed-forward circuit of vestigial autoregulation. Development *134*, 3001–3010.

352. Zecca, M., and Struhl, G. (2010). A Feed-Forward Circuit Linking Wingless, Fat-Dachsous Signaling, and the Warts-Hippo Pathway to Drosophila Wing Growth. PLoS Biol. *8*, e1000386.

353. Zecca, M., Basler, K., and Struhl, G. (1996). Direct and long-range action of a wingless morphogen gradient. Cell *87*, 833–844.